2011

Dynamic Response of Oily Clay to Impact Loading

Carlos Ismael Medina
Lehigh University

Dynamic Response of Oily Clay to Impact Loading

by

Carlos Medina

A Thesis

Presented to the Graduate and Research Committee

of Lehigh University

in Candidacy for the Degree of

Master of Science

in

Civil and Environmental Engineering

Lehigh University

August 12, 2011

This thesis is accepted and approved in partial fulfillment of requirements for the Master of Science.

_____

Date

_____

Thesis Advisor

_____

Chairperson of Department

ACKNOWLEDGEMENTS

I would first like to thank Professor Sibel Pamukcu. I appreciate her guidance and oversight throughout my graduate studies. Also, Professor Mesut Pervizpour who along with Professor Pamukcu served as an advisor and pointed me in the proper direction in order to complete this work. Special thanks go to Professor Naito and his grad students who developed the numerical models. I would also like to thank Trent Muraoka and Dan Zeroka who assisting me in the lab for countless hours. Lastly, I would like to thank my family. Specifically my parents for providing me with support throughout my studies and never allowing me to step backwards.

TABLE OF CONTENTS

LIST OF FIGURES

LIST OF VARIABLES

G	Shear Modulus	MPa
ξ	Damping Ratio	Unit less
A_L	Energy Dissipated	
A_T	Peak Energy	
G_{max}	Maximum Shear Modulus	MPa
ξ_{min}	Minimum Damping Ratio	Unit less
σ	Stress	Pa
υ	Poisson's Ratio	Unit less
E	Young's Modulus	MPa
ρ	Density	kg/m^3
A	Cross Sectional Area	m^2
M	Constrained Modulus	MPa
u	Displacement	m
t	Time	Seconds
ϵ	Strain	m/m
v_L	Longitudinal Wave Velocity	m/s
θ	Angle of Twist	radians
J_z	Polar Moment of Inertia	m^4
v_s	Shear Wave Velocity	m/s
v_R	Rayleigh Wave Velocity	m/s
K_{Rs}	Ratio of Rayleigh Wave to Shear Wave Velocity	Unit less
k_R	Wave Number of Rayleigh Wave	rad/m
ω	Angular Frequency	rad/s

τ	Shear Stress	Pa
γ	Shear Strain	m/m
η	Viscosity	Pa*s
I	Mass Moment of Inertia	kg*m^2
V	Volume	m^3
d	Diameter	m
l	Length of Sample	m
ρ	Density	kg/m^3
J_s	Rotational Mass Polar Moment of Inertia of Sample	kg*m^2
m	Mass	kg
T_T	Active-End Inertial Factor For Torsional Excitation	Unitless
J_A	Rotational Mass Polar Moment of Inertia of Top Platen	kg*m^2
ADF_T	Rotational Apparatus Damping Factor	
ADC_{0T}	Apparatus Damping Coefficient for Torsion	kg*m^2
f_T	Resonant Frequency for Torsion	Hz
RCF	Rotational Motion Transducer Calibration Factor	
RTO	Output Reading from Resonant Column	
TCF	Torque Calibration Factor	
CR_T	Input to Resonant Column	
MMF_T	Torsional Magnification Factor	

γ_r	Reference Strain
γ_h	Hyberbolic Strain
G/G_{max}	Normalized Shear Modulus
ε_{ij}	Strain
ε_{ij}^{e}	Elastic Strain
ε_{ij}^{p}	Plastic Strain
S_{ij}	Deviatoric Stress Component
λ	Plastic Non-negative Multiplier
C_{ijkl}	Stiffness Modulus Tensor
δ_{ij}	Kroenecker Delta
H_{kl}	Second Order Tensor

ABSTRACT

The characterization of the oil based clay response used as a backing material during ballistic impact of light armor testing is essential in assessment of level of potential injury, and effectiveness and certification of the body armor. The current standard for quantification of level of impact relies on the permanent imprint of the impact on clay backing material. Current investigations are in progress for the measurement of magnitude and rate of internal stresses within clay due to ballistic projectile impact. A finite element model of the projectile impact is developed. The dynamic characteristics of the oil based clay backing material are assessed through resonant column tests. The frequency dependent moduli and damping characteristics are determined under various confining pressures and temperatures. The strain and frequency dependency are characterized through appropriate hyperbolic fits.

Chapter 1 INTRODUCTION

The safety and protection of the individuals dedicated to the defense of our nation is a priority of the national research agenda. Body armor and other protective gear are important in preventing damage to the human body. In order to evaluate the effectiveness of body armor, a standardized method for testing Body Armor Protection Systems (BAPS) needs to be developed. The United States National Institute of Justice (NIJ) has developed a standard procedure for testing the BAPS. The test setup consists of the body armor backed by clay. The armor is fired pn and removed at the conclusion of the test to examine clay. The ballistic impact's deformation of the clay is used to assess the severity of the impact and the effectiveness of the armor. The clay used as backing is Roma Plastillina No. 1 oil based modeling clay (RP). The clay and its properties are the main focus of this paper.

1.1 ROMA PLASTILLINA CLAY

Little research has been conducted on RP, the backing material used for testing. Typically, oil based modeling clays consist of oil, waxes, and clay minerals. The exact composition of this clay is unknown due to the privacy rights of the manufacturer. In order to assure the consistency of the material, the clay used was the same color and purchased from the same warehouse.

Modeling clay provides several benefits compared to other materials. Unlike ballistic gelatin, which does not provide a deformation to assess, the RP is left with an impression or deformation due to the impact. Ballistic gelatin is more commonly used to measure the penetration of bullets on human tissue, so it is useless for assessing the damage that is caused by impact. An advantage to using RP is that it is homogenous, so consistent samples can be created

with relative ease. Another advantage is that, since the clay is oil based water content or rather water evaporation is not a concern like it would be in other soils.

While the oil based clay is an advantage for testing and reproducing samples, it is a slight disadvantage when it comes to deriving the properties of the clay. Traditionally clays are classified using their particle distribution and Atterburg limits. Neither of those two concepts can be applied to this clay. In addition, other important soil properties such as void ratio and water content could not be determined. Void ratio could not be determined because attempts at burning off the oil were unsuccessful, which made it difficult to apply some relationships to the clay and limited some of our initial testing.

Several general observations were made about the clay prior to testing. The clay seemed to be very susceptible to temperature change, becoming more malleable when heated and even liquefying at higher temperature. It was also observed that at high temperatures the sulfur in the clay would burn off. Vice versa the clay seemed to become slightly stiffer at cooler temperatures. Handling or disturbing the samples also seemed to cause the clay to be more malleable.

1.2 NEED FOR STUDY

NIJ provides criterion for what deformation would constitute a “kill shot” on the clay backing (44 mm indentation). There has been a movement to not only focus on the deformation created by the impact, but also the stress wave created by the ballistic impact. Previous studies conducted (Carrol & Soderstrom, 1978) & (Moseley & Doty, 1969) suggest that though the penetration of the bullet is prevented by the body armor, damage can still be caused by the impact and concurrent stress wave. These studies state that though the bullet is stopped, the concurrent stress wave can lead to internal damage to the lungs, liver, heart, spleen and spinal

cord. For this reason, the event of a ballistic impact needs to be numerically simulated in order to assess the stress values.

Assessing the impact is currently done by measuring the depth of the indentation after the impact and using high speed cameras to measure the impact velocities. These values are then used to construct a numerical model. The modeling is important in identifying internal strains and stresses. The accuracy of these values are unconfirmed due to the inability to accurately record internal stress values during an event. Furthermore, without lab tests to validate the properties used for the modeling, the accuracy of the results is always going to be in question. The proposed solution to this issue is to use fiber optic sensors to take real time measurements of the event. Through a combination of accurate numerical modeling and corresponding strain measurements, an accurate depiction of the ballistic impact can be created.

Fiber optic sensors provide an unconventional method for measuring strain. Traditionally, strain gauges are intrusive and require flexible backing. Though traditional strain gauges can provide good measurements for strain at the back of the clay layer, they are difficult to install in a manner that does not alter the clay. Whether they have the capability to sustain the impact and capture the signal is also of concern. In contrast, fiber optic sensors are fairly durable, especially in tension. Due to their physical characteristics (diameters of $125\mu m$), fiber optic sensors are not as intrusive and should have minor effects on the clay. Capturing the signal, however, still remains a concern. Once installed in the clay, the fiber optic sensors can be left there for the entire extent of testing. Another benefit of fiber optic sensors is that they can be layered and continuous. As a result, fiber optics can provide measurements that allow us to map out the strain throughout as opposed to other sensors that usually only provide point measurements. Eventually, fiber optic layering can provide a better three dimensional rendering of the strains

occurring in the clay. This three dimensional rendering can be compared to a numerical model in order to verify or establish relationships between the two. This is another reason why accurate soil properties need to found.

1.3 BALL DROP TEST

NIJ provides an outline for testing the oily clay which does not require body armor or an actual ballistic impact (i.e. shooting gun). The impact testing is referred to as the “ball drop” test. The test was created as a calibration procedure in order to verify whether the clay was suitable for backing material. This test is also used to derive the properties that are used for the numerical model. An additional benefit to this test is that it can easily be conducted in a lab setting. This test is a huge asset and was frequently used in our lab in order to verify the model.

The test is simple so that it can easily be reproduced. Firstly, the packaged clay bricks are heated to a temperature of about 40° C. This is done to make the clay more workable and to ease the sample preparation process. The clay is then hammered flat with a mallet and molded into tray 305 x 305 x 102 mm (12 x 12 x 4 in), as shown in figure 1.1. The dimensions provided are the ones used for this test, however tray size may vary. After the clay is packed, the tray is placed back in the oven and reheated to about 40° C. The prepped sample is then ready to be tested. A steel sphere, with a diameter of 63.5 mm and a mass of 1043 g, is dropped from various heights (typically about 2 meters); the setup for this is shown in figure 1.2. In the image the ball is dropped from the top of the frame through a PVC pipe, which served as a guide for the sphere. The maximum deformation allowed for these test is 44 mm. This is the impact that would cause a fatal blow behind a BAPS. If the clay deforms more than the limit, the sample was determined to be unsuitable for testing. Also, this test is used to predict initial soil properties until lab tests

Figure 1.1- Testing Tray Packed with clay and Fiber Optic grid

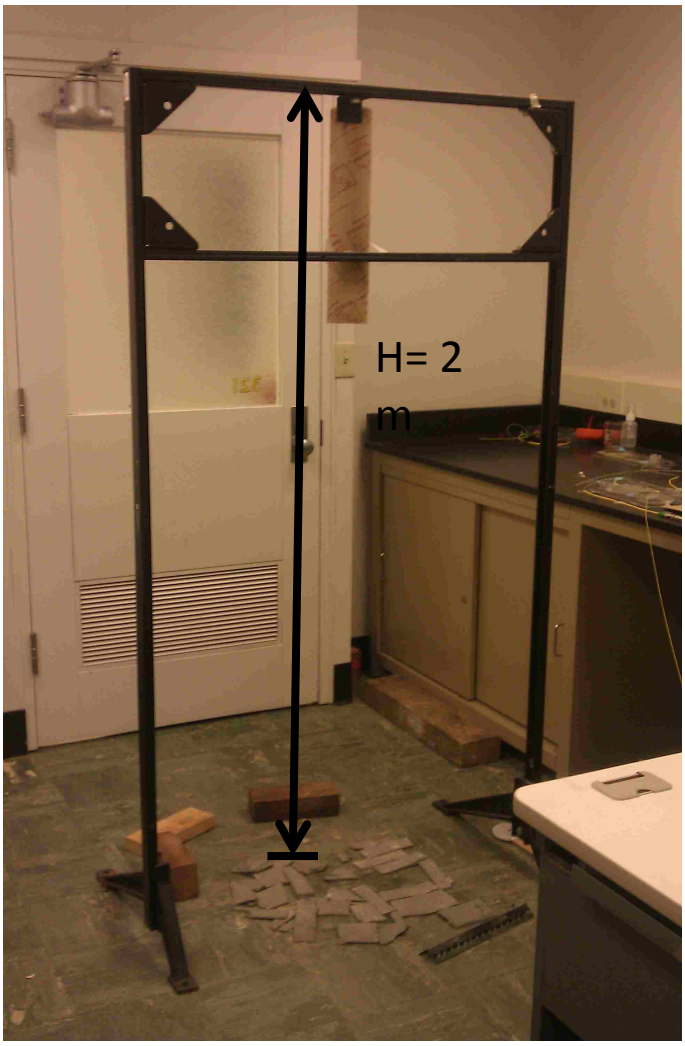

Figure 1.2- Frame used to drop steel ball onto the clay sample.

are conducted. This is done by recording the deformations, and altering the properties of the models until the deformations match.

1.4 FOCUS OF RESEARCH

The purpose of this research is to provide accurate dynamic soil properties for the finite element modeling. Without accurate soil properties, there is no verification of the model or the measurements taken by the sensors. Typically, dynamic soil properties are a function of strain amplitude, effective stress, and number of loading cycles (Hardin & Drnevich, Shear Modulus and Damping in Soils: Design Equations and Curves, 1972). Low strain test are therefore conducted on the clay at varying confining pressures and with increasing strain amplitude. The results of these tests are then interpreted using predictive equations that provide the strain dependent behavior. Also an attempt is made to relate the laboratory data to the Drucker Prager yield criterion that is used to simulate the event. By the end of this study a clear depiction of the clays dynamic clay properties and their interpretation will be shown.

Chapter 2 : BACKGROUND

2.1 DYNAMIC SOIL PROPERTIES

Dynamic soil properties are used in geotechnical engineering for both earthquake and soil dynamic problems. Since, at low strains, the stress-strain relationship of the soil is linear the theory of viscoelasticity is used to describe the dissipation of energy in soils through wave propagation. Soil dynamic properties are found by applying a harmonic oscillation to samples. The harmonic motion applied to the sample creates a hysteresis loop (figure 2.1) which allows us to calculate both the shear modulus (G) and damping ratio (ξ). Figure 2.1 shows the reversal of the harmonic strain that is applied on the sample.

Shear modulus and damping ratios are important when calculating dynamic response of soils or soil structures. The size of the loop varies according to strain amplitude. In figure 2.1, the area within the loop, A_L, is the amount of energy dissipated by the soil during cyclic loading. The area under the triangle, A_T, is the peak energy during a cycle of excitation.

Shear modulus is the relationship between shear strain and stress. It is found using the hysteresis loop. This is done by drawing a line through the endpoints (strain reversals) of the hysteresis loop and finding the slope. The shear modulus and strain allow us to construct the stress curve referred to as the backbone curve. The damping ratio can also be determined by using the hysteresis loop. The damping ratio is used to describe the oscillations' magnitude of decay after a disturbance. By comparing the amount of energy dissipated, A_L, and the peak energy, A_T, the hysteresis loop can give the damping ratio. Both dynamic properties are therefore a function of strain amplitude.

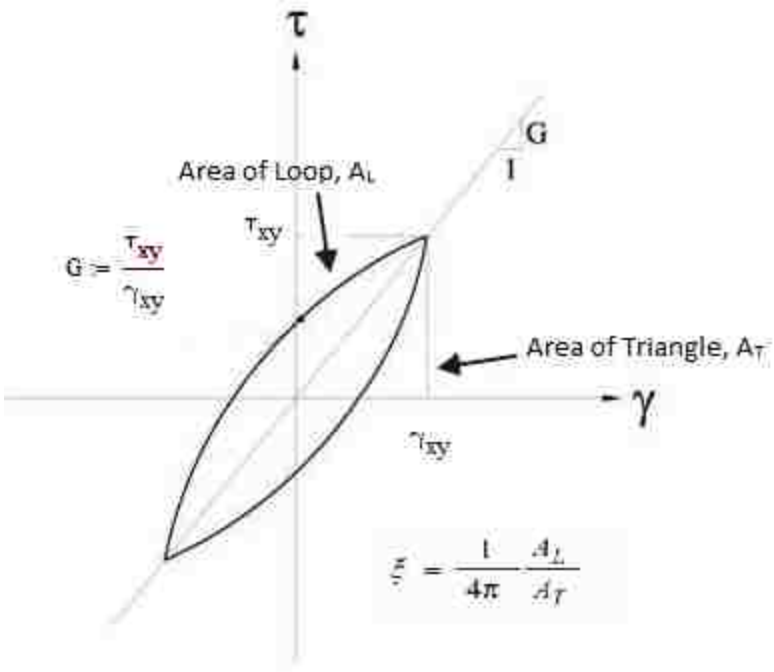

Figure 2.1-Hystoresis Loop

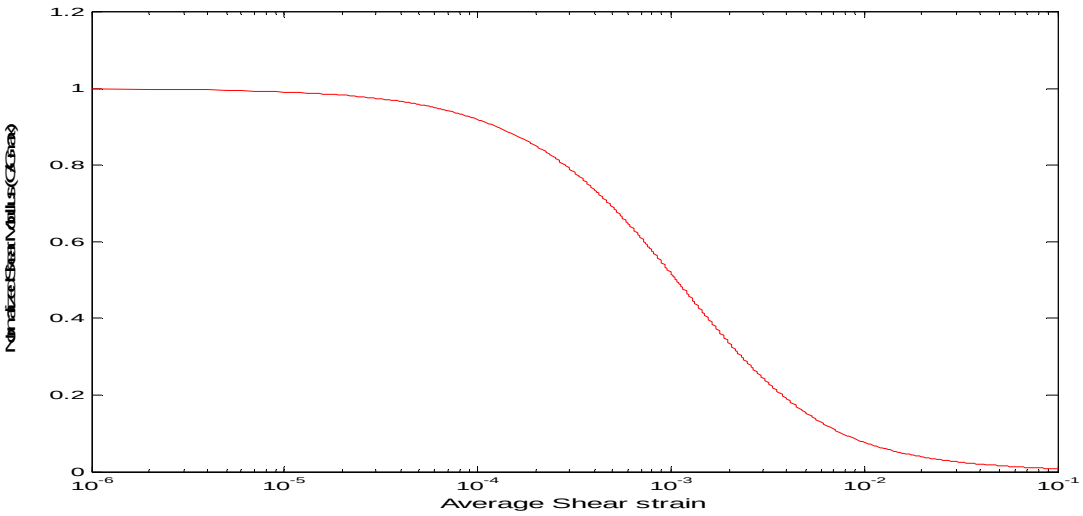

Figure 2.2Degradation of Shear Modulus with Increasing Shear Strain

Soils at low strains behave linearly, meaning that properties like G and ξ are constant low strains (elastic). As the strain amplitude increases, the shear modulus tends to decrease. This is shown in figure 2.2 with normalized shear modulus (G/G_{max}). The maximum value for shear modulus is found at low strains and is called the initial tangent shear modulus (G_{max}). Conversely, the damping ratio increases with strain. The initial value for damping ratio is called the minimum material damping ratio (ξ_{min}).

2.2 YOUNG'S AND SHEAR MODULUS

The moduli of material are used to describe the stress strain relationship of the material. For dynamic soil problems, elastic and shear modulus are a point of emphasize. The elastic modulus is used to describe the relationship between normal stress and normal strain. It can be found using a resonant column or, more commonly, a triaxial machine. The following equation describes elastic modulus:

$$E = \frac{\sigma_1 - 2\nu\sigma_3}{\epsilon_{Axial}} \tag{2.1}$$

In equation 2.1 σ_1 represents the normal stress, σ_3 represents the confining stress of the test and υ is Poisson's ratio of the material. Elastic modulus can be conveniently derived from the stress strain curve created by the triaxial test.

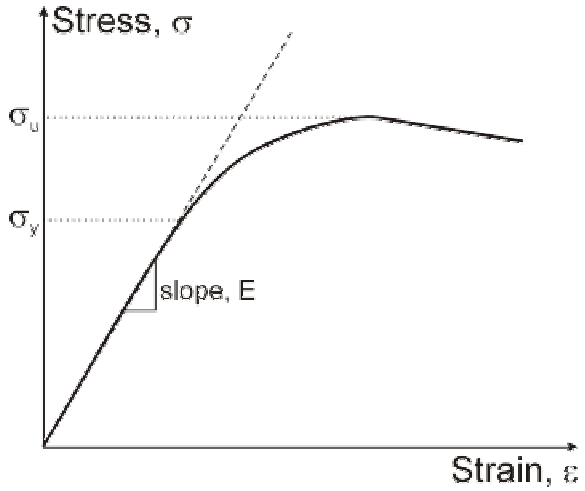

Figure 2.3- Typical Stress-Strain Graph Produced from triaxial test

Shear modulus relates shear stress and shear strain. It can also be defined by the following equation:

— (2.2)

Poisson's ratio relates elastic modulus to shear modulus. Poisson's ratio is the ratio of a material contraction to the extension under an applied load. The equations relating G and E are below:

—— (2.3)

(2.4)

2.3 WAVE PROPAGATION

Dynamic disturbances in soils are characterized by the perspective of wave propagation. Wave velocity and wave attenuation (damping) are two of the most telling soil characteristics. In order to understand wave propagation, the analogy of an infinitely long rod is commonly used. If one looks at the rod, it can have three types of vibration (Steven L.Kramer, 1996). One is when the particles experience longitudinal displacement, the other is when there is torsional displacement, and the third is flexural displacement. Flexural displacement has little application in soils and is typically ignored. Most resonant column tests are conducted for torsional displacement (focus of this study), but they are also capable of longitudinal vibrations so both are covered.

Figure 2.4- Constrained Rod with a Longitudinal Stress Wave

2.3.1 LONGITUDINAL WAVE

The infinitely long rod analogy helps when envisioning longitudinal waves. Figure 2.4 shows the rod, fixed at both the top and bottom so that no radial displacement can occur. Particle displacement can only occur along the axis which is what constitutes a longitudinal wave. In order to derive the wave equation for a longitudinal wave, aspects of the rod's physical

characteristics such as rod density, ρ, cross sectional area, A, and constrained modulus, M, must be known. Also, the assumption that stress is evenly distributed throughout the cross section of the rod must be made. The initial stress traveling along the rod is σ_i, shown at the beginning of the rod in figure 2.4. The rod is continuous so that the stress at any point along the rod can be described by:

$$\sigma_i + \frac{\partial \sigma}{\partial x} * dx \tag{2.5}$$

The strain at the arbitrary point is equal to the initial stress plus the change in stress with respect to the change in distance, shown in figure 2.4. We get the following equation because the external force (i.e., Stress) has to be equal to inertial force that is induced by the internal mass acceleration and, according to dynamic equilibrium, the rates of the forward and the reverse reactions most be equal:

$$\left(\sigma_i + \frac{\partial \sigma}{\partial x} * dx\right) A - \sigma_i A = \rho A \, dx \, \frac{\partial^2 u}{\partial t^2} \tag{2.6}$$

Equation 2.6 simplifies to:

$$\frac{\partial \sigma}{\partial x} = \rho \, \frac{\partial^2 u}{\partial t^2} \tag{2.7}$$

Equation 2.7 is the one-dimensional equation of motion for a longitudinal wave through an infinitely long rod. Furthermore, stress can be related to strain by equation 2.8:

$$\sigma = M\epsilon \tag{2.8}$$

$$\epsilon = \frac{\partial u}{\partial x} \tag{2.9}$$

In the equation of motion, equation 2.8 and 2.9 are used to replace stress. Simplifying even further to:

$$\frac{\partial^2 u}{\partial t^2} = \frac{M}{\rho}\frac{\partial^2 u}{\partial x^2} \tag{2.10}$$

Using material properties for wave velocity the constrained modulus and the density above can be replaced:

$$\frac{\partial^2 u}{\partial t^2} = v_L^2 \frac{\partial^2 u}{\partial x^2} \tag{2.11}$$

Where v_L is the velocity of the longitudinal wave through the solid material.

$$v_L = \sqrt{\frac{M}{\rho}} \tag{2.12}$$

Similar to elastic modulus, constrained modulus is the stress strain relationship of a material due to its normal stress and axial strain. The difference is that constrained modulus is for a continuous rod while elastic modulus is for a rod with a fixed boundary. In a lab setting, this is not easy to test, so we must relate the elastic modulus to the constrained modulus using Poisson's ratio:

$$M = \frac{E(1-\nu)}{(1+\nu)(1-2\nu)} \tag{2.13}$$

2.3.2 TORSIONAL WAVE

Torsional waves, or shear waves, involve a rotation about the axis of the rod. This means that the particle motion is perpendicular to the axis instead of along it. Deriving the wave equation of a torsional wave is exactly like deriving the wave equation to that of the longitudinal wave. If σ_i is replaced with a torque, T_i in figure 2.4 then equation 2.5 becomes:

$$T_i + \frac{\partial T}{\partial x} * dx \tag{2.14}$$

Equation 2.14 gives the torque at a point, dx, away from the initial torque, T_i. Similar to deriving the longitudinal wave equation, dynamic equilibrium is also applied for the torsional wave. The external torque applied on the rod has to be equal to the internal rotation of the system.

$$\left(T_i + \frac{\partial T}{\partial x} * dx\right) - T_i = \rho J_z \, dx \, \frac{\partial^2 \theta}{\partial t^2} \tag{2.15}$$

Equation 2.6 and 2.15 are very similar. From mechanics the following equation is true for torque:

$$T = G J_z \frac{\partial \theta}{\partial x} \tag{2.16}$$

In equation 2.16, G is shear modulus, θ is the angle of twist, J_z is the polar moment of inertia, and x is length of the object to which the torque is applied. Like the longitudinal equation, the torsional equation simplifies to:

$$G \frac{\partial^2 \theta}{\partial x^2} = \rho \ \frac{\partial^2 \theta}{\partial t^2} \tag{2.17}$$

The following equation relates shear modulus and density in equation 2.17 to the shear wave velocity through a solid:

$$v_s = \sqrt{\frac{G}{\rho}} \tag{2.18}$$

Plugging in shear wave velocity (v_s) as described in equation 2.18 to equation 2.17 the final derivation:

$$\frac{\partial^2 \theta}{\partial t^2} = v_s^2 \ \frac{\partial^2 \theta}{\partial x^2} \tag{2.19}$$

2.3.3 Rayleigh Waves

Rayleigh waves are acoustic surface waves that occur in solids. They are produced in earthquakes and other dynamic loading making them an interest to geotechnical engineering. Rayleigh waves are unique in that they only travel along the surface of a solid. They can be loosely described as a combination of longitudinal and torsional waves. Figure 2.5 shows how particle displacement begins to occur in a circular motion as the wave extends away from the point of origin. The image below shows the circular motion of a Rayleigh wave as it moves in a planar direction. Rayleigh wave velocity is related to torsional wave by equation 2.20 in which K_{Rs} is the ratio of Rayleigh wave velocity to shear wave velocity.

$$v_R = K_{Rs} v_s \tag{2.20}$$

Equation 2.20 is important because it relates the shear wave, which can easily be tested in a lab, to Rayleigh wave velocity. Another way of finding Rayleigh wave velocity is by the following equation:

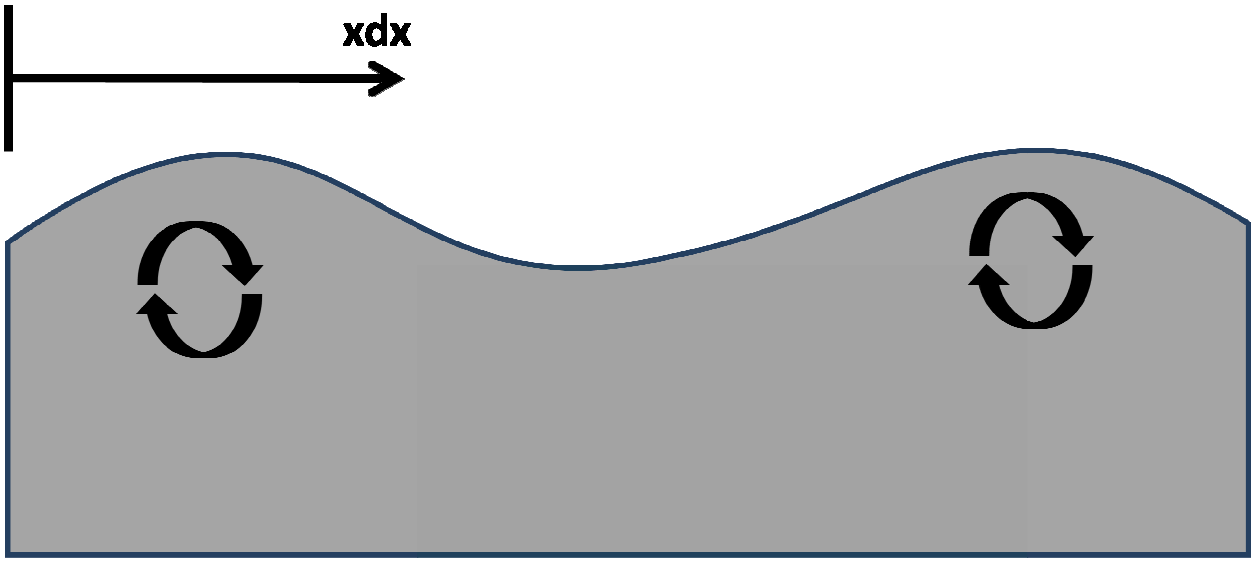

Figure 2.5- Rayleigh Wave

— (2.21)

In the equation above k_R stands for the wave number of Rayleigh waves and ω for the harmonic frequency.

2.4 DAMPING/ATTENUATION

Attenuation of stress waves or damping refers to the fact that the amplitude of stress waves decays as they propagate away from the source through soil. Damping can be described by two mechanisms; material damping and geometric damping. The former is of greater importance to us. Material damping in coarse grained soils occurs because of two mechanisms. The friction caused by soil particles rubbing against each other is the first of these mechanisms. The second which typically happens in saturated soils is the interaction between the fluids (pore water pressure) and the solids. Pore pressure disturbance can cause the fluids to absorb some of the energy transmitted by the wave.

To mathematically explain material damping in soils, the analogy of a viscous damper is used. In viscoelastic wave propagation, soils are modeled using the Kelvin-Voigt model.

$$\tau = G\gamma + \eta \frac{\partial \gamma}{\partial t} \tag{2.22}$$

Equation 2.22 describes the stress strain relationship of the Kelvin-Voigt solid in shear. τ is shear stress, γ is shear strain and η is the viscosity of the material. The first term in equation 2.22 refers to the elastic properties of the material, and the second term is the viscous part of the material. If a harmonic shear strain was applied:

$$\gamma = \gamma_0 \sin \omega t \tag{2.23}$$

Equation 2.22 can be combined with the equation 2.23 resulting in:

$$\tau = G\gamma_0 \sin \omega t + \omega \eta \gamma_0 \cos \omega t \tag{2.24}$$

Equation 2.24 produces an elliptical stress strain loop, the hysteresis loop. The elastic energy dissipated in a single cycle is the area within the ellipse. This is shown mathematically by:

$$\Delta W = \int_{t_0}^{t_0 + 2\pi/\omega} \tau \frac{\partial \gamma}{\partial t} dt = \pi \eta \omega \gamma_0^2 \tag{2.25}$$

Equation 2.25 indicates that the energy dissipated is dependent on the frequency of the loading. As implied above, this is not necessarily true for coarse grained soils because elastic energy can be dissipated through the friction caused between soil particles. However, in moist soils or fine grained soils this relationship is true. As stated above the dynamic loading causes the pore water pressure to fluctuate. This is referred to as “squirting”. Due to the frequency dependent nature of soil-fluid interaction, squirting is a frequency dependent behavior. Using the hysteresis loop the following is true.

$$\xi = \frac{\Delta W}{4\pi W} \tag{2.26}$$

Where W is peak energy stored in a cycle. The area of the triangle in the hysteresis loop is:

$$W = \frac{G\gamma_0^2}{2} \tag{2.27}$$

Material damping then simplifies to:

$$\xi = \frac{\pi\eta\omega\gamma_0^2}{4\pi\frac{G\gamma_0^2}{2}} = \frac{\eta\omega}{2G} \tag{2.28}$$

While material damping absorbs some of the load caused by the stress wave, it does not entirely account for its dissipation. The remaining energy is dissipated through geometric damping. Geometric damping is simple; imagine a stress wave beginning at an epicenter and propagating through the solid in a spherical manner. As the stress wave moves through the material, the energy of the wave never changes yet the area to which the stress is applied continues to grow. Eventually, the stress will spread throughout the media and become small enough to neglect. This is geometric or radiation damping.

2.5 RESONANT COLUMN

A resonant column is tool designed to test soil samples in a non-destructive manner. This makes it effective for measuring soil dynamic properties. The resonant column functions by applying a harmonic cyclic load to a sample. Since this is a low strain test, the samples are barely damaged and can be reused in other laboratory tests. Resonant column testing is based on the theory of wave propagation, in which a cylindrical specimen is subjected to a harmonic axial or torsional load. For this study, only torsional loads were applied.

The properties can be derived by controlling the frequency and amplitude of the torsional load applied to the sample. For this test, a Drnevich Resonant column was used. It consists of a free-fixed specimen setup where the top, or free end, applies the load. This is shown in figure 2.6. The load applied to the top of the specimen creates a torque which can be described by:

$$T = GJ\frac{\partial\theta}{\partial x} = G\frac{I}{\rho}\frac{\partial\theta}{\partial x} \tag{2.29}$$

Equation 2.29 is based on the elastic resistance of the sample. I is the mass moment of the specimen's inertia. In order for our analysis to make sense, the torque on the top of the specimen has to be equal to the torque of the loading system, in other words there should be no loss between the sample and the cap. This coupling between loading system and specimen is important. The torque of the loading system can be described using Newton's second law and changing it for torsion:

$$T = -I_0 l\frac{\partial^2\theta}{\partial t^2} \tag{2.30}$$

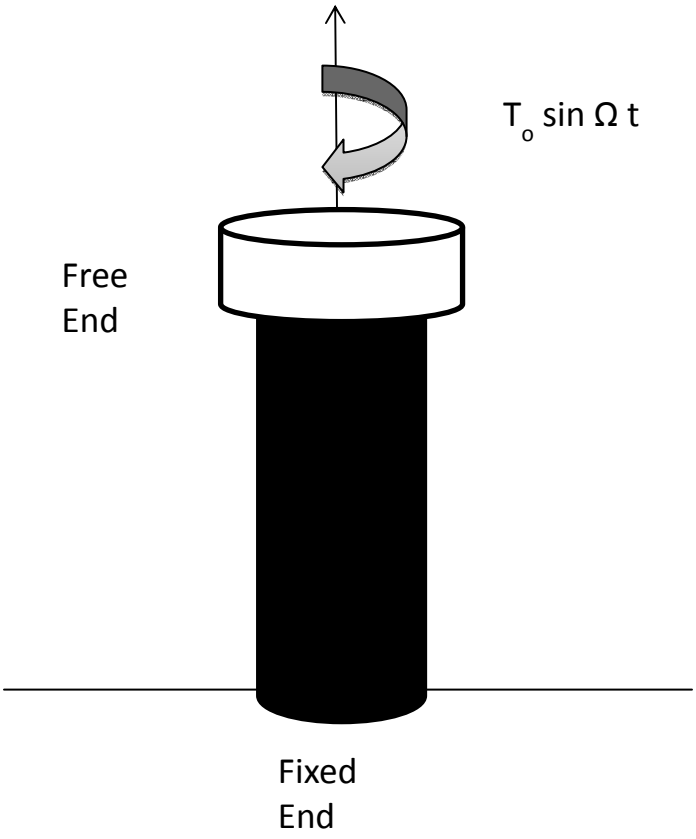

Figure 2.6- Free-Fixed Specimen

Where I_0 is the mass polar moment of inertia for the top loading system, and $\frac{\partial^2\theta}{\partial t^2}$ is the angular acceleration. The rotation applied by the top cap is harmonic. So its rotation can be described by using the following equation:

$$\theta(x,t) = \Theta(x)(C_1 \cos\omega t + C_2 \sin\omega t) \tag{2.31}$$

$\Theta(x)$is the shape function for the sample harmonic torsion.

$$\Theta(x) = C_3 \cos kx + C_4 \sin kx \tag{2.32}$$

The bottom of the specimen is fixed thereby making the rotational boundary condition of the bottom zero. The bottom is taken to be our starting point (z=0) in order to drop out the C_3=0 term. Setting the torsion of the sample's top (2.29) and the loading system (2.30) equal to each other and inserting equation 2.31 for the rotation into both produces the following equation:

$$G\frac{I}{\rho}\frac{\partial\theta}{\partial x} = -I_0 l \frac{\partial^2\theta}{\partial t^2} \tag{2.33}$$

$$G\frac{I}{\rho}C_4 k \cos kz\,(C_1 \cos\omega t + C_2 \sin\omega t) = I_0 l(C_4 \sin kx)\omega^2\,(C_1 \cos\omega t + C_2 \sin\omega t) \tag{2.34}$$

This equation is then solved for ω at the fundamental or natural frequency, $\omega_n = k_n v_s$. Equation 2.34 then simplifies to:

$$\frac{I}{I_0} = \frac{\omega_n l}{v_s} \tan \frac{\omega_n l}{v_s} \tag{2.35}$$

In 2.35, three of the variables are known (I, I_0, l), the other, ω_n, is found experimentally through the resonant column. v_s can be found using equation 2.35. v_s is then related to shear modulus using equation 2.18.

Chapter 3 : LABORATORY TESTING

Dynamic soil properties can be determined in both lab and in-situ settings. Tests such as the Seismic Cross-Hole and Seismic Cone measure shear wave velocity in geologic material. Data from the Cone Penetration Test (CPT) and Standard Penetration Test (STP) can be empirically related to values such as shear modulus. For the RP clay these methods are not required, because the application of the test is experimental.

Lab tests are divided into two groups. The first group consists of low strain tests. These tests include resonant column, ultrasonic pulse test, and the piezoelectric bender element test. Tests such as these provide the low strain properties of the geologic material and the elastic properties of the soil. The second group is comprised of high strain tests. These consist of the cyclic shear test and cyclic torsional test. As implied by category, these tests apply higher strains on the samples which typically result in an increase in porewater pressure. For these tests it is important to monitor the volumetric strain in drained conditions and the increase in porewater pressure in undrained conditions. In low strain tests, this is not required because the loads applied are low and are not enough to induce a significant increase in porewater pressure.

3.1 RESONANT COLUMN EQUIPMENT

Tests were conducted on a Drnevich Resonant column. The equipment was purchased from Soil Dynamics Inc. It consisted of a fixed-free experimental setup used for cylindrical specimens, as shown in figure 2.6. The top (free-end) provides a torque on the top of the cylindrical specimen. The dynamic soil properties can be accurately derived with appropriate coupling between the top of the sample and the loading system. The resonant column allows for

several diameter samples. The various setups include a 35.7mm, a 71mm, or a specimen with a 71 mm outside diameter and 35.7 mm inside diameter (i.e. hollow sample). The setup used for our experiment was the 71 mm. The schematic of the resonant column is show in figure 3.1.

3.1.1 TORSIONAL DRIVE COILS AND MAGNET

In figure 3.1 and 3.2, the torsional drive coils are attached to the coil support brackets. Each of the four coils is numbered. The numbers correspond to the support brackets. The drive coils slide on the support brackets and are fastened in place. Care needs to be taken when fastening the coils because they damage easily. In figure 3.1, the torsional drive coils fit right next to the torsional magnet. Figure 3.2, shows clearly how the magnet and drive coil fit together. The magnet fits inside of the gap in the torsional drive coils. The separation between the magnet and the drive coils should be uniform in all four which may require some adjusting to the torsional drives.

The torsional magnet is actually part of the top platen system. The top platen system sits on top of the specimen and delivers the torsion on the specimen. So, the torsional magnet and the drive coils provide torsional excitation to the specimen. The shear strain amplitude produced can be controlled by varying the amplitude of the voltage delivered to the drive coils.

3.1.2 LONGITUDINAL DRIVE COILS AND MAGNET

Figure 3.1, also shows the placement of the longitudinal drive coil as well as that of the longitudinal magnet. The longitudinal drive coil is located above the top platen system. The longitudinal magnet is large and fits over the drive coil. Similar to the torsional drive coils and magnet, the longitudinal drive coil and magnet provided a compression wave in the specimen.

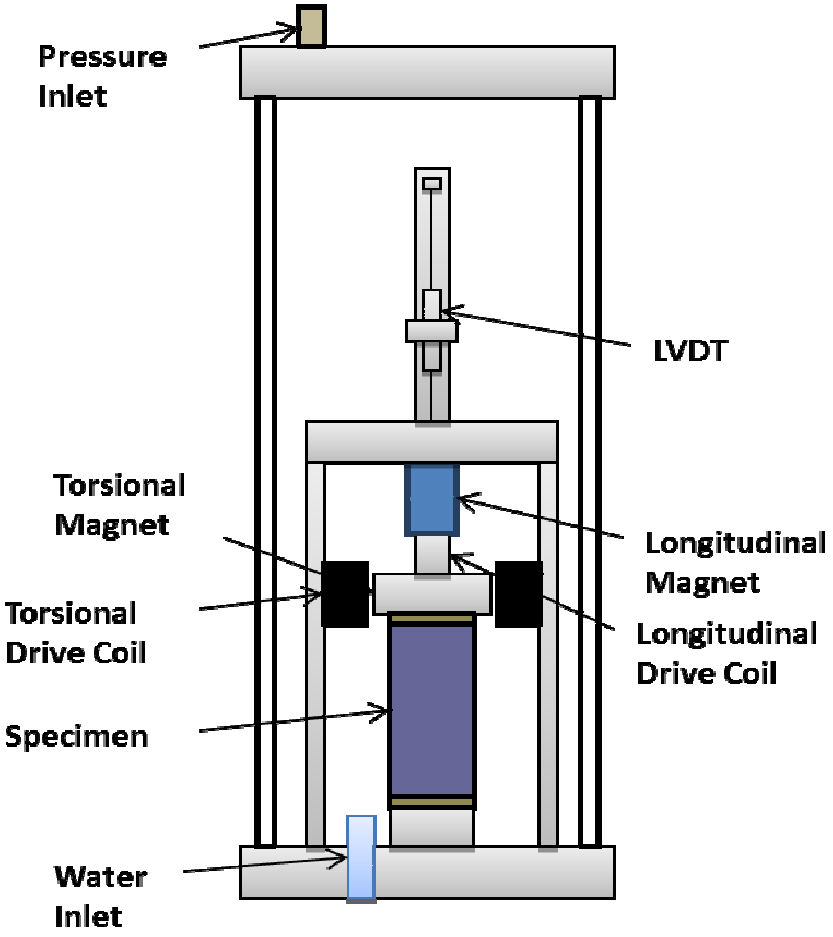

Figure 3.1-Schematic of Resonant Column

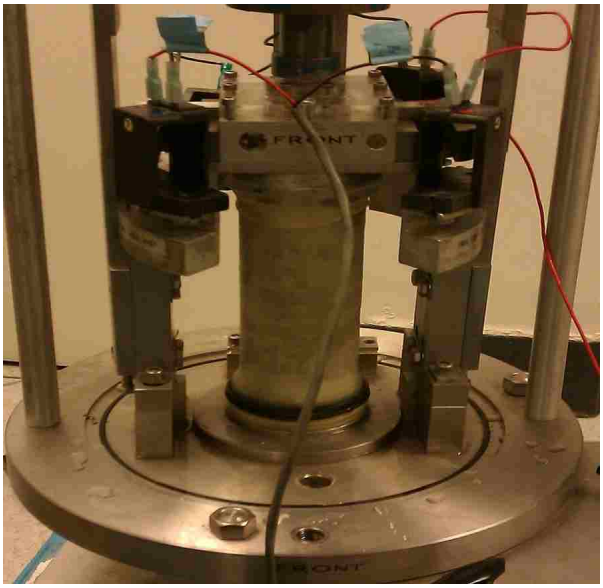

Figure 3.2- Sample Setup

Note that the longitudinal magnet and coil are not shown in figure 3.2. This is because the setup was only for torsional excitation, the focus of this study.

3.1.3 TOP PLATEN SYSTEM

The top platen system provides the stress wave in the sample. It consists of two accelerometers, torsional magnets, longitudinal drive coils, top platen and porous stones. The top platen is different from the top platen system. The top platen system is the entire system. The top platen, on the other hand, is the removable piece that corresponds to the type or size of the specimen that is being tested. Placement of the accelerometers is shown in figure 3.5. The accelerometers are Colombia Research Laboratories, Inc. model 200-1-H. Their purpose is to measure the reflected wave response. Each accelerometer corresponds to one mode of displacements, torsional or longitudinal. The LVDT is a Scheavitz model; it is connected to the top platen system in figure 3.4. The LVDT measures longitudinal displacement and is accurate to within 0.01 mm.

3.1.4 BOTTOM PLATEN SETUP

The base supporting the sample is rigidly fixed to maintain the fixed conditions necessary for the assumption of wave propagation. The bottom platen has a porous stone that allows for drainage. Additionally the bottom platen has inlets for vacuum, water and a pressure transducer (measures porewater pressure). It is important to note that the chamber is not to be filled entirely. The porewater transducer is a P SI-Tronix, Inc. Model LC-0100-G11-111. The transducer is located under the specimen. The porewater pressure was not measured because the material in question was comprised of oil based clay.

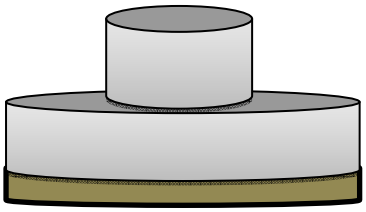

Figure 3.3- Top Platen

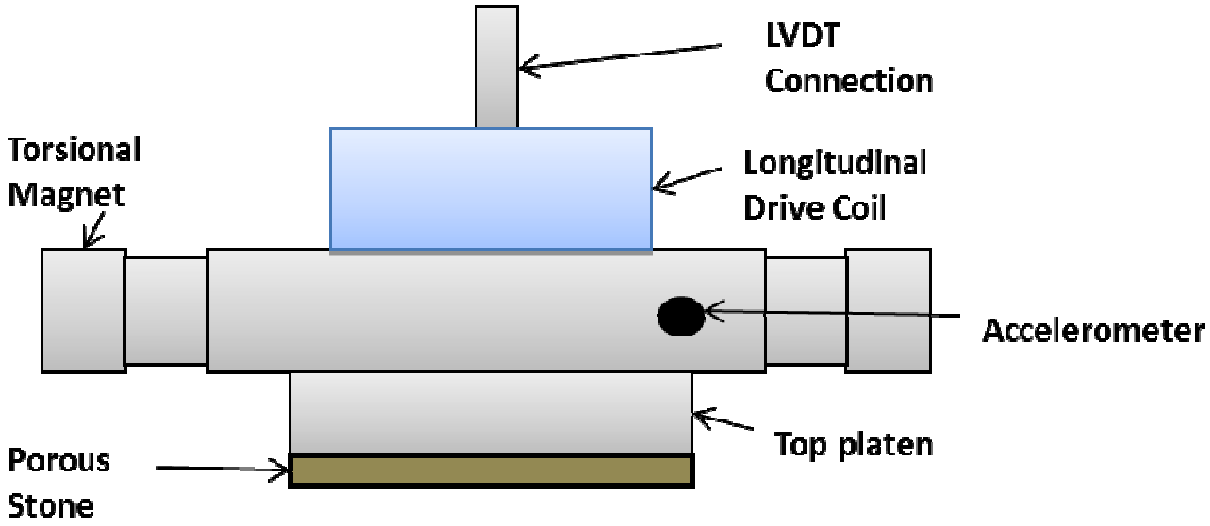

Figure 3.4- Top Platen System Side View

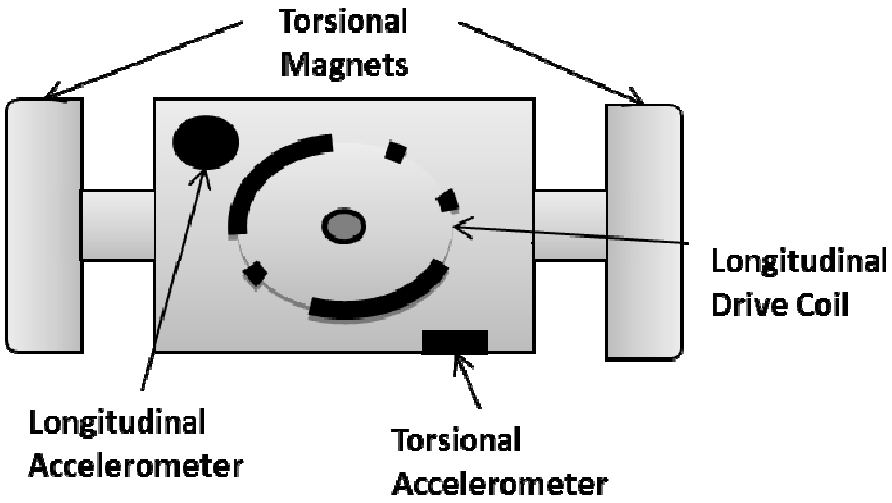

Figure 3.5- Top Platen System Top View

3.1.5 OTHER

The chamber that surrounds the sample is an acrylic tube. Silicon jell is carefully placed around the ends of the tube in order to prevent pressure from escaping the chamber. Also, the top is sealed off with metal chamber lid. The lid provides connections for the LVDT, accelerometers, drive coils. It also supplies an inlet from which to apply pressure to the specimen. The chamber allows for pressures up to 700 kPa (100 psi). The building pressure had a limit of 175 kPa (25 psi).

3.2 ELECTRICAL EQUIPMENT/AUXILIARY EQUIPMENT

Besides the resonant column, there are other external apparatuses that help in collecting data, applying shear strain, and controlling both the shear strain amplitude and the frequency of the excitation applied to the sample. The Drnevich resonant column comes with a control box, which is constructed by Soil Dynamics Inc. The control box serves as the router for the electronics. It also provides a control for the modes of excitation, either torsional or longitudinal. The connections are shown in the wiring schematic (figure 3.6). It is important to note that the switch box in the image is actually incorporated in the Drnevich control box. The switch box is the part of the control box that allows us to switch from torsional to longitudinal excitations and controls what voltage reading is displayed on the Digital Multimeter, Fluke 8010A (Digital Voltmeter). By setting the switch, the voltmeter can display either the accelerometer reading (output) or the power delivered to the drive coils (input). The power supply amplifier is a Techron Model 5507. It has two channels available. For this setup, channel one is used for longitudinal excitation, and channel two for torsional excitation.

A function generator is used to control the frequency of the excitation and the type of wave used for the signal. Two BK Precision 3011B 2MHz function generators are used. One function generator controls the torsional excitations and the other the longitudinal excitations. The function generator is capable of creating square, triangular, and sinusoidal waves. Typically, tests are conducted using a sinusoidal signal. The accuracy of the frequency can be recorded up to 0.1 Hertz.

The function generator and the power amplifier deal with the input signal. The output signals (accelerometer readings) must be amplified to be used. This is done with two Columbia Research Laboratories, Inc. Model 4102 charge amplifiers. The final piece of equipment is the

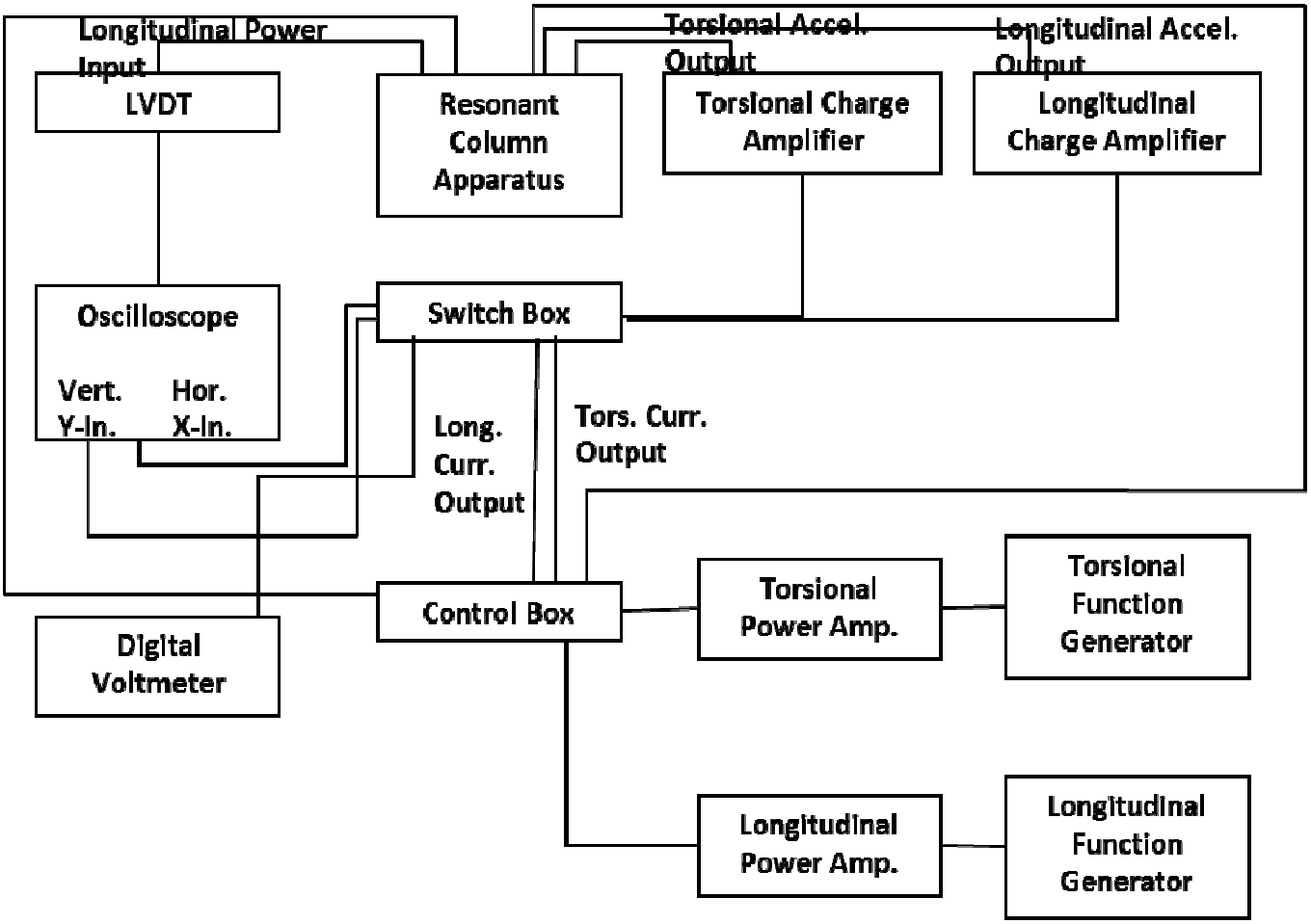

Figure 3.6-Wiring Schematic

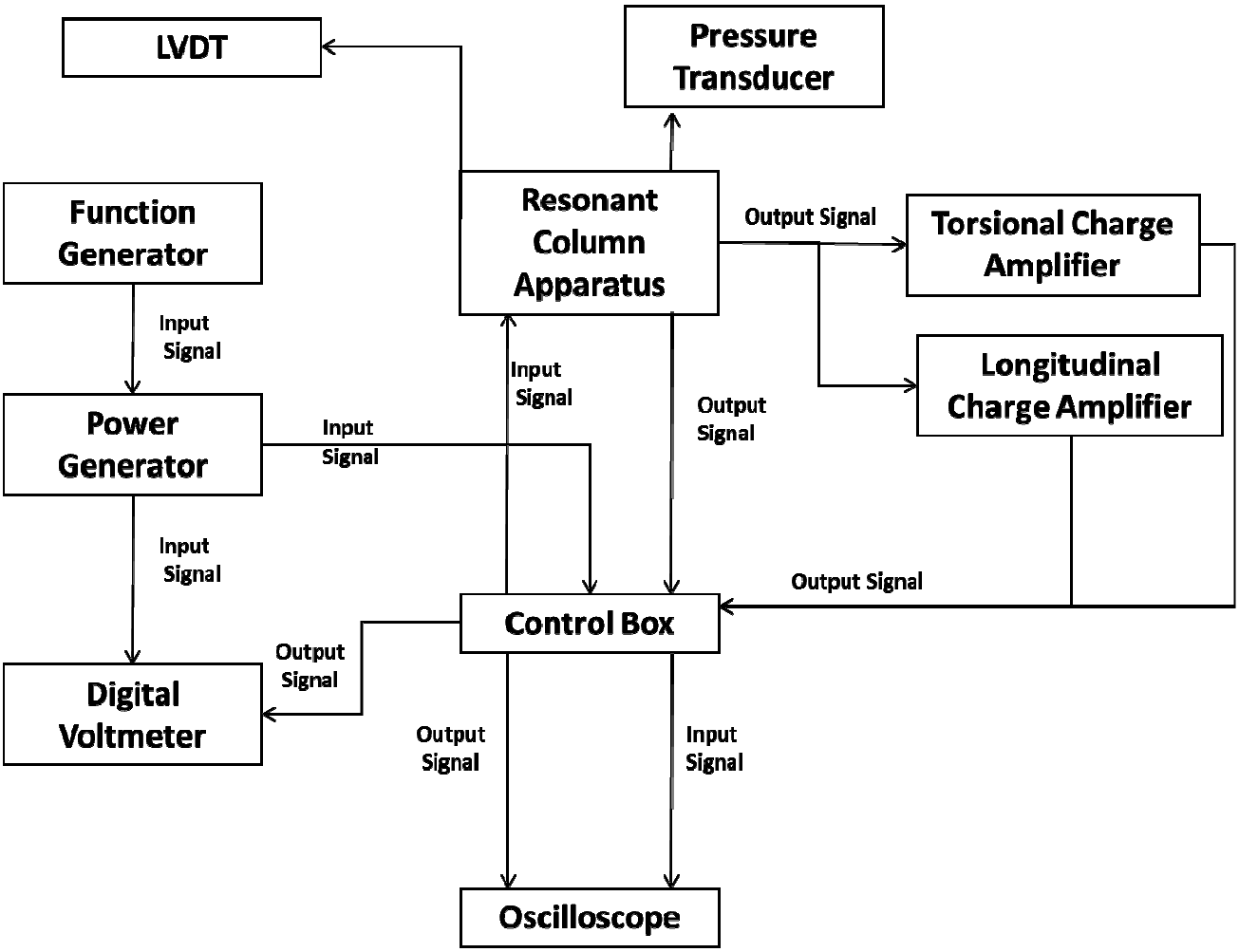

Figure 3.7-Consolidated Wiring Schematic

oscilloscope. The one used in this setup is a Hameg HM 205-3. Both the input and output are displayed on the oscilloscope. The oscilloscope shows the signal in both time domain and X-Y mode. Channel one of the oscilloscopes displays the output signal and channel two displays the input signal.

Chapter 4 : DATA ANALYSIS AND INTERPRETATION

The auxiliary equipment assists in collecting and attaining data from the resonant column apparatus. The data needs to be converted into more understandable values. Several sources provide guidelines for data reduction (ASTM D4015, Drnevich, Hardin, & Shippy, 1978, Hardin & Drnevich, 1972). The results of the data reduction are fitted using predictive equations and comparisons are drawn.

4.1 DATA REDUCTION

Several preliminary measurements need to be taken prior to running the test. As previously stated, cylindrical samples are used for testing. Typically, the length of the sample should be about twice its diameter. There is some leeway for this but the sample should not be used if its length is less than 1.5 the diameter. Since physical properties like density (ρ) are used to determine constants for the data reduction, accurate measurements need to be taken prior to testing. Before every test the diameter (d), length (l), and Mass (m) are taken. Metric units are used in data reduction equations (meters and Kg).

$$V = 2\pi \frac{d^2}{4} l \tag{4.1}$$

To determine the constants used to arrive at shear modulus and damping, physical properties are used. The properties that need to be calculated are volume (V, equation 4.1), density, and the rotational mass polar moment of inertia (J_s). The equations for density and rotational mass polar moment of inertia are provided below:

$$\rho = \frac{m}{V} \tag{4.2}$$

$$J_s = \frac{md^2}{8} \tag{4.3}$$

J_s is used to calculate the active-end inertial factor for torsional excitation.

$$T_T = \frac{J_A}{J_s} \tag{4.4}$$

T_T denotes the active-end inertial factor for torsional excitation. The other variable, J_A, is the top platen's rotational mass moment of inertia. J_A is typically calculated experimentally ($J_A = 0.003\ kg/m^2$) with the use of a calibration rod with known material properties. This process is shown in appendix A.1. The rotational apparatus damping factor, ADF_T, is calculated as:

$$ADF_T = \frac{ADC_{0T}}{2\pi f_T J_s} \tag{4.5}$$

ADC_{0T}, a system constant, is calculated during the calibration process. This is shown in appendix A.3. The value used for the apparatus damping coefficient, ADC_{0T}, was $0.004\ kg - m^2/sec$. The other value, f_T, is the resonant frequency for torsion of the test at that strain amplitude. Shear modulus can be determined using the following equation:

$$G = \rho(2\pi l)^2 \left(\frac{f_T}{F_T}\right)^2 \tag{4.6}$$

Resonant frequency for torsion is determined during the test by plotting the input signal vs. output signal on the oscilloscope, in other words the X-Y mode of the oscilloscope. The frequency on the function generator is increased until a clear circle is shown in the X-Y mode of

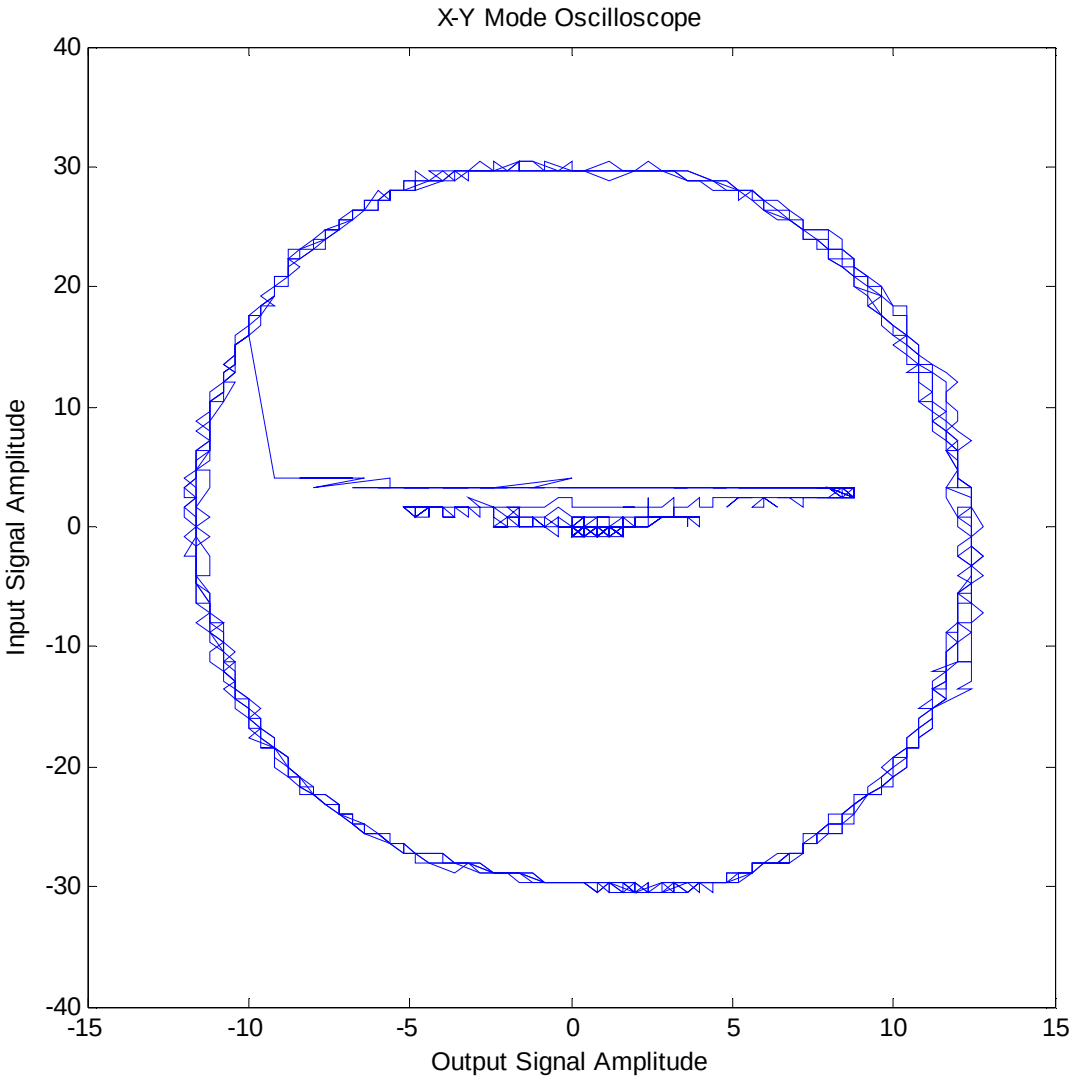

Figure 4.1- Circle shows 180 Phase between input and output signal

the oscilloscope. This is shown in figure 4.1. The image in figure 4.1 is circular meaning that the input and output signals are 180° phase. When the signal is in 180° phase the corresponding frequency is taken to be the resonant frequency. F_T is the dimensionless frequency factor found using figure 4.2. The frequency factor is a function of T_T, which is the ratio of the polar mass moment of inertia of top platen to the sample. It is important to note that in figure 4.2, ADF_T is assumed to be zero and damping is less than 10 %. Since ADF_T is typically rather small the assumption is justified and damping typically stayed below 10%. The next important parameter that needed to be calculated was shear strain amplitude, γ:

$$\gamma = \left(0.4\ \frac{d}{l}\right)(RCF)(RTO) \tag{4.7}$$

RCF is the rotational motion transducer calibration factor. It is dependent on the calibration of the accelerometer.

$$RCF = \frac{acceleration\ calibration\ factor}{2\pi f_T} \tag{4.8}$$

The acceleration calibration factor is a constant found during calibration. The Columbia Research Laboratory found the calibration of the accelerometers to be 28.1. RCF is given the following units Pk-rad/$Volt_{RMS}$. RTO is the output reading from the resonant column apparatus or the accelerometer reading.

Torsional magnification factor, $MMF_{T,}$ is necessary in order to determine damping ratio and is defined as follows:

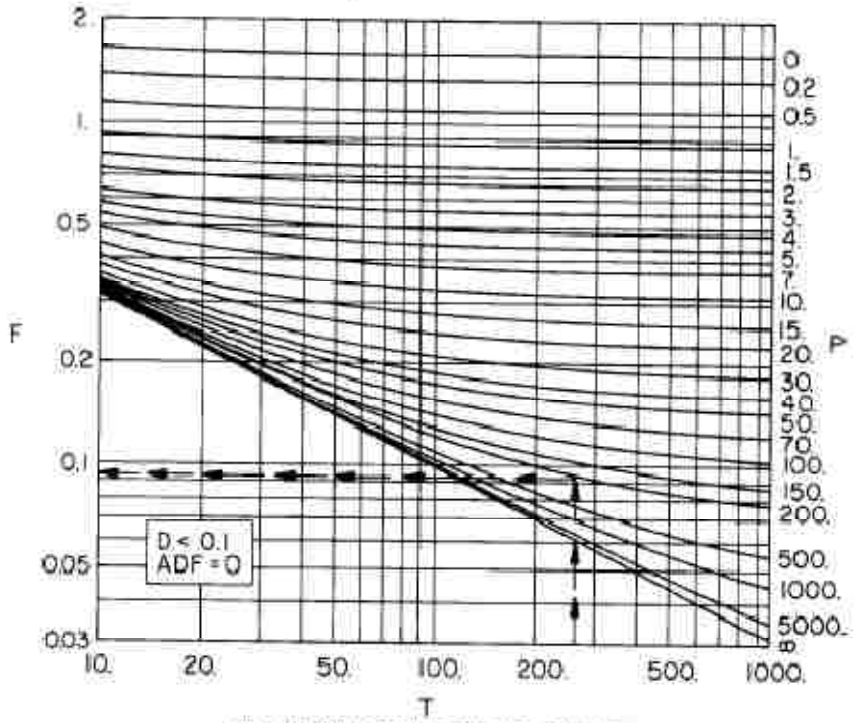

FIG. 2 (a) Dimensionless Frequency Factors[2]

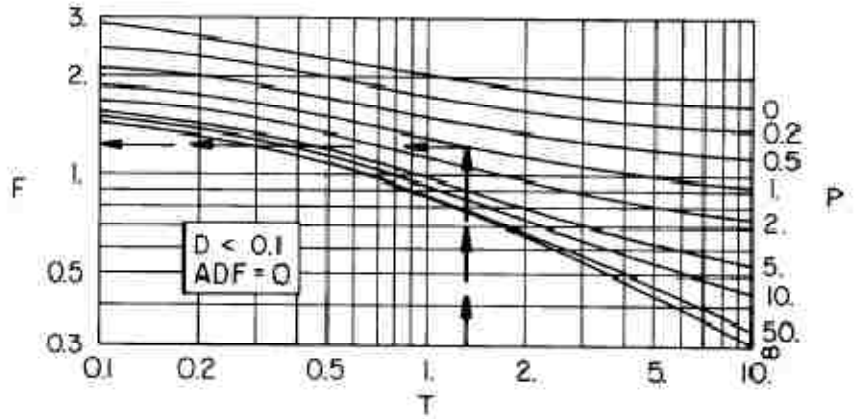

FIG. 2 (b) Dimensionless Frequency Factors[2] *(continued)*

Figure 4.2- Dimensionless Frequency Factor Graph from ASTM D4015

$$MMF_T = \frac{(RCF)(RTO)J_s(2\pi f_T)^2}{(TCF)CR_T} \tag{4.9}$$

CR_T being the measured voltage associated with the current to the torsional drive coils (input to resonant column system). TCF is the torque calibration factor and is determined during calibration shown in Appendix A.2. Damping ratio, ξ, is computed by:

$$\xi = \frac{1}{A(MMF_T)} \tag{4.10}$$

A is the amplification coefficient found in figure 4.3. Like the dimensionless frequency factor it is also a function of T_T.

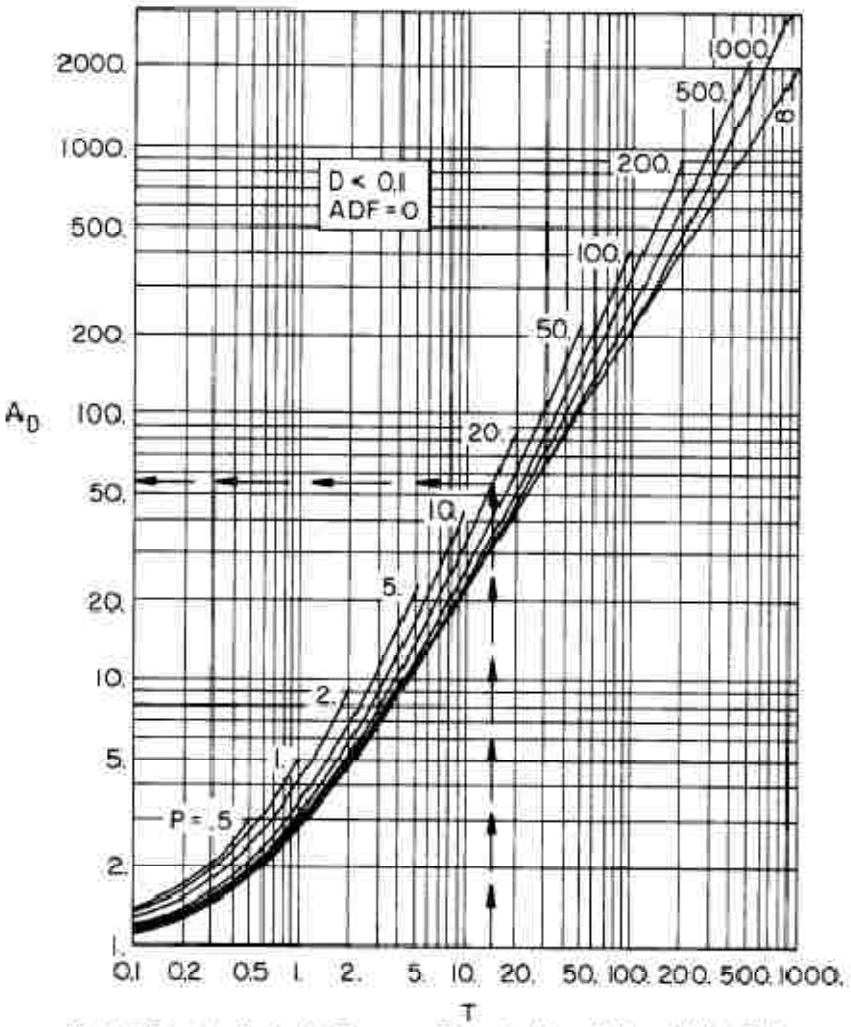

FIG. 4 (a) Damping Factors for Resonance Determined from Motion at Active End*

Figure 4.3- Amplification Coefficient based on the Dimensionless Frequency Factor from ASTM D4015

4.2 CURVE FITTING

In processing resonant column data it is common practice to fit the normalized shear modulus with the hyperbolic model that predicts the reduction of modulus as a function of strain. Using the low strain data collected, shear modulus can be predicted for larger strains. Additionally, allows us to compare trends of different soils or samples. The factors or trends of the reduction of normalized shear modulus in soils have been heavily researched (Hardin and Drnevich 1972, Stokoe 1999, Zhang 2005).

When interpreting resonant column results many issues arise. Most issues arise from the variability of the soil properties. The clay used removes some of these issues because it is almost completely homogeneous. Other issues, such as Plasticity index, can be ignored. The main concerns when testing RP clay were temperature monitoring, and sample preparation. Temperature, as originally stated, caused the clay to become more malleable, as did remolding. In order, to simplify the results, they are separated by confining stress, temperature, and preparation method.

4.2.1 Reference Strain (γ_r):

Hardin and Drnevich stressed the importance of normalizing the strain. In most analysis this step is ignored as strain is an already dimensionless parameter. Hardin and Drnevich define their reference strain,γ_r as:

$$\gamma_r = \frac{\tau_{max}}{G_{max}} \tag{4.11}$$

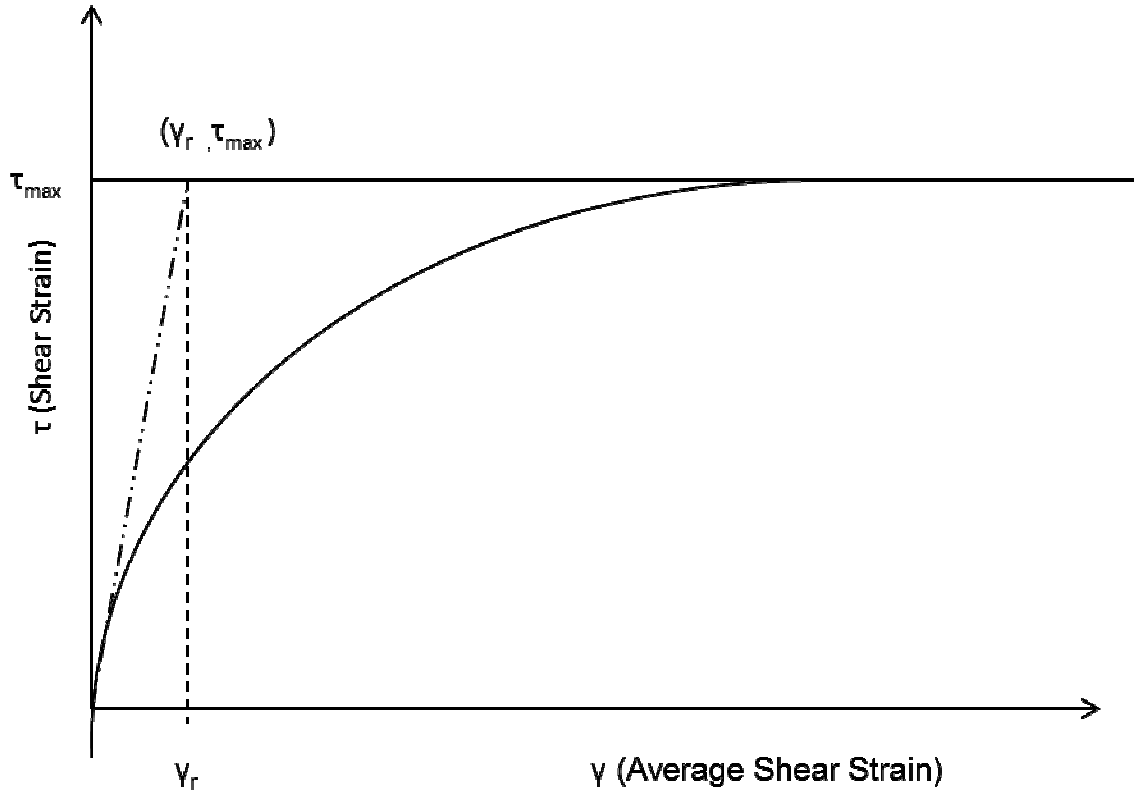

Figure 4.4- Shear Stress-Strain Graph (Hardin & Drnevich, 1972)

Reference strain is the point where a line with a slope of extends from the origin and intercepts the maximum shear stress, . This is clearly shown in figure 4.4. Stokoe's concept of reference strain was different. In Stokoe's approach the static value, does not need to be found. Stokoe defines his as the point when—— . Ours —— remains greater than 0.5 so applying Stokoe methodology was simply not possible.

Both and , can be determined experimentally. Though, not both can be found using the resonant column. can be determined using a traditional undrained triaxial shear test. values can be found using the resonant column test.

4.2.2 NORMALIZED SHEAR MODULUS

Fitting normalized shear modulus with hyperbolic curves is an effective tool for interpreting the stress strain relationship of the RP clay. It also helps to predict the behavior of the soil after its initial elastic range at low strains. Once the reference strain, as defined by Hardin and Drnevich, is found one can proceed interpreting the data. The basic hyperbolic stress strain relationship is as follows:

$$\tau = \frac{\gamma}{\frac{1}{G_{max}} + \frac{1}{\tau_{max}}} \tag{4.12}$$

Equation 4.12 gives what is typically referred to as the backbone curve. The backbone curve is the stress curve of the soil. Using the shear modulus relationship, $G = \tau/\gamma$, in equation 4.12 a normalized relationship can be expressed.

$$\frac{G}{G_{max}} = \frac{1}{1+\frac{\gamma}{\gamma_r}} \tag{4.13}$$

Equation 4.13 is only true if the stress strain relationship is hyperbolic. Typically this is not the case. Therefore, the relationship needs to be modified in order to account for the variability. For this Hardin and Drnevich introduced hyperbolic strain,γ_h. Hyperbolic strain distorts the strain scale in order to accurately fit data. Hyperbolic strain is given:

$$\gamma_h = \frac{\gamma}{\gamma_r}\left[1 + a\, e^{-b\left(\frac{\gamma}{\gamma_r}\right)}\right] \tag{4.14}$$

Hyperbolic strain incorporates two constants, a and b, that modify the normalized strain in order to get a more accurate fit. Hyperbolic strain is used in equation 4.13 to replace the reference strain ratio, $\frac{\gamma}{\gamma_r}$:

$$\frac{G}{G_{max}} = \frac{1}{1+\gamma_h} \tag{4.15}$$

4.2.3 DAMPING FIT

Once the coefficients for hyperbolic strain are defined similar relationships can be used to predict damping in soils. Normalized damping is described as follows:

$$\frac{\xi}{\xi_{max}} = \frac{\gamma_h}{1+\gamma_h} \tag{4.16}$$

Equations 4.15 and 4.16 are very similar. Equation 4.16 relates the constants found in the previous section to damping. Basically, equation 4.16 is the same as $1 - {}^{G}/_{G_{max}}$. This relationship is convenient and gives a clear hyperbolic curve. The only issue is that ξ_{max} is found using empirical correlations. Since there is no data existing for the synthetic oil based clay, ξ_{max} remained undefined.

Stokoe used another method for determining the relationship between normalized shear modulus and damping ratio (Stokoe, Darendeli, Gilbert, Meng, & Choi, 2004). Instead of fitting a hyperbolic equation to damping data using ξ_{max} he established a fit that incorporated ξ_{min} instead. The advantage was that ξ_{min} can be determined during resonant column test.

$$\xi = f\left({}^{G}/_{G_{max}}\right) + \xi_{min} \tag{4.17}$$

Zhang (Zhang, Andrus, & Juang, 2005) further modifies this approach by subtracting ξ_{min} from the other damping ratio:

$$\xi - \xi_{min} = f\left(G/G_{max}\right) \tag{4.18}$$

Typically, $f\left(G/G_{max}\right)$ can be defined using a quadratic equation. Like the one below:

$$\xi - \xi_{min} = A\left(G/G_{max}\right)^2 + B\left(G/G_{max}\right) + C \tag{4.19}$$

4.3 DRUCKER-PRAGER CAP MODEL

Currently the dynamic impact of the ballistic impact is modeled using Drucker-Prager yield criterion. Drucker-Prager a constitutive model for the behavior of geotechnical material is widely used in finite element stress analysis. Drucker-Prager provides a mathematical model of the behavior of granular or frictional material. The model is an elastic-perfectly plastic model (bilinear relationship). The yield surface on the model is dependent on the hydrostatic pressure and the associated flow rule. Hydrostatic pressure is in turn highly dependent on volumetric strain. For our purpose, Drucker-Prager with cap (hardening) is used instead of without hardening. The difference is that the cap model includes a second yield function or surface that closes the cone in the principal stress space. The cap better simulates the hardening (softening in soils) in the numerical model.

It is important to compare the resonant column results to the results of the finite element or numerical solution. In this section the stress matrix using Drucker-Prager criteria is reduced to its one dimensional equation. By deriving the one dimensional stress strain relationship a comparison of the predicted shear modulus values of the numerical solution to the predictive equations developed by Hardin and Drnevich can be drawn.

4.3.1 GENERAL THEORY PLASTICITY

Drucker-Prager is a plasticity model that provides an inviscid relationship between stress rate, $d\sigma_{ij}$, and strain rate, $d\varepsilon_{ij}$. For multiaxial loading, general strain rate can be decomposed into its elastic and plastic components:

$$d\varepsilon_{ij} = d\varepsilon_{ij}^{e} + d\varepsilon_{ij}^{p} \tag{4.20}$$

ε_{ij}^{e} is the elastic component of strain and ε_{ij}^{p} is the plastic component. Assuming that the elastic behavior is isotropic, the elastic strain can be defined by:

$$d\varepsilon_{ij}^{e} = \frac{1}{2G} dS_{ij} \tag{4.21}$$

S_{ij} is the deviatoric stress component and is defined by the following equation:

$$S_{ij} = \sigma_{ij} - \frac{\sigma_{kk}}{3}\delta_{ij}$$

The plastic strain increment or plastic strain rate is given by the associated flow laws for the active yield surface:

$$d\varepsilon_{ij}^{p} = d\lambda \frac{\partial f}{\partial \sigma_{ij}} \tag{4.22}$$

f in equation 4.22 is the function that describes the yield surface and $d\lambda$ is the plastic non-negative multiplier, with

$$d\lambda \begin{cases} = 0 \; when \; f < 0 \; of \; f = 0 \; but \; df < 0 \\ > 0 \; when \; f = 0 \; and \; df = 0 \end{cases}$$

Using Hooke's law for the strain rate:

$$d\sigma_{ij} = C_{ijkl}\left(d\varepsilon_{kl} - d\varepsilon_{kl}^{p}\right) = C_{ijkl} d\varepsilon_{kl} - d\lambda C_{ijkl} \frac{\partial f}{\partial \sigma_{kl}} \tag{4.23}$$

$C_{ijkl}$is the stiffness or elastic modulus tensor. In isotropic media the stiffness tensor relates the resulting internal stresses with the resulting strains or deformation. The stiffness tensor is given by:

$$C_{ijkl} = K\delta_{ij}\delta_{kl} + G(\delta_{ik}\delta_{jl} + \delta_{il}\delta_{jk} - \frac{2}{3}\delta_{ij}\delta_{kl}) \quad (4.24)$$

K is the bulk modulus of the material and G is shear modulus. The other term introduced here is the Kronecker delta (δ_{ij}). Plugging equation 4.24 into the previous equation 4.23 gives:

$$d\sigma_{ij} = 2Gd\varepsilon_{ij} + Kd\varepsilon_{kk}\delta_{ij} - d\lambda\left[\left(K - \frac{2}{3}G\right)\frac{\partial f}{\partial \sigma_{mn}}\delta_{mn}\delta_{ij} + 2G\frac{\partial f}{\partial \sigma_{kl}}\right] \quad (4.25)$$

The above gives change of stress as a function of shear and bulk modulus.

4.3.2 YIELD SURFACE FOR DRUCKER PRAGER WITH CAP

Chapter 5 Now that the stress rate is defined in terms of shear modulus and bulk modulus the yield function needs to be derived for the Drucker-Prager cap model. The yield function in a Drucker-Prager cap model is a $f(\sigma_{ij}, \varepsilon_{ij}^{p}, k)$=0. The constant k is defined by:

$$k = \frac{3c\cos\varphi}{\sqrt{3}(3-sin\,\varphi)} \quad (4.26)$$

c and φ are the cohesion and the friction angle of the material that is being used respectively. These values are easily be determined using a triaxial test. The consistency condition is assumed to be:

$$df = \frac{\partial f}{\partial \sigma_{ij}}d\sigma_{ij} + \frac{\partial f}{\partial \varepsilon_{ij}^{p}}d\varepsilon_{ij}^{p} + \frac{\partial f}{\partial k}dk = 0 \quad (4.27)$$

This ensures the plastic process and that the stress and strain remain on the yield surface. The general form for the yield function for isotropic hardening in Drucker-Prager is:

$$f(\sigma_{ij}, \varepsilon_p) = \alpha(\varepsilon_p) I_1 + \sqrt{J_2} - k(\varepsilon_p) = 0 \tag{4.28}$$

Equation 4.28 is a function of stress and ε_p, uniaxial effective strain. The constant α can also be defined using triaxial test results by the following equation:

$$\alpha = \frac{2 \sin \varphi}{\sqrt{3}(3 - \sin \varphi)} \tag{4.29}$$

For simplicity, assume that the loading surface ($I_1 - \sqrt{J_2}$) is constant, $\alpha(\varepsilon_p) = \alpha$. This allows us to assume the hardening behavior of the material to be dependent on the single uniaxial stress-strain relation through the hardening parameter k,

$$f(\sigma_{ij}, \varepsilon_p) = \alpha I_1 + \sqrt{J_2} - k(\varepsilon_p) = 0 \tag{4.30}$$

To derive the Drucker-Prager isotropic-hardening elastic-plastic constitutive relationship one must find the increment for isotropic hardening, dk:

$$dk = \frac{dk}{d\varepsilon_p} d\varepsilon_p \tag{4.31}$$

This is obtained from equation 4.30. The following equation gives the increment of uniaxial effective strain in terms of C:

$$d\varepsilon_p = C \sqrt{d\varepsilon_{ij}^p d\varepsilon_{ij}^p} \tag{4.32}$$

Combining the above equation with equation 4.31 it can be simplified to:

$$dk = \frac{dk}{d\varepsilon_p} C \sqrt{d d\varepsilon_{ij}^p d\varepsilon_{ij}^p} \tag{4.33}$$

Applying the associated flow laws from equation 4.22 it can further be simplified to:

$$dk = \frac{dk}{d\varepsilon_p} C \sqrt{\frac{\partial f}{\partial \sigma_{ij}} \frac{\partial f}{\partial \sigma_{ij}}} d\lambda \tag{4.34}$$

Combining equation 4.34 with the consistency equation (4.27) reduces the later to:

$$df = \frac{\partial f}{\partial \sigma_{ij}} \left(C_{ijkl} d\varepsilon_{kl} - d\lambda C_{ijkl} \frac{\partial f}{\partial \sigma_{kl}} \right) + \frac{\partial f}{\partial \varepsilon_{ij}^{p}} d\lambda \frac{\partial f}{\partial \sigma_{ij}} + \frac{\partial f}{\partial k} \frac{dk}{d\varepsilon_p} C \sqrt{\frac{\partial f}{\partial \sigma_{ij}} \frac{\partial f}{\partial \sigma_{ij}}} d\lambda = 0$$

$$df = \frac{\partial f}{\partial \sigma_{ij}} C_{ijkl} d\varepsilon_{kl} - d\lambda \left(\frac{\partial f}{\partial \sigma_{ij}} C_{ijkl} \frac{\partial f}{\partial \sigma_{kl}} - \frac{\partial f}{\partial \varepsilon_{ij}^{p}} \frac{\partial f}{\partial \sigma_{ij}} - \frac{\partial f}{\partial k} \frac{dk}{d\varepsilon_p} C \sqrt{\frac{\partial f}{\partial \sigma_{ij}} \frac{\partial f}{\partial \sigma_{ij}}} \right) = 0 \tag{4.35}$$

The part of 4.35 that is within the parenthesis is represented by the scalar function, h, for simplicity:

$$h = \frac{\partial f}{\partial \sigma_{ij}} C_{ijkl} \frac{\partial f}{\partial \sigma_{kl}} - \frac{\partial f}{\partial \varepsilon_{ij}^{p}} \frac{\partial f}{\partial \sigma_{ij}} - \frac{\partial f}{\partial k} \frac{dk}{d\varepsilon_p} C \sqrt{\frac{\partial f}{\partial \sigma_{ij}} \frac{\partial f}{\partial \sigma_{ij}}} \tag{4.36}$$

Solving equation 4.35 for the scalar function, $d\lambda$, gives:

$$d\lambda = \frac{\frac{\partial f}{\partial \sigma_{ij}} C_{ijkl} d\varepsilon_{kl}}{h} = \frac{H_{kl} d\varepsilon_{kl}}{h} \tag{4.37}$$

H_{kl} is a second order tensor that is associated with the yield function and is defined as:

$$H_{kl} = \frac{\partial f}{\partial \sigma_{ij}} C_{ijkl} \tag{4.38}$$

Taking the derivative of the Drucker-Prager yield function from above with respect to σ_{ij} gives:

$$\frac{\partial f}{\partial \sigma_{ij}} = \alpha \delta_{ij} + \frac{1}{2\sqrt{J_2}} S_{ij} \tag{4.39}$$

Equation 4.39 is combined with the second order tensor from equation 4.38 and 4.24 to the second order tensor in terms of G and K:

$$H_{kl} = \frac{\partial f}{\partial \sigma_{ij}} C_{ijkl} = \left(\alpha \delta_{ij} + \frac{1}{2\sqrt{J_2}} S_{ij}\right)\left(K\delta_{ij}\delta_{kl} + G(\delta_{ik}\delta_{jl} + \delta_{il}\delta_{jk} - \frac{2}{3}\delta_{ij}\delta_{kl})\right)$$

$$H_{kl} = 3K\alpha\delta_{kl} + \frac{G}{\sqrt{J_2}} S_{kl} \tag{4.40}$$

The loading function, f, is not expressed as a function of ε_{ij}^{p} explicitly, so $\frac{\partial f}{\partial \varepsilon_{ij}^{p}} = 0$. In order to determine the scalar function, h, we obtain the function $\frac{dk}{d\varepsilon_p}$ and the parameter C. The hardening parameter, k, can be expressed using the effective stress, σ_e, for Drucker-Prager material.

$$\sigma_e = \frac{\sqrt{3}(\alpha I_1 + \sqrt{J_2})}{1+\sqrt{3}\alpha} \tag{4.41}$$

Then:

$$k = \frac{1+\sqrt{3}\alpha}{\sqrt{3}} \sigma_e \tag{4.42}$$

From here combine with equation 4.31:

$$\frac{dk}{d\varepsilon_p} = \frac{1+\sqrt{3}\alpha}{\sqrt{3}} \frac{d\sigma_e}{d\varepsilon_p} = \frac{1+\sqrt{3}\alpha}{\sqrt{3}} H_p \tag{4.43}$$

H_p is determined from a uniaxial tension stress-strain curve, $d\sigma = H_p d\varepsilon$. H_p is the modulus of the material up to its plastic yield point. The effective strain, ε_p, is defined as:

$$d\varepsilon_p = \frac{dW_p}{\sigma_e} = \frac{\sigma_{kl} d\varepsilon_{kl}^{p}}{\sigma_e} = C\sqrt{\frac{\partial f}{\partial \sigma_{ij}} \frac{\partial f}{\partial \sigma_{ij}}} \tag{4.44}$$

Now parameter C can be defined as:

$$\boldsymbol{C} = \frac{\boldsymbol{\sigma_{kl} d\varepsilon^p_{kl}}}{\boldsymbol{\sigma_e \sqrt{\frac{\partial f}{\partial \sigma_{ij}} \frac{\partial f}{\partial \sigma_{ij}}}}} = \frac{\boldsymbol{\sigma_{kl} \frac{\partial f}{\partial \sigma_{kl}}}}{\boldsymbol{\sigma_e \sqrt{\frac{\partial f}{\partial \sigma_{ij}} \frac{\partial f}{\partial \sigma_{ij}}}}} \tag{4.45}$$

h is found by combining equations 4.39, 4.40, 4.41, 4.43, and 4.45 in equation 4.36:

$$h = G + 9K\alpha^2 + \frac{\alpha I_1 + \sqrt{J_2}}{3k}\left(1 + \sqrt{3}\alpha\right)^2 H_p = G + 9K\alpha^2 + \left(\alpha + \frac{1}{\sqrt{3}}\right)^2 H_p \tag{4.46}$$

Using equation 4.37 plastic strain increment is then given as:

$$d\varepsilon^p_{ij} = d\lambda \frac{\partial f}{\partial \sigma_{ij}} = \frac{\frac{\partial f}{\partial \sigma_{mn}} C_{mnst} d\varepsilon^p_{st}}{h} \frac{\partial f}{\partial \sigma_{ij}} = \frac{H_{st} d\varepsilon^p_{st}}{h} \frac{\partial f}{\partial \sigma_{ij}}$$

Again applying Hooke's law:

$$d\sigma_{ij} = C_{ijkl}\left(d\varepsilon_{kl} - \frac{\frac{\partial f}{\partial \sigma_{mn}} C_{mnst} d\varepsilon_{st}}{h} \frac{\partial f}{\partial \sigma_{kl}}\right) = C_{ijkl}\left(\delta_{sk}\delta_{tl} - \frac{\frac{\partial f}{\partial \sigma_{mn}} C_{mnst}}{h} \frac{\partial f}{\partial \sigma_{kl}}\right) d\varepsilon_{st} =$$

$$\left(C_{ijkl}\delta_{sk}\delta_{tl} - \frac{\frac{\partial f}{\partial \sigma_{mn}} C_{ijkl} C_{mnst}}{h} \frac{\partial f}{\partial \sigma_{kl}}\right) d\varepsilon_{st} = \left(C_{ijst} - \frac{H_{st} H_{ij}}{h}\right) d\varepsilon_{st}$$

$$d\sigma_{ij} = \left(C_{ijst} - \frac{H_{st} H_{ij}}{h}\right) d\varepsilon_{st} \tag{4.47}$$

Now the most general form of the Drucker-Prager isotropic-hardening elastic-plastic constitutive relationship is formed:

$$d\sigma_{ij} = \left[2G\delta_{im}\delta_{jn} + (K - \frac{2}{3}G)\delta_{ij}\delta_{mn} - \frac{\left(\frac{G}{\sqrt{J_2}}\right) S_{ij} + 3K\alpha\delta_{ij}}{G + 9K\alpha^2 + \left[\left(\alpha + \frac{1}{\sqrt{3}}\right)^2 H_p\right]} \left(\frac{G}{\sqrt{J_2}} S_{mn} + 3K\alpha\delta_{mn}\right)\right] d\varepsilon_{mn} \tag{4.48}$$

Equation 4.48 gives the change in shear stress by making i=m=1 and j=n=2. Also the Kronecker delta allows us to cancel out many of the parameters.

$$d\sigma_{12} = \left[2G\delta_{11}\delta_{22} + (K - \frac{2}{3}G)\delta_{12}\delta_{12} - \frac{\left(\frac{G}{\sqrt{J_2}}\right)S_{12} + 3K\alpha\delta_{12}}{G + 9K\alpha^2 + \left[\left(\alpha + \frac{1}{\sqrt{3}}\right)^2 H_p\right]}\left(\frac{G}{\sqrt{J_2}}S_{12} + 3K\alpha\delta_{12}\right)\right] d\varepsilon_{12}$$

$$d\sigma_{12} = \left[2G - \frac{\left(\frac{G}{\sqrt{J_2}}\right)^2 S_{12}S_{12}}{G+9K\alpha^2+\left[\left(\alpha+\frac{1}{\sqrt{3}}\right)^2 H_p\right]}\right] d\varepsilon_{12} \quad (4.49)$$

Equation 4.49 defines the shear stress-strain relationship. In other words, it can construct the backbone curve. The backbone curve can then be used to plot normalized shear modulus to strain. We can see whether Drucker-Prager can effectively model the clay by comparing this to the measured normalized shear modulus values.

Chapter 5 : DATA ANALYSIS AND INTERPRETATION

5.1 SAMPLE PREPORATION

5.1.1 UNDISTURBED SAMPLES

The behavior of the synthetic oil based clay is mostly dependent on the temperature and preparation method of the samples. Special care needs to be taken when the preparing samples. A method for preparing the cylindrical test samples needed to be established prior to testing in order to minimize human error and increase the reliability of the samples. Any disturbances to the clay may cause it to become more malleable. Remolding and variations in temperature are considered disturbances because they also have an effect on the clay. For initial tests, samples were constructed directly from packaged clay bricks with minimal disturbance, referred to as undisturbed samples. The undisturbed samples were initially constructed by bonding several bricks together. The layers were cut out using a mold that had a 71.1 mm diameter. The sample layers were then scarred and compressed together. Several issues arose from constructing this way. The bonding between layers wasn't strong enough to resist the torsion and many times the sample would break apart. Also, the layering caused damping to increase and shear modulus values to decrease, similar to a softening affect. This was due to the mechanisms caused by the weak bonding between layers.

In order to correct these issues samples were constructed from a single clay brick. By constructing samples from a single clay brick, the layering mechanisms could be excluded as a discrepancy. The clay bricks were trimmed to a 64 mm diameter (largest diameter possible for the samples). A molding ring of the one dimensional consolidation test was used for trimming.

Figure 5.1- Circular Clay Layers

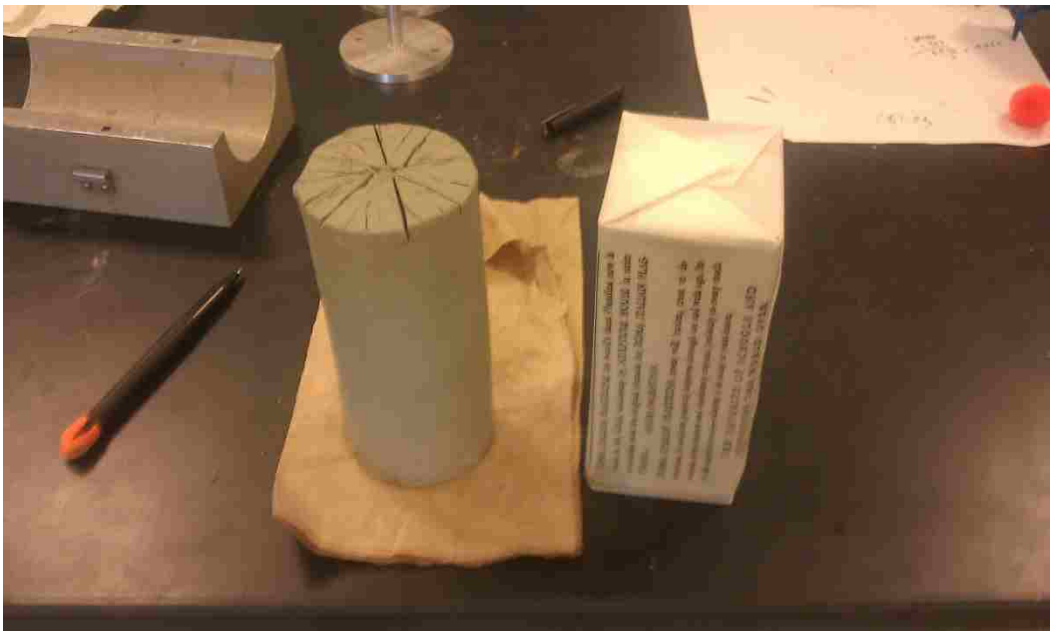

Figure 5.2- Whole Clay Sample

5.1.2 REMOLDED SAMPLES

As stated throughout this paper, the clay in question can either stiffen or become more malleable depending on the conditions applied. Initially, the tests were conducted on undisturbed samples (continuous samples). However, the clay used as the backing for the drop ball test is actually rolled and hammered into the box prior to testing. In order to construct an accurate numerical model of the ballistic event, the clay should be tested under similar conditions.

It is important to keep the remolding process constant throughout testing. The method developed in our lab was very simple in order to assure this. Firstly, the clay was flattened using a roller. The flattened clay was then rolled into long slender cylinders and placed into molds. The sample molds had an inside diameter of 72 mm and a height of 144 mm. The molds were then filled to about a quarter of their length and compacted using a standard compaction hammer. Each layer was given 10 blows by the hammer. Typically, it took 5 layers to completely fill the mold and create a sample. Using the following equation the energy delivered to each layer can be determined:

$$Energy = \frac{[\#\ of\ Blows][\#\ of\ Layers][Weight\ of\ Hammer][Drop\ Height\ of\ Hammer]}{Volume\ of\ Mold}$$

$$Energy = \frac{[10\ blows][5\ layers]\left[\frac{2.5 \times 9.81}{1000}\,kN\right][0.305\ m]}{570 \times 10^{-6} m^3} \approx 656\ kN - m/m^3$$

These samples are referred to as remolded samples. The clay did show signs of rebound after initial disturbance. Due to the rebound, the decision was made to test the remolded samples at a finite time after they were created. This was set to 48 hours after disturbing. Like the undisturbed samples these were tested in both heated and non-heated conditions at varying confining pressures.

5.1.3 HEATED SAMPLES

Besides remolding the clay the DOD also heats the clay in an oven. Typically, the DOD wants the clay to be around 70°F, which is around the lab's room temperature. The temperature was maintained by heating the clay to 100°F and limiting the time a sample could be used to 30 minutes. The clay is very susceptible to temperature so the heating process had to be simulated during lab tests. Samples were heated to 100°F in the oven for at least 8 hours, in order to assure the entire sample was properly heated. Certain modification had to be made during this stage of testing. Since resonant column test can take several hours to transpire, due to the consolidation of samples as the test is run, an effective manner of heating the sample throughout the duration of the test needed to be developed.

When running similar triaxial tests a circulation system was used that helped maintain the required temperature. This was not possible for the resonant column due to insufficient inlets. Instead, hot water was placed in the chamber prior to testing and was replaced throughout the test. The tap water used for heating was 120°F when placed. The temperature within the cell was carefully monitored using thermostats inside the chamber. Additionally, the water was removed after the tests to verify that the temperature had not dropped below the intended target. The temperatures of the samples were taken prior to and after the tests were concluded. The goal was to maintain a temperature above 90°F. Both the remolded and undisturbed samples were heated in this manner.

5.2 RESULTS

Four sets of samples were created using combinations of the previously mentioned sample preparation methodology. They will be referred to as undisturbed, undisturbed heated, remolded, and remolded heated. The samples were also subjected to varying confining pressures. A summary of the important properties are shown in table 5.1. As previously stated, G_{max} and $\boldsymbol{\xi_{min}}$ represent the elastic behavior of the clay. Undisturbed samples were expected to be the stiffest and this is shown in that it has the highest G_{max} value and lowest $\boldsymbol{\xi_{min}}$ value. Comparing undisturbed samples to remolded samples shows that the clay loses a large amount of strength during the remolding process. More strength is lost remolding than heating the samples. This is shown in that the undisturbed heated samples have a $G_{max}$of 41 MPa compared to remolded sample's 35.2 MPa. The disturbed sample loses close to 40% of its strength were heating only causes it to lose 28%. Surprisingly, the loss of shear modulus for heated samples is similar to that of their non-heated counterparts, 27% for disturbed and 28% for undisturbed. The ranges for shear modulus show a lot of overlap for the shear strains tested. The samples seem to overlap in the 10-30 MPa range except for the undisturbed samples, which consistently stayed above. Figures 5.3 through 5.7 show the effects of confining pressure on shear modulus. As anticipated the increase of confining pressure causes an increase in shear modulus, but besides that no definitive pattern was determined.

Damping is shown in table 5.1, as well as figure 5.8. It's difficult to distinguish any trends in damping due to confining pressure (figures 5.9 through 5.12). Looking at damping by comparing the preparation method does show some distinctive characteristics. The remolded samples have higher initial values of damping, ξ_{min}, than the undisturbed samples. This is attributed to the mechanisms of the remolded clay. The remolding process leaves voids and some

Table 5.1- Summary of Test

	Non-Heated		Heated	
	Undisturbed	Disturbed	Undisturbed	Disturbed
ξ_{min} (%)	4.21	8.52	5.35	8.82
ξ (%)	4-9	5-10	8-13	8.5-14
G_{max} (MPa)	56.9	35.2	41.0	25.7
G (MPa)	33-57	13-35	17-41	4-26

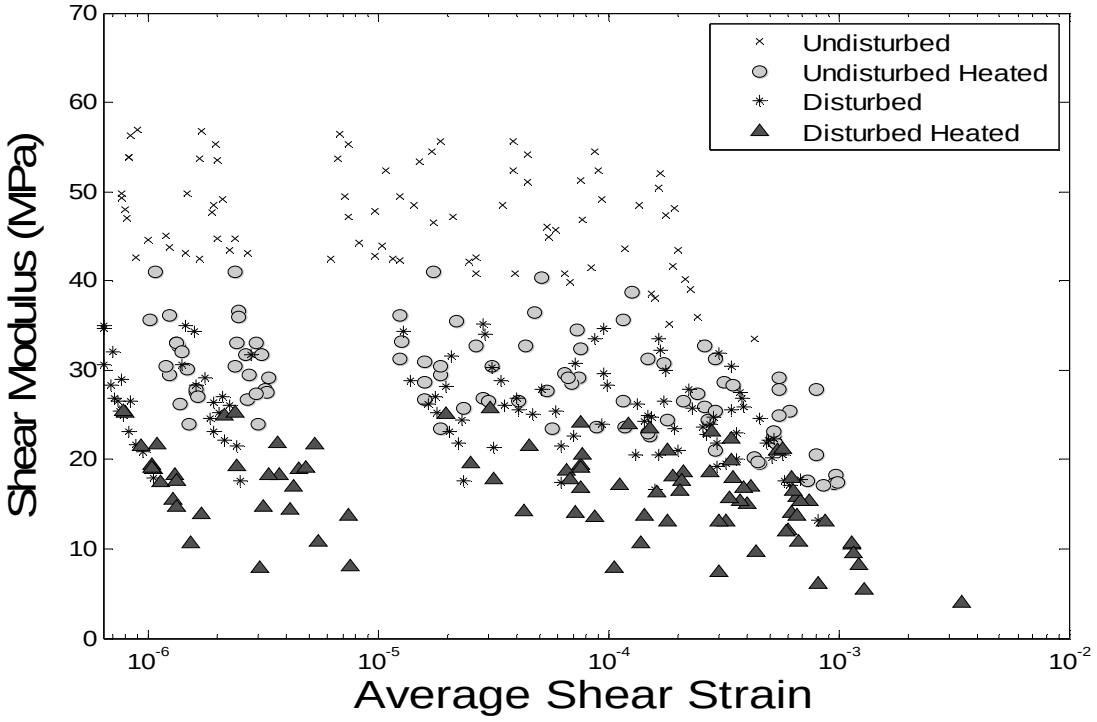

Figure 5.3- Shear Modulus by Preparation Method

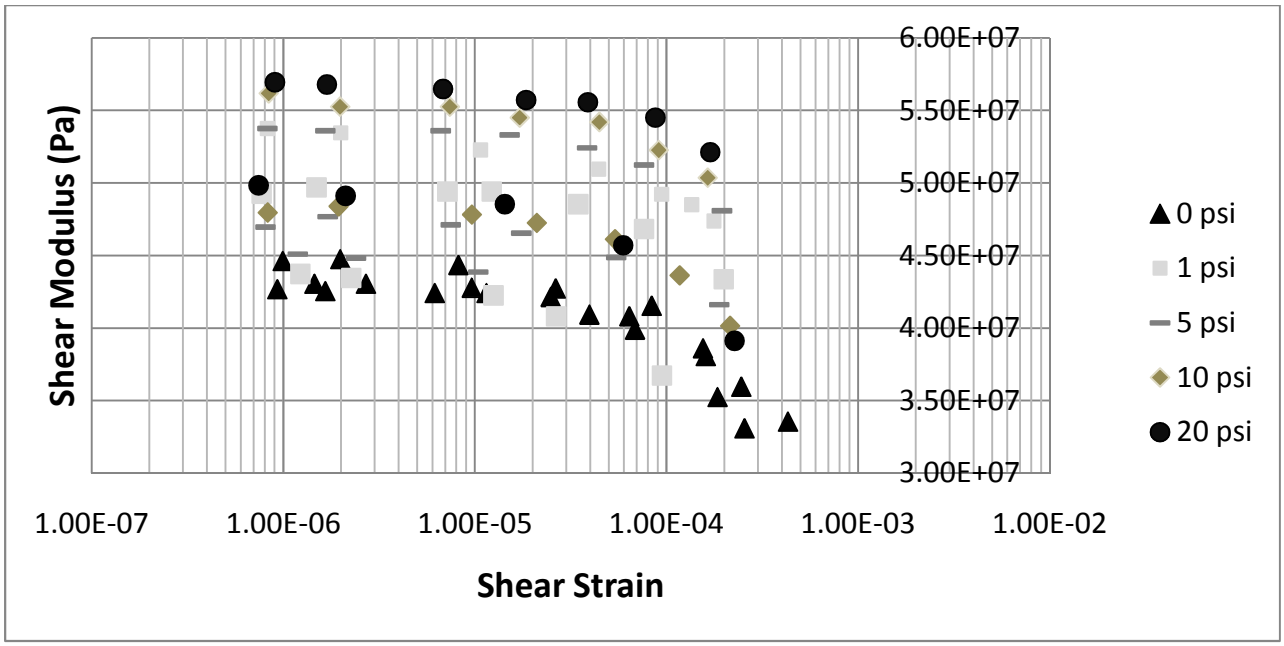

Figure 5.4- Shear Modulus for Undisturbed Samples

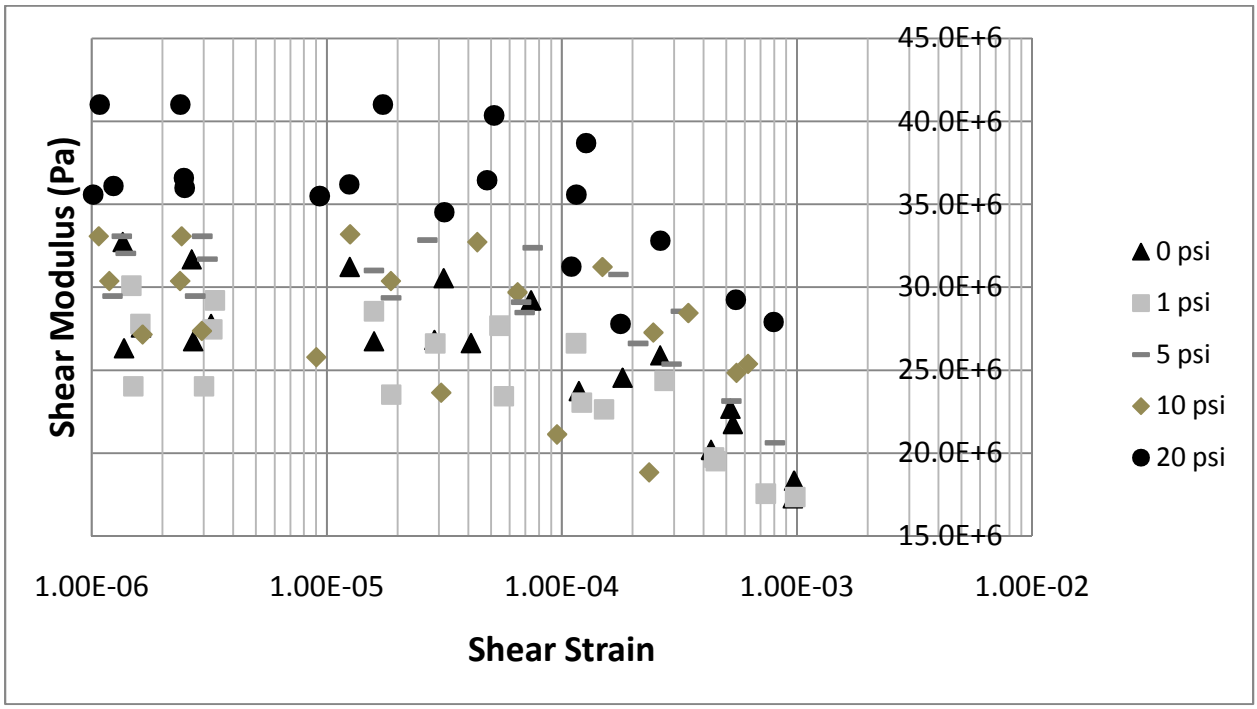

Figure 5.5- Shear Modulus for Undisturbed Heated

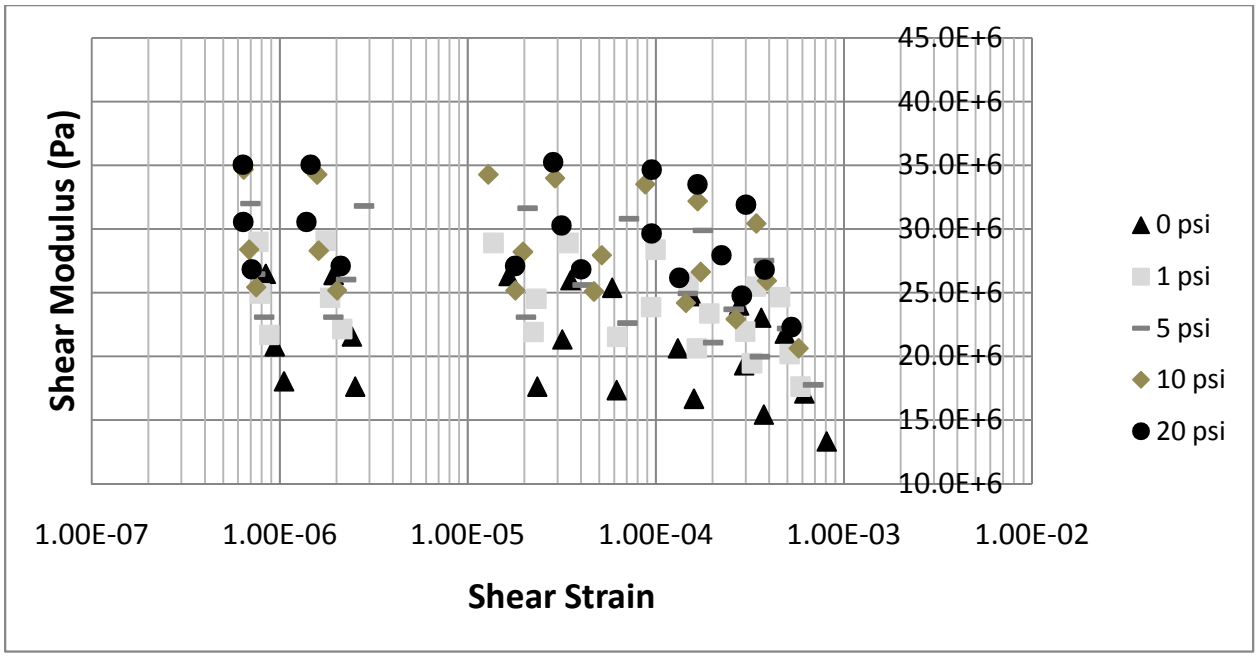

Figure 5.6- Shear Modulus for Remolded

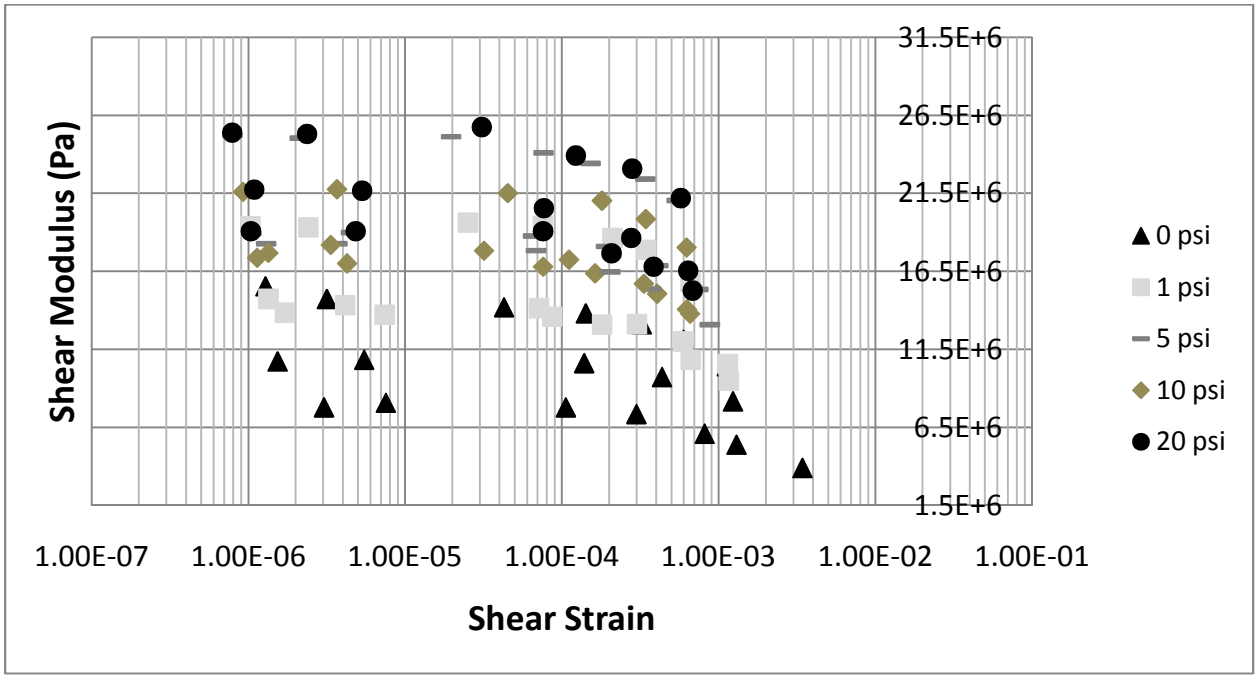

Figure 5.7- Shear Modulus for Remolded Heated

layering. The layering likely plays a large role in the dissipation of energy in the clay. In figure 5.8, the undisturbed and remolded look almost identical except that the remolded data is shifted up. Other more significant interpretations of the damping data are done later when the analytical predictive equations are used.

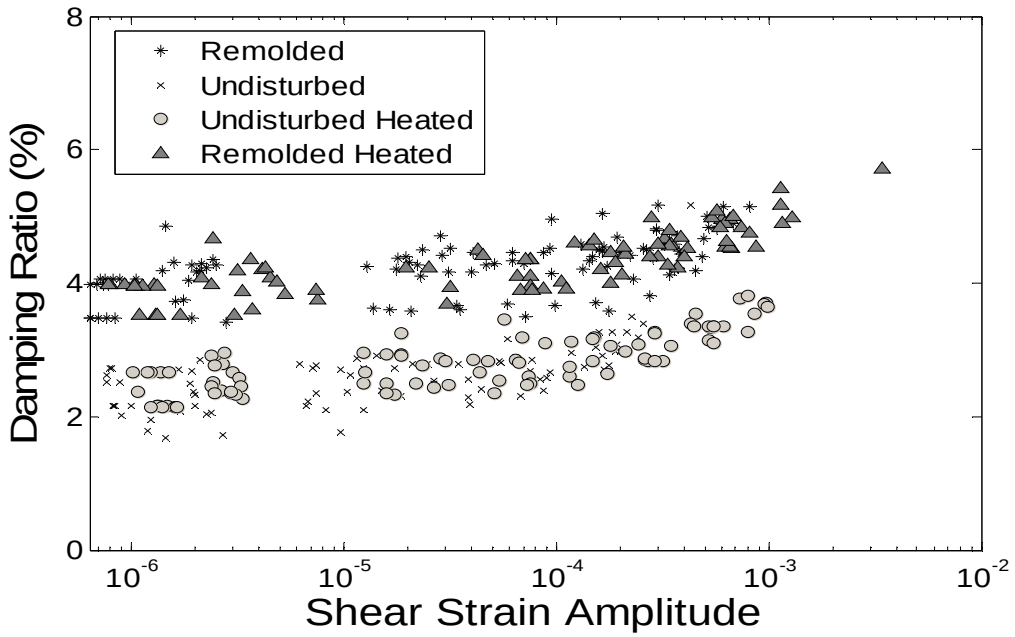

Figure 5.8- Damping Ratio by Preparation Method

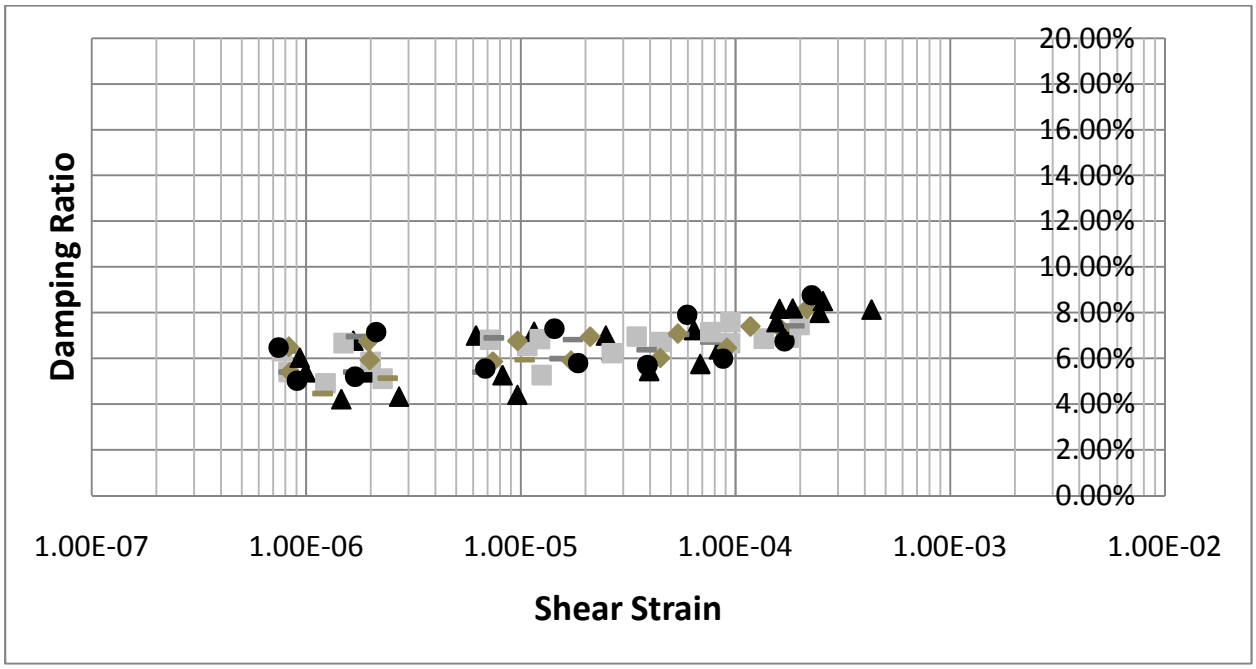

Figure 5.9- Damping Ratio for Undisturbed

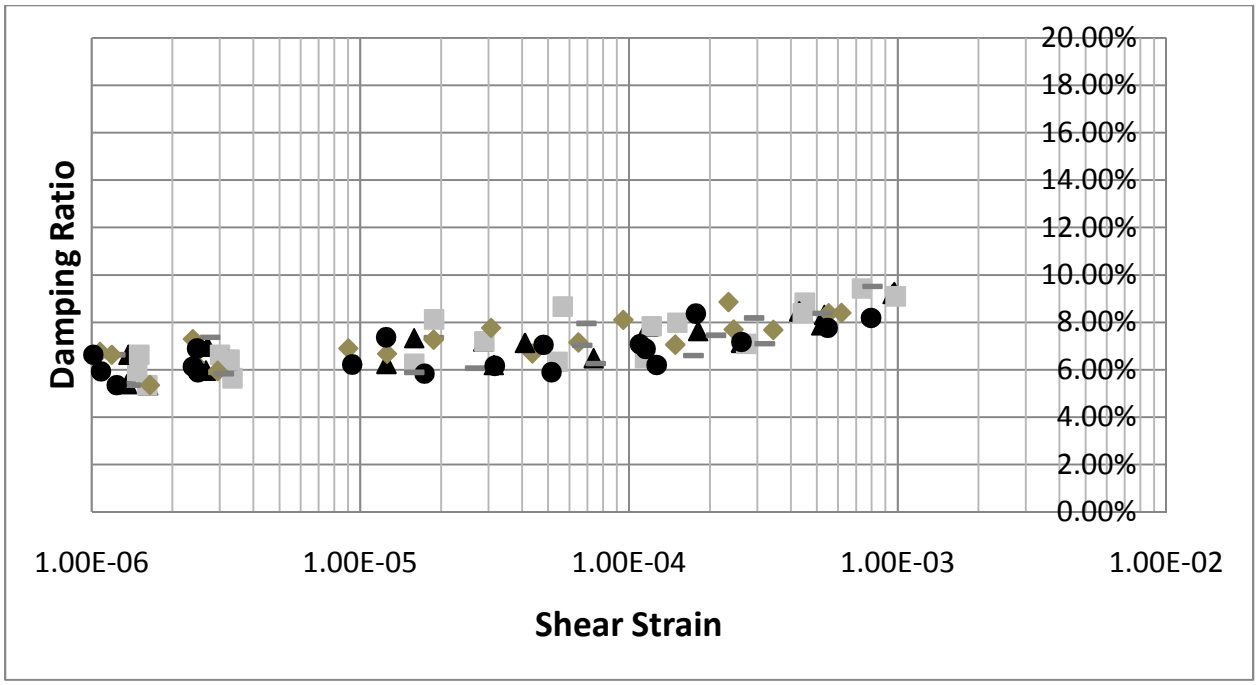

Figure 5.10- Damping Ratio for Undisturbed Heated

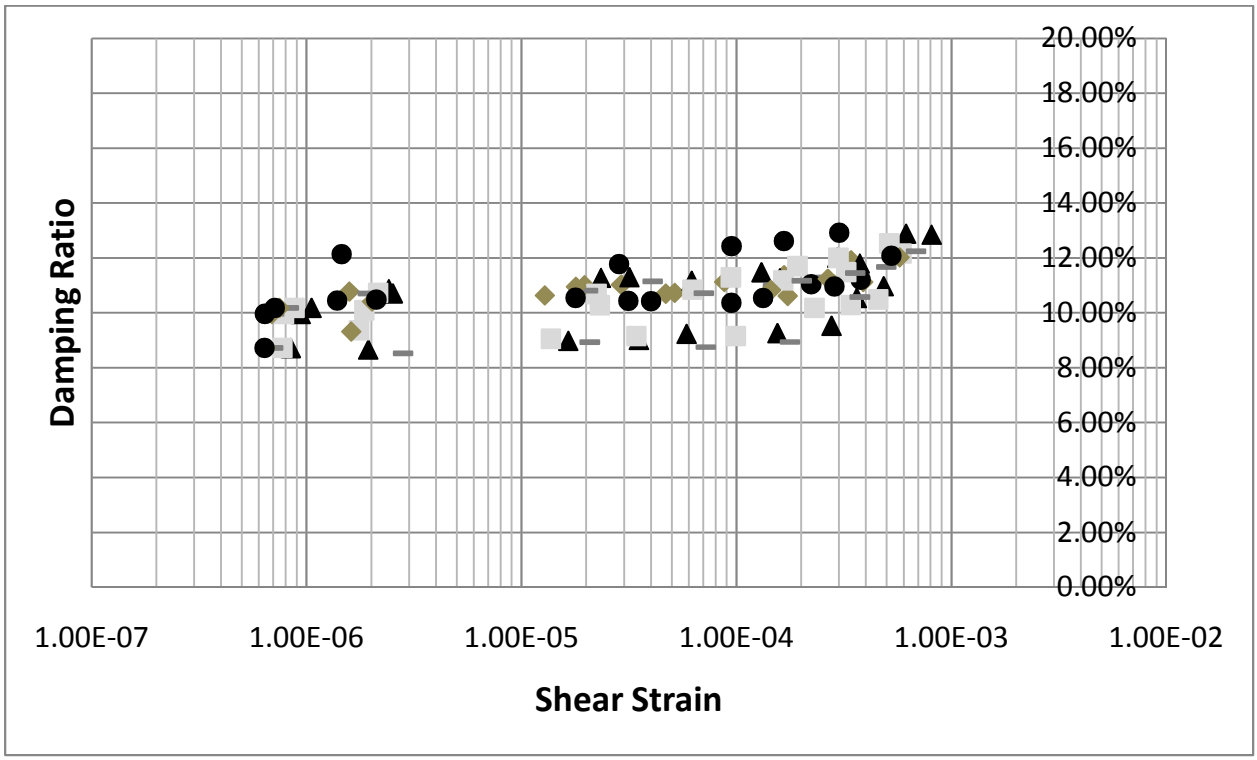

Figure 5.11- Damping Ratio for Remolded

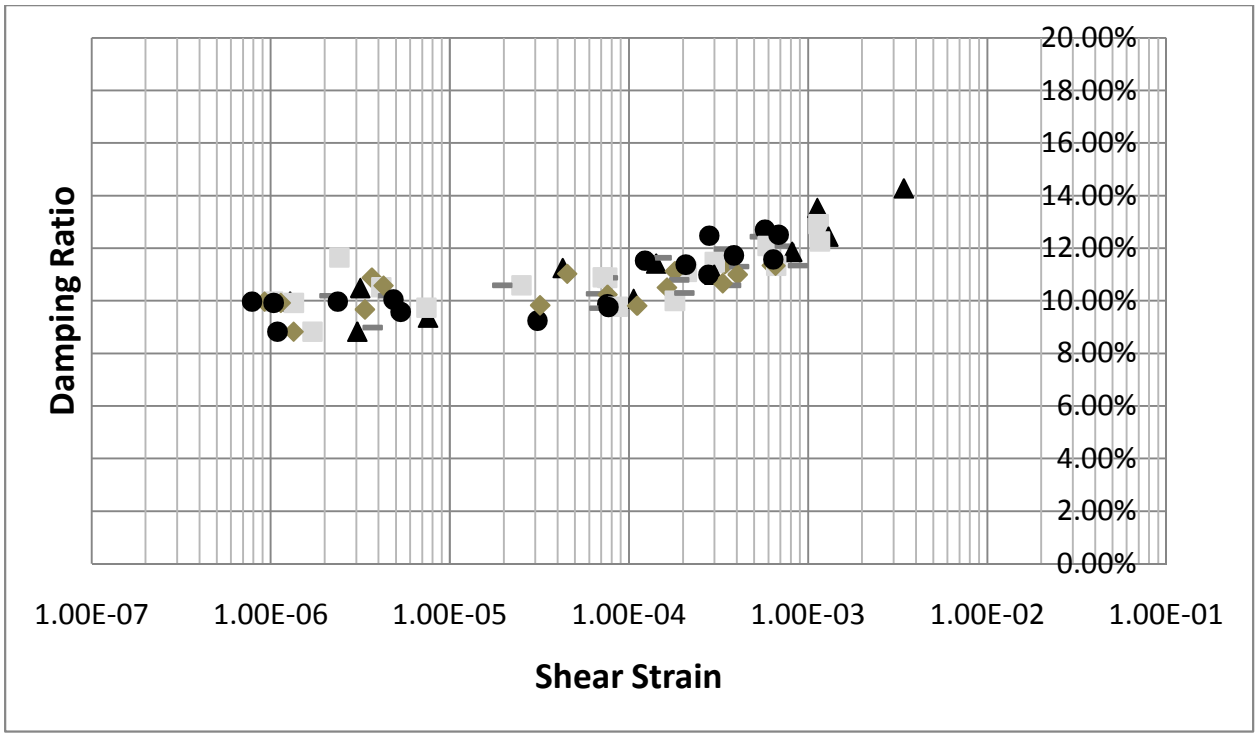

Figure 5.12- Damping Ratio for Remolded Heated

5.3 ANALYSIS USING PREDICTIVE EQUATION

Section 4.2 describes the analytical methods that are applied to the resonant column results. In this section it is explained that certain variables are necessary prior to the analysis of the data. For example, the triaxial test needs to be conducted in order to determine the maximum shear stress of the clay for all four of the sample types. Table 5.2 provides the necessary properties from both the static test ($\boldsymbol{\tau_{max}}$) and the dynamic test ($\boldsymbol{G_{max}}$). The reference strain of the samples at their corresponding cell pressure is also given in table 5.2. Reference strain is found using equation 4.11. Figure 5.13 shows all the normalized shear modulus reduction curves. The appendix shows more detailed figures of each test (i.e remolded, undisturbed, etc,). Typically, confining pressure had little significance on the reduction curves; this is also shown in figure 5.13 were most of the curves overlap except for a few outliers. In order to simplify the congestion the averages of the reduction curves were taken, ignoring confining pressure. This is shown in figure 5.14 where the data is separated by preparation method.

Looking at figure 5.14, the undisturbed samples decrease in normalized shear modulus at an earlier shear strain than the other three samples. This means that the soil retains its strength longer as the shear strain amplitude increases for undisturbed heated samples and both heated and unheated remolded samples. Also the difference between the two remolded sets of data is very small compared to the two undisturbed samples. The most important trend shown in figures 5.13 and 5.14 is that the shear modulus degrades later than typical clays. This behavior is similar to non-Newtonian fluids. If the backbone curve were reconstructed it would show that the RP clay is very stiff. Whereas typical clays, studied by Hardin & Drnevich (1972), show a softer relationship. The reconstruction of the backbone curve is done later.

Table 5.2- Summary of Static and Dynamic Properties

Non Heated Sample (Undisturbed)					
	0 psi	1 psi	5 psi	10 psi	20 psi
τ_{max} (kPa)	46	46	46	46	46
G_{max} (MPa)	44.6	53.8	53.8	56.2	56.9
γ_r	1.031×10^{-3}	8.55×10^{-4}	8.55×10^{-4}	8.185×10^{-4}	8.084×10^{-4}
Heated Sample (Undisturbed)					
	0 psi	1 psi	5 psi	10 psi	20 psi
τ_{max} (kPa)	25.1	25.1	25.1	25.1	25.1
G_{max} (MPa)	32.7	30.1	33.1	33.2	41.0
γ_r	7.676×10^{-4}	8.339×10^{-4}	7.583×10^{-4}	7.56×10^{-4}	6.122×10^{-4}
Non Heated Sample (Disturbed)					
	0 psi	1 psi	5 psi	10 psi	20 psi
τ_{max} (kPa)	44	44	44	44	44
G_{max} (MPa)	26.5	29.1	32.0	34.7	35.2
γ_r	1.66×10^{-3}	1.512×10^{-3}	1.375×10^{-3}	1.268×10^{-3}	1.25×10^{-3}
Heated Sample (Disturbed)					
	0 psi	1 psi	5 psi	10 psi	20 psi
τ_{max} (kPa)	25.1	25.1	25.1	25.1	25.1
G_{max} (MPa)	15.5	19.6	25.2	21.8	25.7
γ_r	1.619×10^{-3}	1.281×10^{-3}	9.96×10^{-4}	1.151×10^{-3}	9.767×10^{-4}

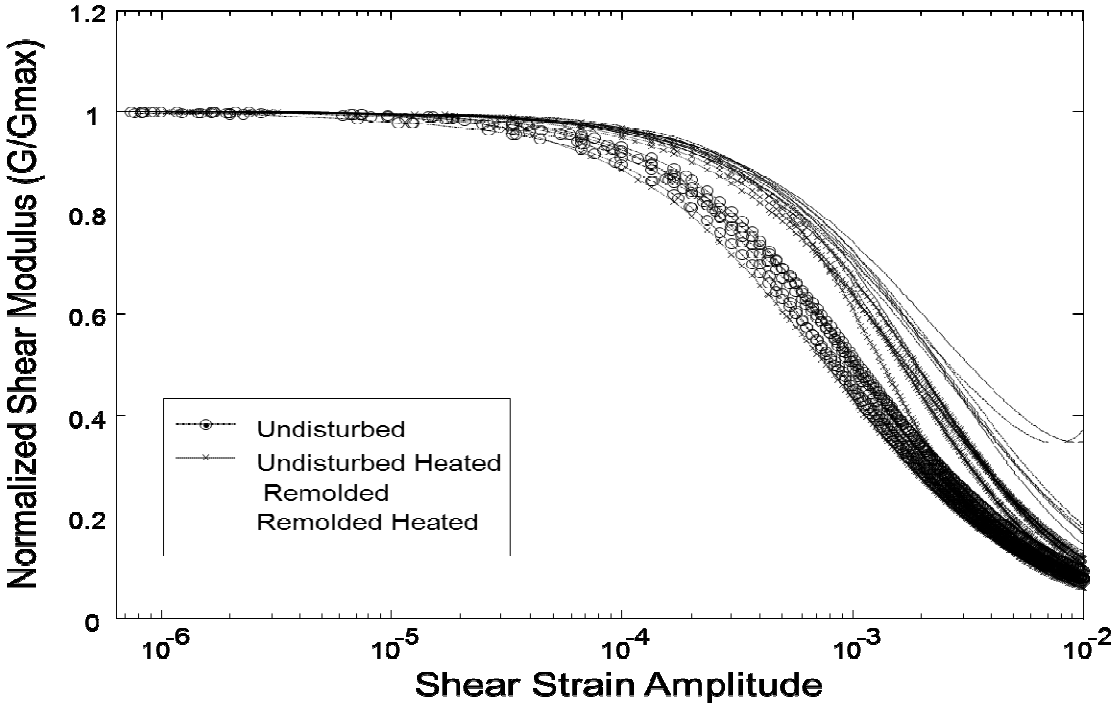

Figure 5.13- Modulus Reduction Curves

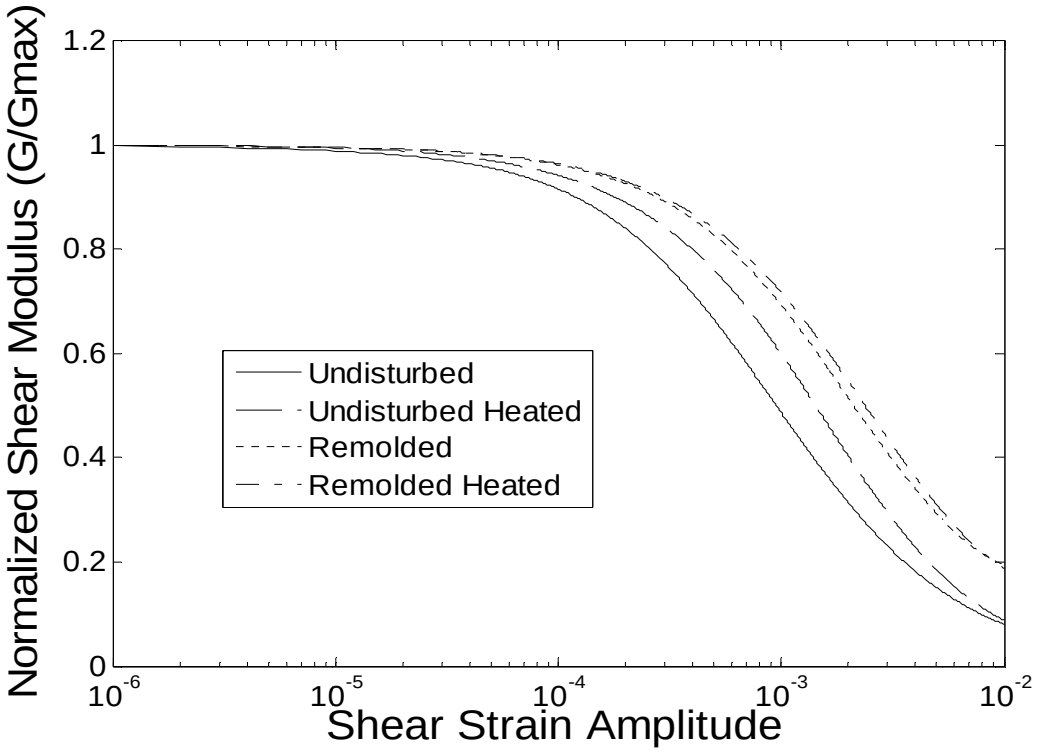

Figure 5.14- Average Modulus Reduction Curves

5.4 PREDICTIVE CURVES FOR DAMPING

Damping is frequency dependent according to the Kelvin-Voigt model. To compare damping from a resonant column test, it is looked at as a function of $G/G_{max.}$ Using G/G_{max} allows for the data collected from samples of different dimensions to be compared, basically normalizing frequency. Since empirical correlations could not be used for the RP clay, the method laid out by (Zhang, Andrus, & Juang, 2005) was used. Using equation 4.19, the quadratic curve was used to fit the data. These are the results:

$$\xi - \xi_{min} = 17.31\left(G/G_{max}\right)^2 - 47.98\left(G/G_{max}\right) + 30.9 \quad (5.1)$$

$$\xi - \xi_{min} = 2.433\left(G/G_{max}\right)^2 - 13.39\left(G/G_{max}\right) + 11.37 \quad (5.2)$$

$$\xi - \xi_{min} = 3.655\left(G/G_{max}\right)^2 - 18.38\left(G/G_{max}\right) + 14.97 \quad (5.3)$$

$$\xi - \xi_{min} = 3.115\left(G/G_{max}\right)^2 - 15.43\left(G/G_{max}\right) + 12.33 \quad (5.4)$$

Equation 5.1 is the damping fit for undisturbed samples, equation 5.2 is for the heated undisturbed samples, equation 5.3 is for remolded, and equation 5.4 is for heated remolded. Figure 5.15 graphically shows all of the equations. The undisturbed sample shows a more drastic increase in damping as the normalized shear modulus decreases. Looking at figures 5.16 and 5.17, there are no dramatic variations. Specifically both of the heated samples show almost identical trends, figure 5.16. In table 5.1, the fits are used to predict values for ξ_{max}, though the heated remolded sample and the heated undisturbed sample show similar trends their ξ_{max} value is different due to ξ_{min}. As stated before damping is not a function of confining pressure. The fact that the trends in damping support the trends found in the normalized shear modulus fits

with the fact that the clay behaves more similar for heated undisturbed than the two remolded samples.

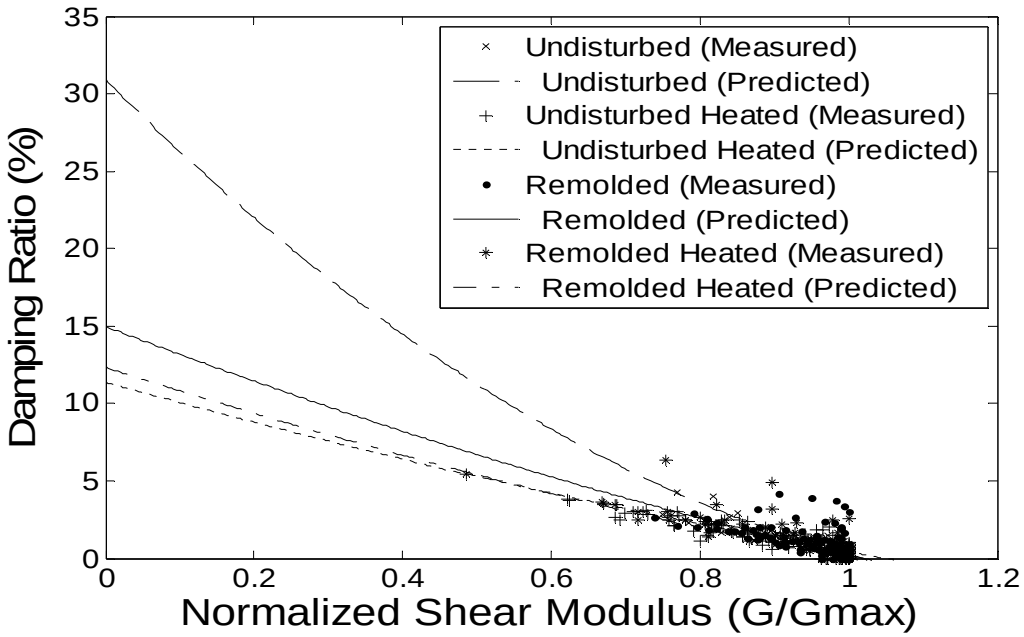

Figure 5.15- Damping Ratio predictive curves

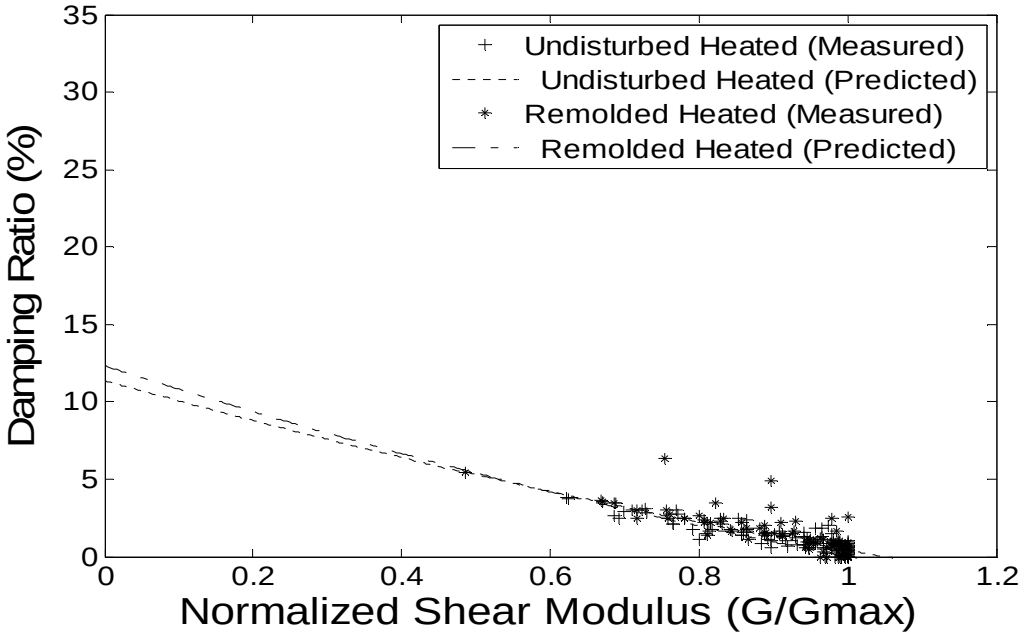

Figure 5.16- Heated Samples predictive curves

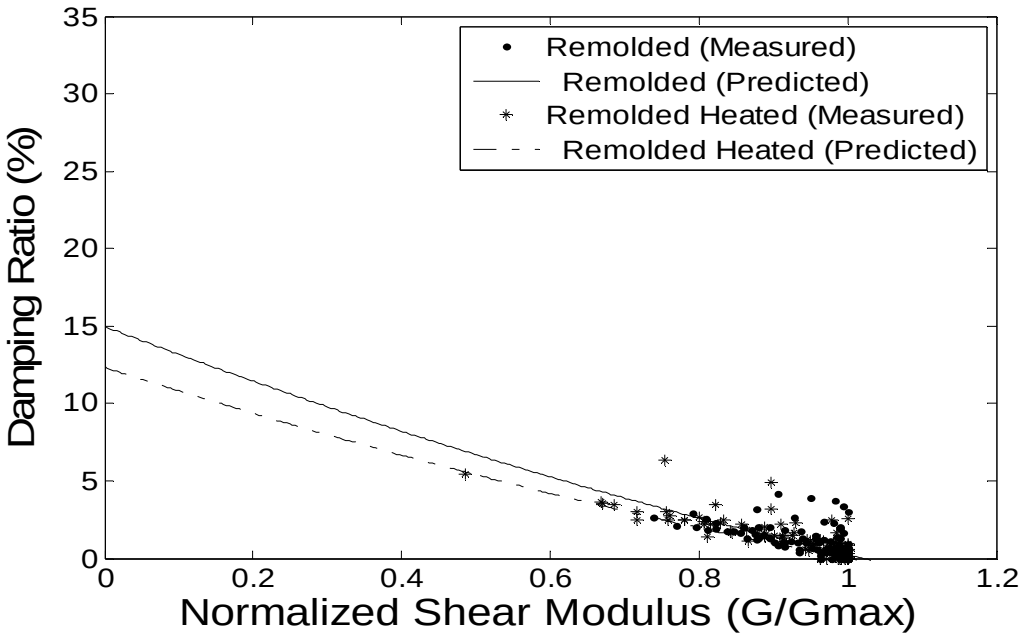

Figure 5.17- Remolded Samples predictive curves

5.5 COMPARISONS TO DRUCKER PRAGER CAP MODEL

Now the results from the resonant column can be compared to the one dimensional equation derived for the Drucker-Prager cap model. Only the samples with no confining pressure applied were compared to the 1D equation (equation 4.49). The parameters used for the Drucker-Prager cap model were directly taken from the model created through the testing/calibration method. The properties of which are listed in table 5.3. It is important to note that shear modulus was never inputted to the finite element program. The program assigns a value to shear modulus using elastic modulus and Poisson's ratio (equation 2.3). The shear modulus that the finite element model uses is therefore smaller than the one measured using the resonant column, 1.388 MPa to 44.6 MPa. Equation 4.49 is also very dependent on J_2 , second invariant of deviatoric stress. This value is dependent on the yield stress of the clay. In order to show the sensitivity of the model, the yield stress and modulus are varied. The matlab program is included in the appendix.

Figure 5.18 and 5.19 compare the data from the currently being used for analysis to the one measured. In the graphs the yield stress was varied in order to show the effects on the shear modulus reduction curves. Due to the lower shear modulus values and higher yield stress the strain at which the material becomes plastic is shifted further to the right in both figures 5.18 and 5.19. Also, in figure 5.19 we can see that the Drucker-Prager model predicts a stress strain relationship that is on a different scale than the Hardin/Drenvich prediction. Figure 5.20 shows the stiffer stress strain relationship of the Hardin/Drnevich when compared to the others. Also notice that the yield stress needed to be reduced by a factor of ten in order to be comparable to the predictive curve.

Figures 5.21 and 5.22 were constructed using a higher elastic modulus (132.908 MPa). Figure 5.21 looks like it gives a better prediction for yield strain; still Drucker-Prager is going to predict a material that is stiffer than the measured results. This is shown in more detail in Figure 5.23. It is determined using figure 5.23 that a yield stress of 5 kPa would give a similar stress strain relationship to the measured data. Obviously a higher elastic modulus would also have to be used in order to get the best fit possible with the collected data.

Table 5.3- Model Values

Finite Element Model Parameters	
Friction Angle (φ)	60°
Cohesion (c)	46 kPa
E (Elastic Modulus)	4.136 MPa
Yield Stress	60 kPa
Poisson's Ratio (ν)	0.49
J_2	34.641 kPa

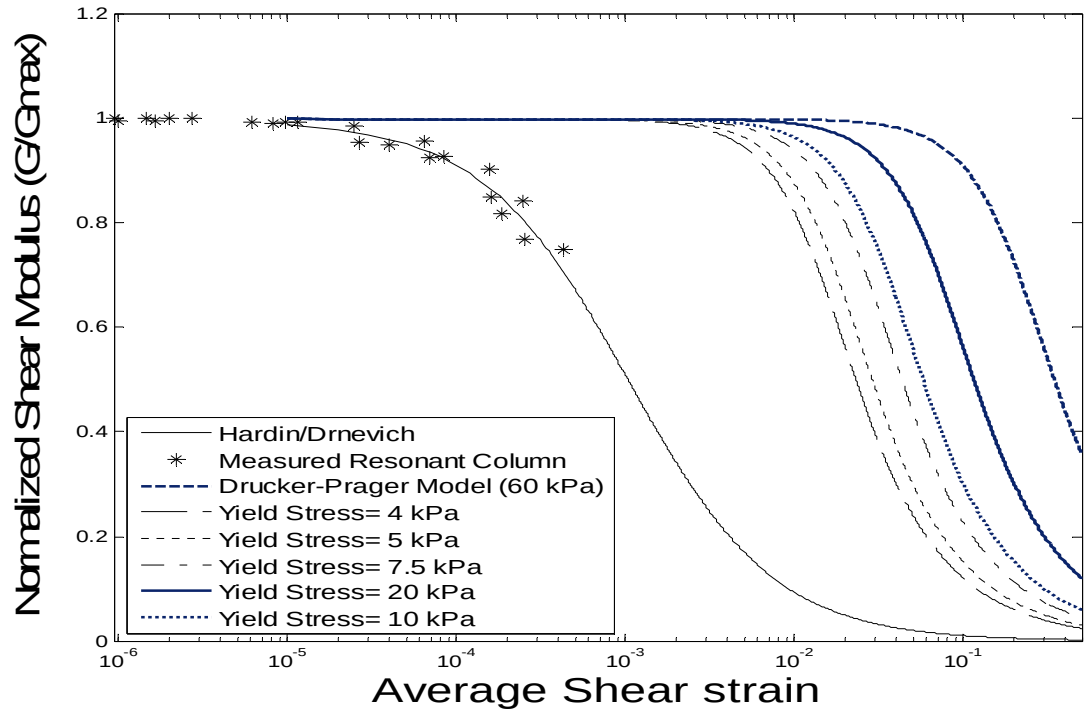

Figure 5.18- Modulus Reduction Curves using Model Values

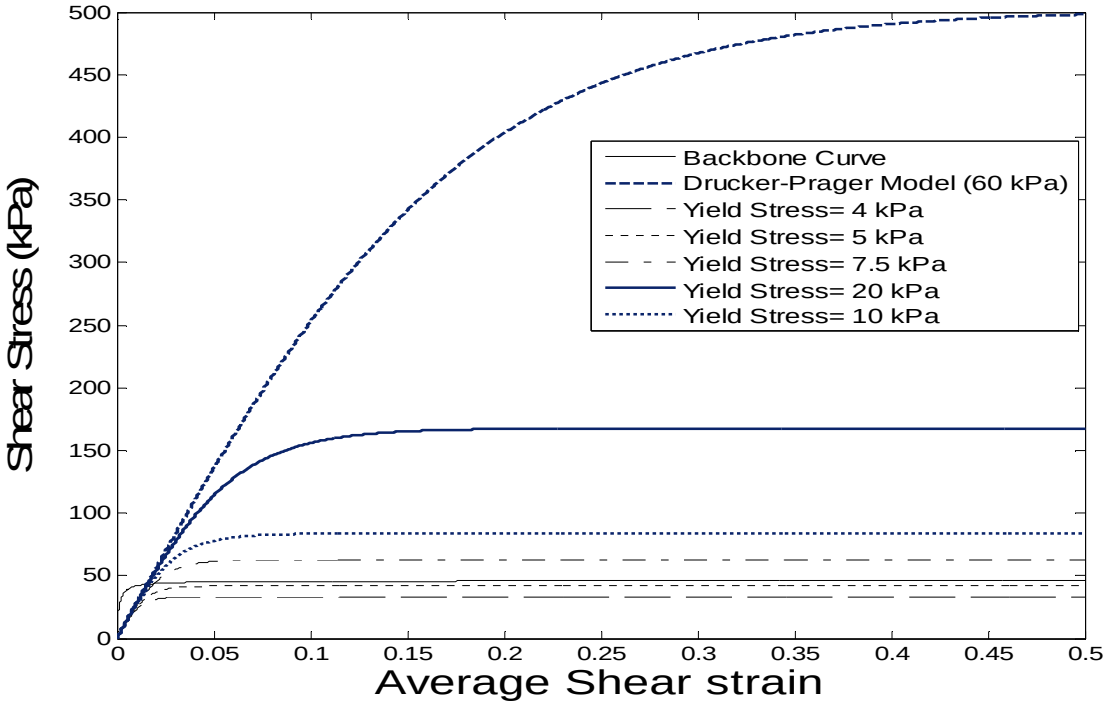

Figure 5.19- Stress-Strain curves using Model Values

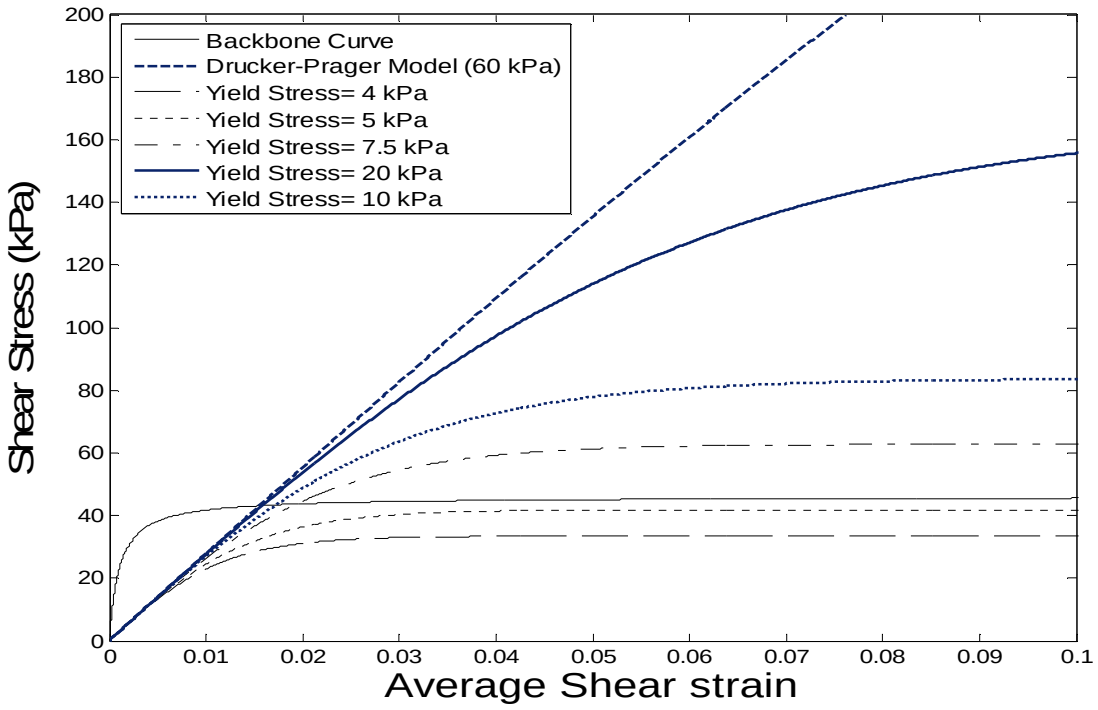

Figure 5.20- Stress-Strain curves using Model Values

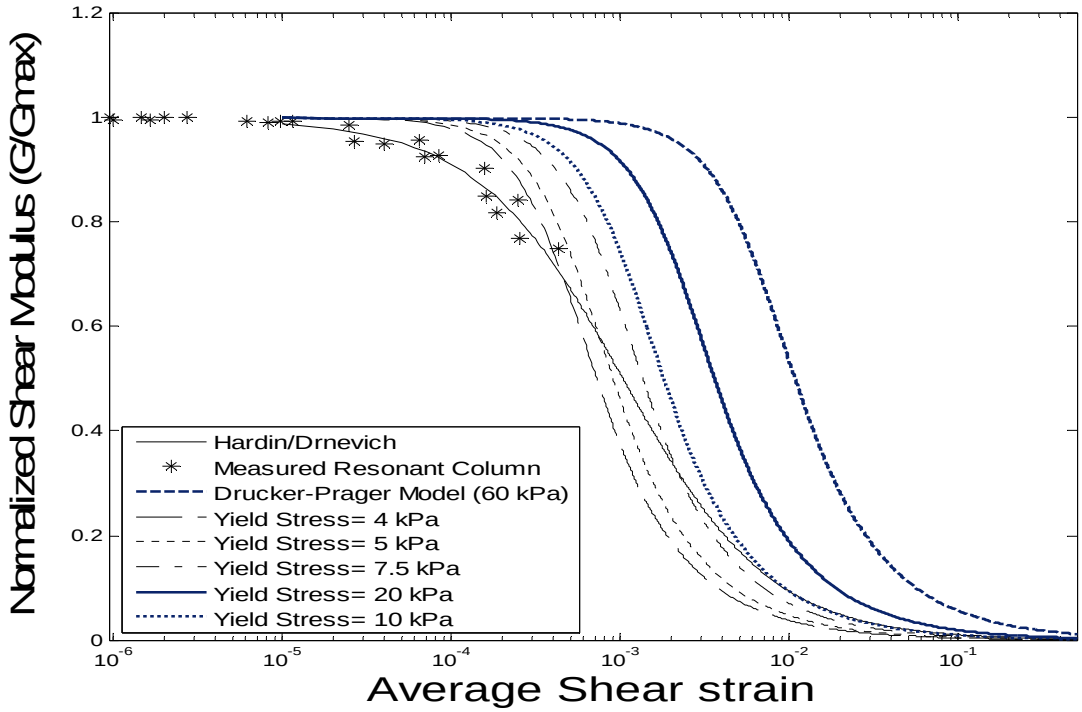

Figure 5.21- Modulus Reduction Curves using Calculated Shear Modulus

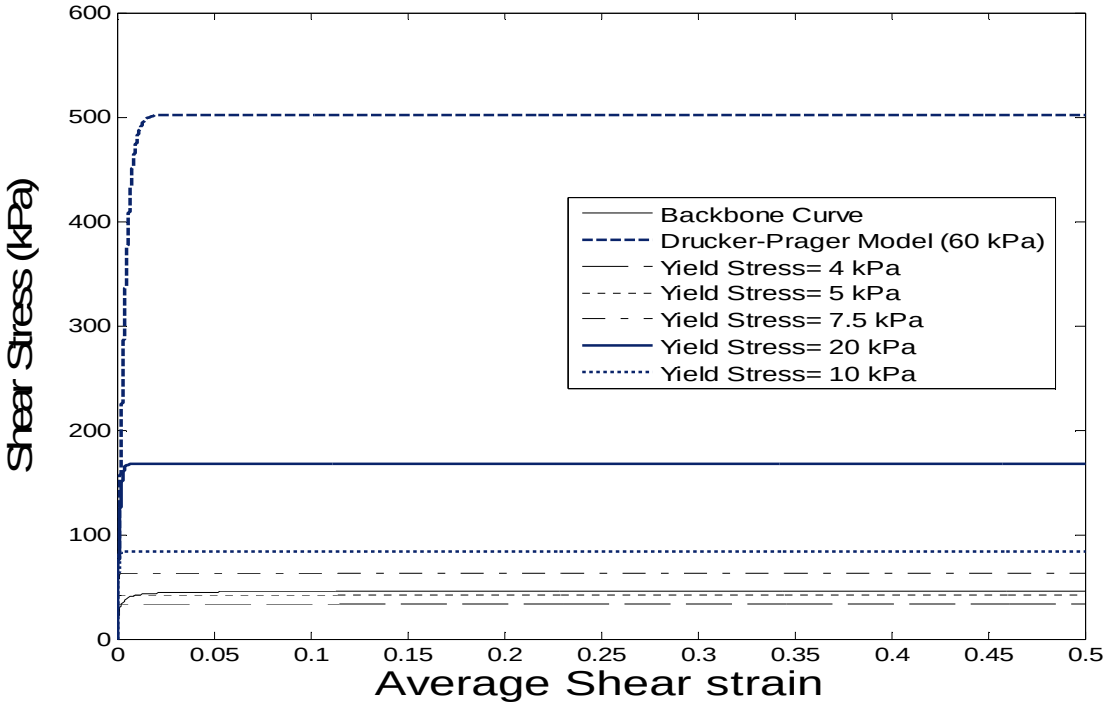

Figure 5.22- Stress-Strain relationship using Calculated Shear Modulus

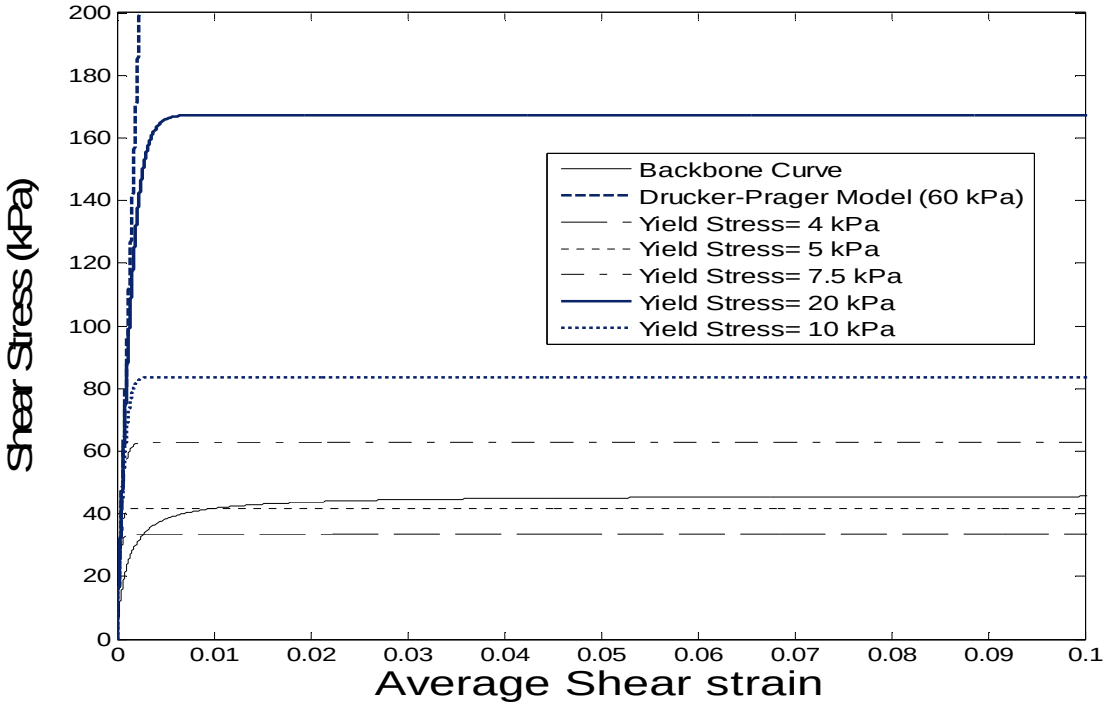

Figure 5.23- Stress-Strain relationship using Calculated Shear Modulus

5.6 CONCLUSSION/RECOMMENDATIONS

In conclusion, this paper presented shear modulus values for four sets of samples; undisturbed, remolded, undisturbed heated and remolded heated. The study determined that the clay is considerably affected by remolding and temperature. It behaves more like a non-Newtonian fluid when heated. These results show a material that is stiffer than typical clays.

The study also offers a comparison of the behavior of Drucker-Prager yield criterion with a cap to the experimental results of our resonant column. The results of our tests show a huge difference between the models that is currently being used. With some adjustments the model though could be made to match our measurements pretty closely. Drucker-Prager typically predicts soils to be stiffer or have a more constant shear modulus, our clay also shows that it is stiffer than typical clays. Additionally, the study provides values for maximum shear modulus as well as ranges for damping and maximum damping.

In order to gain a greater understanding of the material tests need to be conducted at higher strains. Though the predictive equations assist in characterizing the soils behavior at such strains running a high strain test would reduce the error in these estimates. Also, the resonant column test should be compared to other constitutive models such as CAM Clay, and Von Mises.

Appendix A. CALIBRATION

In order to accurately measure dynamic soil properties, it is necessary to first calibrate the resonant column. Calibrating the resonant column allows us to provide assurance of the recorded; also it allows us to become intimate with both the equipment and the testing procedure. It's also important to take an inventory of the equipment prior to beginning calibration process in order to assure everything is accounted for and functioning properly. It's also important to oil and clean pieces in order to prevent loss created by the friction of the rubbing pieces.

A.1 POLAR MASS MOMENT OF INERTIA FOR TOP PLATEN

Polar mass moment of inertia for the top mass of the resonant column is an integral property for determining dynamic properties of soil using the equipment. Typically polar mass moment of inertia can be determined by the physical properties of the object. In the resonant column though, the complex shape of the top mass makes it difficult to accurately measure the physical properties. It then becomes easier and more accurate to measure the value, J_A, experimentally instead of using physical measurements this is directly from "Drnevich Resonant Column Apparatus Operating Manual". This method is also briefly described in ASTM D4015. In order to begin the calibration process it's necessary to have a calibration rod, which is usually provided by the company that produces the resonant column. In this calibration the rod needed to be manufactured. The manufactured rod is based on the description provided in ASTM D 4015. It is recommended that a calibration rod with a known stiffness be used. The rod used in our calibration process was aluminum alloy 2024. The aluminum rod has a known shear modulus 2.646 GPA. The rod is used to perform standard test at very low strain amplitudes. From dynamics the following relationship is known:

$$f_n = \frac{1}{2\pi}\sqrt{\frac{K_{cr}}{J_0}} \quad \text{A.1}$$

Where K_{cr} is the torsional spring constant of calibrating rod (N-m/Rad) and J_0 is the polar mass moment of inertia (Kg-m^2). Equation A.1 can be rearranged in order to find the polar mass moment of inertia of the top platen. This is shown below:

$$J_0 = \frac{K_{cr}}{(2\pi f_n)^2} \quad \text{A.2}$$

Torsianal spring constant can be accurately solved because the value for shear modulus of the rod is known:

$$K_{cr} = \frac{GI_p}{l} \quad \text{A.3}$$

I_p in the equation above stands for the polar moment of inertia for the rod and l is the length of the rod.

$$I_p = \frac{\pi d^4}{32} \quad \text{A.4}$$

In order to authenticate the calibration process, two rods were used to find the polar mass moment of inertia. The length of both rods varied, one was 134 mm and the other 119 mm. Both rods had a diameter of 9.525 mm (0.375 in). The rods were placed in the fixed on the resonant column using screw to attach them to the top and bottom platen. A sketch of the calibration rods can be found on figure A.1. Using the large rod the resonant frequency was found to be 37.65 Hz. The resonant frequency of the smaller rod was about 39.6 Hz. The results of the resonant

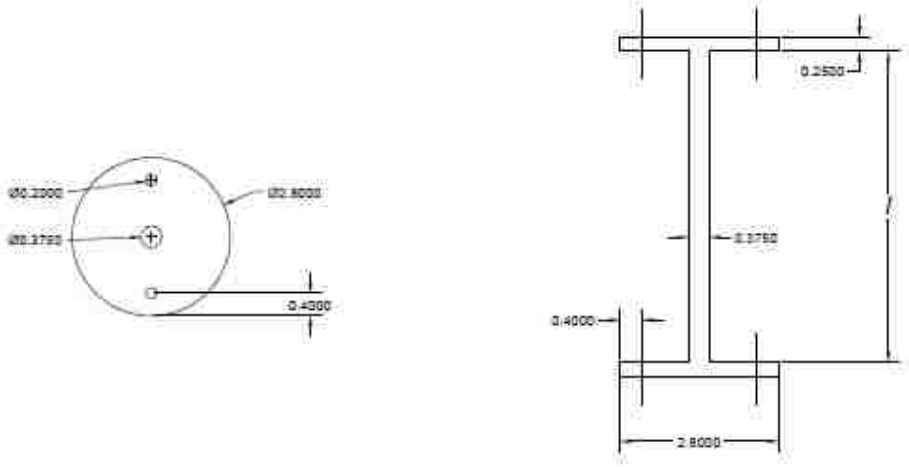

Figure A.1-Shop Drawing of Calibration Rods

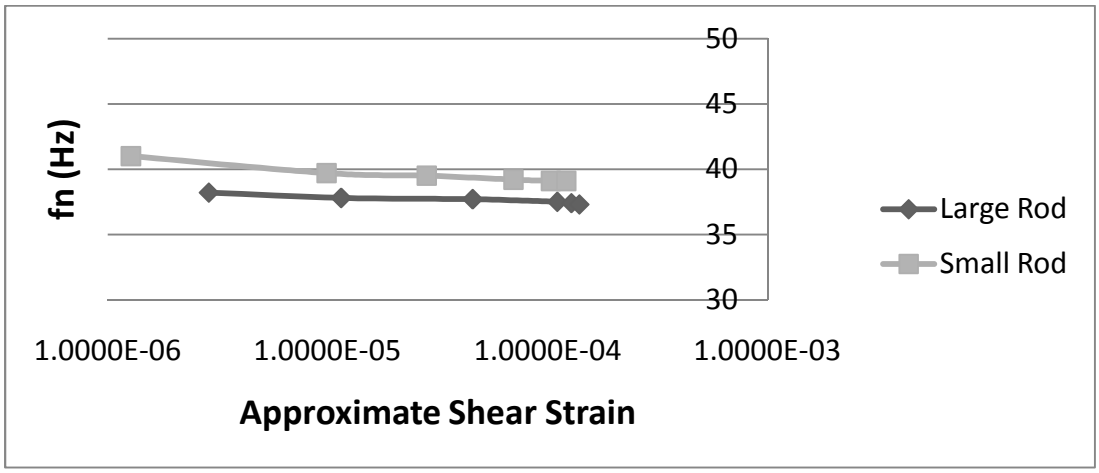

Figure A.2- Resonant frequency of the calibration rods

column test on the two calibration rods is also shown in figure A.2 where the independent variable is the approximate equivalent shear strain for the aluminum rods using the equation Drnevich created for soil samples.

The polar mass moment of inertia were experimentally determined to be $2.858 \times 10^{-3}\ m^2kg$ and $2.893 \times 10^{-3}\ m^2kg$, for the large and small rods respectively. For the final value of polar mass moment of inertia the polar mass moment of inertia of the top attachment of the calibration rod needs to be subtracted. Then by adding the polar mass moment of inertia of the copper porous stone for soil testing results in our final values, final value is referred to as J_A. These values are $2.935 \times 10^{-3}\ m^2kg$ and $2.87 \times 10^{-3}\ m^2kg$. Both numbers are very close. Due to some modifications to the porous stone to increase the friction between the top platen system and sample the value used was actually $3.0 \times 10^{-3}\ m^2kg$. A set of sample calculations are included below.

Hardin Calibration Method (Directly from Manual):
Physical Characteristics of Sample (Large Aluminum Rod):

$G := 2.646\,10^{7}\cdot kPa = 2.646\times 10^{4}\cdot MPa$ Based on Tatsuoka and Silver paper and some online research. Drnevich uses a G of 23.7 GPa but

$D := 0.375\,in$ $I_P := \frac{\pi\cdot D^4}{32} = 8.081\times 10^{-10}\,m^4$

$l_1 := (5.764\,in - 2\cdot 0.25\,in) = 0.134\,m$ $K_{cr} := \frac{G\cdot I_P}{l_1} = 159.919\,N\cdot m$

For Natural Frequency I used an average value

$f_{n1} := 37.65\,Hz$ $J_{o1} := \frac{K_{cr}}{\left(2\cdot\pi\cdot f_{n1}\right)^2} = 2.858\times 10^{-3}\,m^2\cdot kg$

Small Aluminum Rod:

$D := 0.375\,in$ $I_P := \frac{\pi\cdot D^4}{32} = 8.081\times 10^{-10}\,m^4$

$l_2 := (5.2\,in - 2\cdot 0.25\,in) = 0.119\,m$ $K_{cr} := \frac{G\cdot I_P}{l_2} = 179.109\,N\cdot m$

For Natural Frequency I used an average value

$f_{n2} := 39.6\,Hz$ $J_{o2} := \frac{K_{cr}}{\left(2\cdot\pi\cdot f_{n2}\right)^2} = 2.893\times 10^{-3}\,m^2\cdot kg$

Both Rods give a close estimate for polar mass of inertia

$J_{ATop} := 4.301\times 10^{-5}\,m^2\cdot kg$ $J_{Platen} := 0.0001199\,m^2\cdot kg$ Directly from manual

$J_{A1} := J_{o1} - J_{ATop} + J_{Platen} = 2.935\times 10^{-3}\,m^2\cdot kg$

$J_{A2} := J_{o2} - J_{ATop} + J_{Platen} = 2.97\times 10^{-3}\,m^2\cdot kg$

Besides using different calibration rods the polar mass moment of inertia was also verified using alternative methods. The second method used to calculate J_A was taken from (Tatsuoka & Silver, 1980). This method has some advantages over the other. The most important being that material properties, such as shear modulus, are not needed in order to find J_A. It is important to note that this method was used as verification of the previous one. It is not discussed in the ASTM standards for resonant column so it was used to verify whether the numbers resulting from the previous method were reasonable. In order to use this method it is important to understand some the derivation. Firstly, the following relationship is known to be true for shear modulus:

$$G = \rho\left(\frac{2\pi f_n l}{F}\right)^2 \qquad \text{A.5}$$

In equation A.5, f_n is the resonant frequency, l is the length, ρ is the density and F is the dimensionless frequency factor. This equation is the same as 4.6 in the data reduction section. Dimensionless frequency factor can be read of a chart provided in ASTM D4015 (this is also shown in figure 4.2).Dimensionless frequency factor is also described by the following equation:

$$F\tan F = \frac{J}{J_A - \frac{K_S}{(2\pi f_n)^2}} \qquad \text{A.6}$$

J, in equation A. 6, is the total rotational moment of inertia of a sample. K_S is the spring constant. Spring constant can be related to the resonant frequency of the system, f_{OT}.

$$f_{OT} = \frac{1}{2\pi}\sqrt{\frac{K_S}{J_A}} \qquad \text{A.7}$$

Equation A.7 is then solved for K_s, the spring constant, and then plugging that into equation A.6, for dimensionless frequency factor. This gets ride of the spring constant in equation A.6.

$$F \tan F = \frac{J}{J_A\left[1-\frac{f_{OT}}{fn}\right]^2} \qquad \text{A.8}$$

For this method two calibration samples with different rotational moments of inertia need to be tested. The calibration samples basically consist of rods and top and bottom masses. In figure A.3 this is shown more clearly. As you can see in figure A.3 both of the rods of the calibration samples need to have the same physical properties (i.e. length, rotational moment of inertia, and density). Also the rods should have the same shear modulus value. Then equation A.5 can be made equal to each other because they have the same shear modulus. That gives use the following relationship:

$$\rho\left(\frac{2\pi f_{n1} l}{F_1}\right)^2 = \rho\left(\frac{2\pi f_{n2} l}{F_2}\right)^2 \qquad \text{A.9}$$

As seen in equation A.9, most of the terms are the same and can actually be dropped out. Dropping those like terms leaves the following:

$$\frac{f_{n1}}{F_1} = \frac{f_{n2}}{F_2} \qquad \frac{f_{n1}}{f_{n2}} = \frac{F_1}{F_2} \qquad \text{A.10}$$

This equation shows that the rods have linear relationships with each other. (Tatsuoka & Silver, 1980) Using this relationship the following is established:

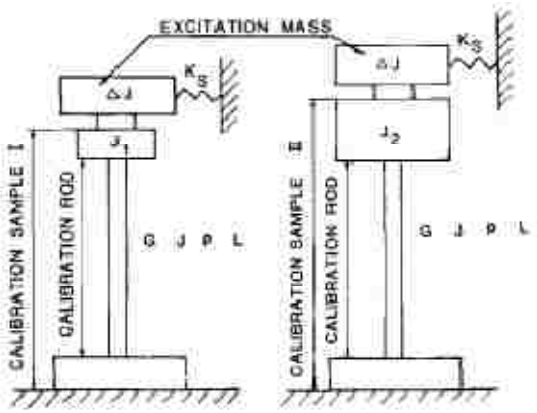

Figure A.3- From (Tatsuoka & Silver, 1980) Calibration Rods

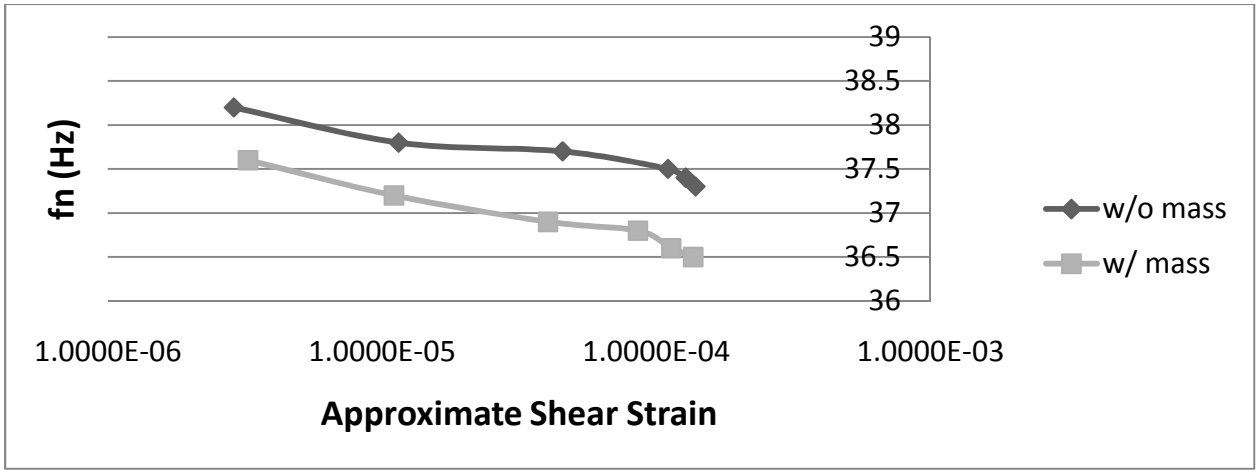

Figure A.4- Results for New Method of Calibration

$$J_A = \frac{J_2 - J_1}{\left(\frac{f_{n1}}{f_{n2}}\right)^2 - 1} \qquad \text{A.11}$$

Equation A.11 is pretty straight forward and convenient. Basically, two rods with the same properties are tested. By adding more weight to the top of one, therefore increasing its mass moment of inertia and reducing its natural frequency, J_A can be experimentally determined. For my calibration, the same rod was used, one without a mass attached and another with a mass attached. As previously stated this changes the mass moment of inertia of either rod, also by using the same rod we reduce the possibility of having different physical properties, which was a point of emphasize for the author.

Figure A.4 shows the test results for each rod. The rod without a mass has a higher frequency than the rod with the mass, which was expected. It was recommended to use the most linear part of the data. Most materials are linear from 10^6 to 10^5 strain range. This range was extrapolated from then data and interpreted using a linear equation. This is shown in Mathcad on the following page. In the calculations the following relationship was used in equation A. 11, $\Delta J = J_2 - J_1$, this basically ends up being the mass moment of inertia of the copper porous stone, which is $1.199 \times 10^{-3}\ m^2 kg$ (value has been used throughout text and is taken from Drnevich's manual).

Using Tatsuoka and Silver Method:

$fn_1(\gamma) := 37.841 - 3084.8\gamma$

$fn_2(\gamma) := 37.079 - 3918.5\gamma$

$\Delta J := 0.0001199 \cdot kg \cdot m^2$

$$J_{Avg} := \frac{\Delta J}{\left(\frac{fn_1(0.00001105)}{fn_2(0.00001105)}\right)^2 - 1} = 2.849 \times 10^{-3}\, m^2 \cdot kg$$

This value does not include the mass moment of inertia of the copper porous stone. If the porous stone is included the final value becomes $2.969 \times 10^{-3}\ m^2kg$. This values measures up favorably with the previous method for measuring mass moment of inertia, this is shown in table A.1. There is about a 0.5% error between the values.

	ASTM D4015 (Average Value)	(Tatsuoka & Silver, 1980)
J_A, mass moment of inertia of top platen	$2.952 \times 10^{-3}\ m^2kg$	$2.969 \times 10^{-3}\ m^2kg$

Table A.1- Polar mass moment of inertia of top platen

A.2 Torque Calibration Constant

Besides mass moment of inertia of top platen there are other system constants that need to be determined during the calibration process. In this section the constant that is determined is the Torque Calibration Constant (TCF). ASTM D4015 describes the process for verifying the TCF. The method consist of taking two measurements one at 0.707 time the resonant frequency of the rod, the other being at 1.414 times the resonant frequency of the rod. The resonant frequency of the rod used was 37.6 Hz (average value for the larger rod). The measurements were taking at 26.6 Hz (0.707 times f_n) and 53.2 Hz (1.414 times f_n). The measurements were made on varied amplitude of power delivered to the drive coils or CRT in order to verify the results. Using these measurements C_1 and C_2 (constants used to find TCF) can be found. C_1 corresponds to the 0.707 reading and C_2 to the 1.414 reading. The constants are defined by the following equations:

$$C_1 = \frac{RCF * RTO_{0.707}}{2CRT_{0.707}} \quad \text{A.12}$$

$$C_2 = \frac{RCF * RTO_{1.414}}{CRT_{1.414}} \quad \text{A.13}$$

RCF is a calibration factor that is given for the accelerometer. The equation for RCF is given in chapter 4 (equation 4.8). RTO is the accelerometer reading in voltage and CRT is the power delivered to the drive coil, this is explained in chapter 4.

$$TCF = \frac{(C_1 + C_2)K}{2} \quad \text{A.14}$$

In equation A.14 the constant K is the stiffness of the rod that is being used to calibrate the equipment. For this phase of the calibration process the larger rod was used, its stiffness was 159.91 N-m (using equation A.3). ASTM does stipulate that the C values cannot be more than

10% apart. Also it states that the voltage readings should be ten times higher than the signal when the machine is off, in other words the noise of the signal (which is about 0.001), so as to make sure that the instrumentation is measuring the forcing function. A set of calculations are included on the next page. This number is lower than any previous ones. I repeated the test several times.

	Current Calibration	Previous Calibration
TCF, Torque Calibration Factor	0.03	0.049

Table A.2- Torque Calibration Factor comparison

Torque Calibration Factor using ASTM D4015

$f_n := 36.7 \cdot Hz$ $f_{0.707} := 26.6 \cdot Hz$ $f_{1.414} := 53.1 \cdot Hz$

$RCF_{0.707} := \frac{4.4723}{f_{0.707}^2 \cdot s^2} = 6.321 \times 10^{-3}$ $RCF_{1.414} := \frac{4.4723}{f_{1.414}^2 \cdot s^2} = 1.586 \times 10^{-3}$

$CRT_{0.707} := 1.04$ $CRT_{1.414} := 1.04$ $K := 159.91$

$RTO_{0.707} := 0.0$ $RTO_{1.414} := 0.13$

$C_1 := \frac{0.5 \cdot RTO_{0.707} RCF_{0.707}}{CRT_{0.707}} = 1.808 \times 10^{-4}$ $C_2 := \frac{RTO_{1.414} RCF_{1.414}}{CRT_{1.414}} = 1.996 \times 10^{-4}$

$TCF := \frac{(C_1 + C_2) \cdot K}{2} = 0.03$

A.3 Apparatus Damping Coefficient for Torsion

The final constant that needs to be verified is the apparatus damping coefficient for torsion. This is basically done by conducting what is typically referred to as a "free vibration" test. Basically, the rod is excited and allowed to vibrate freely. In this case the calibration rod is excited at its resonant frequency and then shut it off. That is shown in figure A.5. Figure A.6 takes the data from A.5 and plots the peaks versus No. of cycles in order to process the data more efficiently. The data from these graphs are used in the following equation that is taken from ASTM D4015.

$$ADC_{oT} = 2f_{oT}J_A\delta_T \qquad \text{A.15}$$

Mass moment of inertia, J_A, was found earlier in the calibration process. The other parameter, f_{oT}, is the torsional motion resonant frequency measured during damping determination. In this case that was taken to be the resonant frequency of the rod. The other parameter is δ_T or logarithmic decrement for torsional motion. Logarithmic decrement for torsion is given by the following equation:

$$\delta_T = \frac{1}{n}\log\left(\frac{A_1}{A_n}\right) \qquad \text{A.16}$$

In equation A.16, the A values refer to the amplitude of the cycle. A_1 is the notation for the amplitude of the first cycle and A_n the amplitude of the n^{th} cycle. The results using figure A.6 give a $\delta_T = 0.01933$. This value is plugged into equation A.15. ADC_{oT} then is about 0.004 which matches the number that is on the calibration sheets.

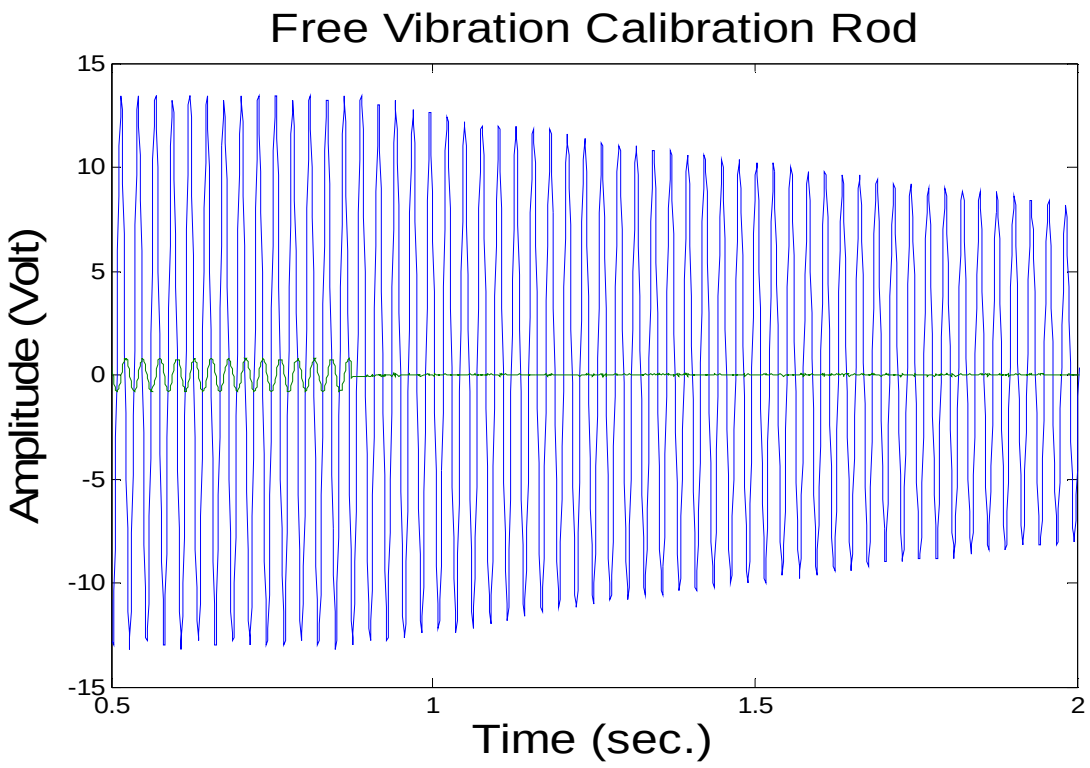

Figure A.5- Free Vibration of the calibration rod

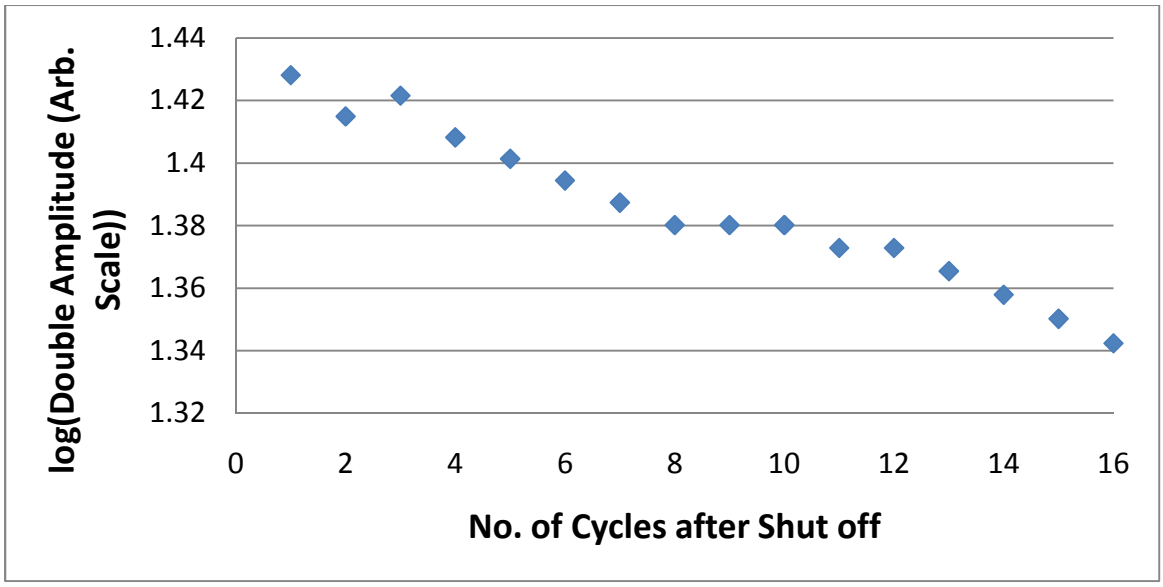

Figure A.6- Peaks versus number of cycles

A.4 Sample Test

Now that I have the three system constants, shown in table A.3. A test was run in order to verify whether the calibration yielded reasonable results. Using a rod with known properties a frequency sweep was conducted in order to determine the resonant frequency of the rod at varying strain amplitudes. Some assumptions needed to be made. For example, the dimensionless frequency factors actually fall out of the range that is provided. In order to use the charts that are provided for F (Dimensionless frequency factor) and A (Damping factor), ADF has to be equal to zero. This is not the case here but in order to continue it was necessary to ignore this rule and just assume that ADF is about zero (the other option would have been to use a program that is giving in ASTM but the program makes some assumptions in order to converge that I was not sure about). Also, damping factor was out of the range of the charts, but in Drnevich's manual he states that A can be assumed to be twice the value of T_T, Active-end factor for torsional motion for most cases. This resulted in shear modulus values that varied from 2.81 x 10^4 - 2.69 x 10^4 MPa. As previously mentioned aluminum alloy has a shear modulus of about 2.646 x 10^4 MPa. The slight variance could be attributed to two reasons; dimensionless frequency factor being slightly off, or the material might have a higher stiffness than we predicted. Also the Damping ratio matched pretty closely for both free vibration and steady state damping.

J_A, mass moment of inertia of top platen	TCF, Torque Calibration Factor	ADC_{oT}, Apparatus damping coefficient for torsion
$2.952 \times 10^{-3}\, m^2 kg$	0.03	0.004

Table A.3- Summary of Calibration

ft (Hz)	Jm (kg/m2)	Tt	ADFt	TCF	γ (Shear Strain)	G	Dt (damping ratio)	FV Damping	Error
38.2	0.0029	9835.23	56.52	0.03	0.00029%	2.81E+10	0.80%	0.75%	6.29%
37.7	0.0029	9835.23	57.27	0.03	0.00456%	2.74E+10	0.29%	0.29%	1.75%
37.5	0.0029	9835.23	57.58	0.03	0.01104%	2.71E+10	0.35%	0.40%	16.04%
37.4	0.0029	9835.23	57.73	0.03	0.01281%	2.69E+10	0.51%	0.77%	49.27%

Table A.4- Results of Aluminum Rod

Appendix B. DATA REDUCTION CURVES

B.1 UNDISTURBED

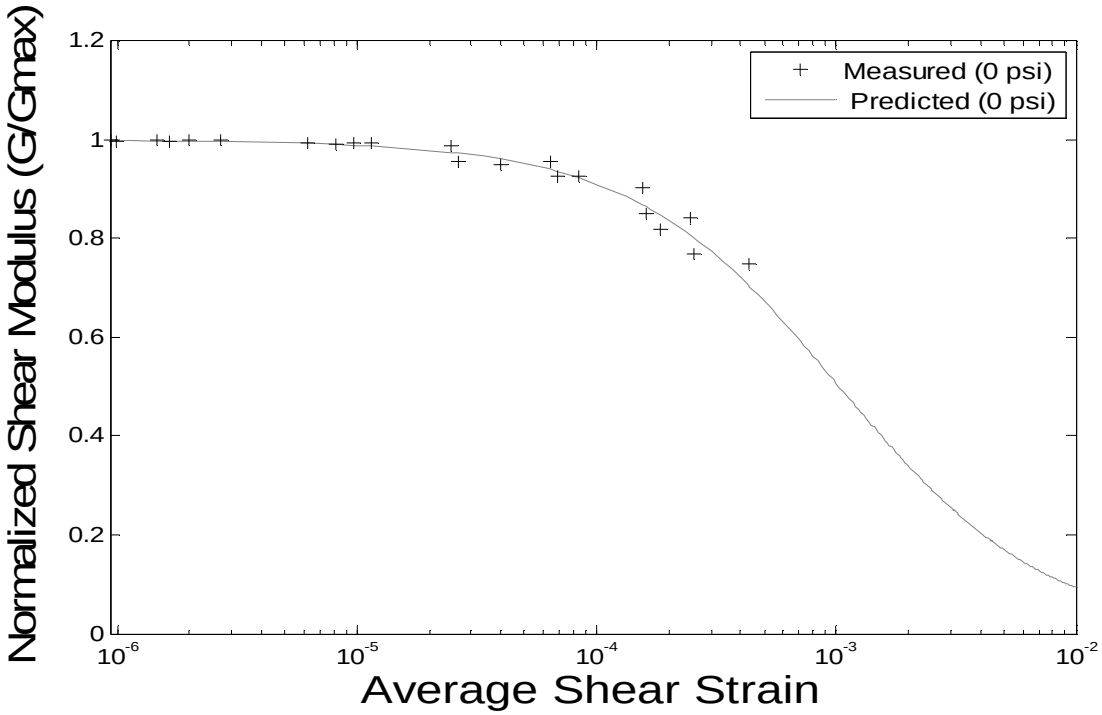

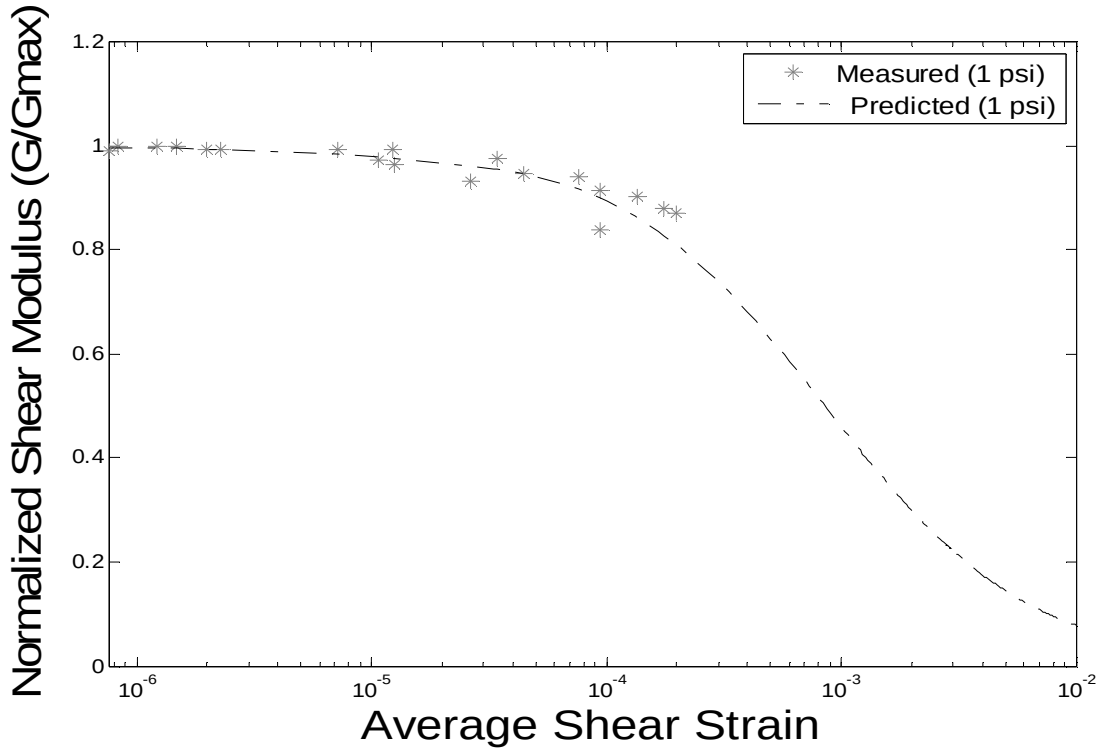

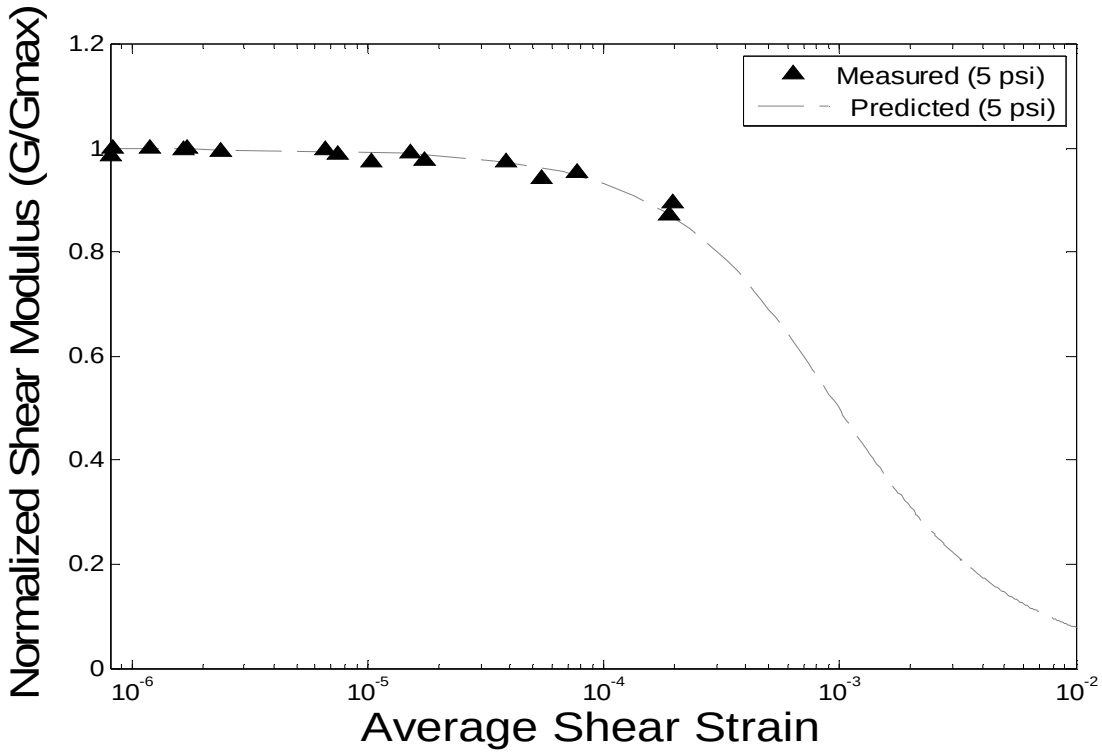
Normalized Shear Modulus (G/Gmax)
Average Shear Strain
Measured (5 psi)
Predicted (5 psi)
1.2
1
0.8
0.6
0.4
0.2
0
10-6
10-5
10-4
10-3
10-2

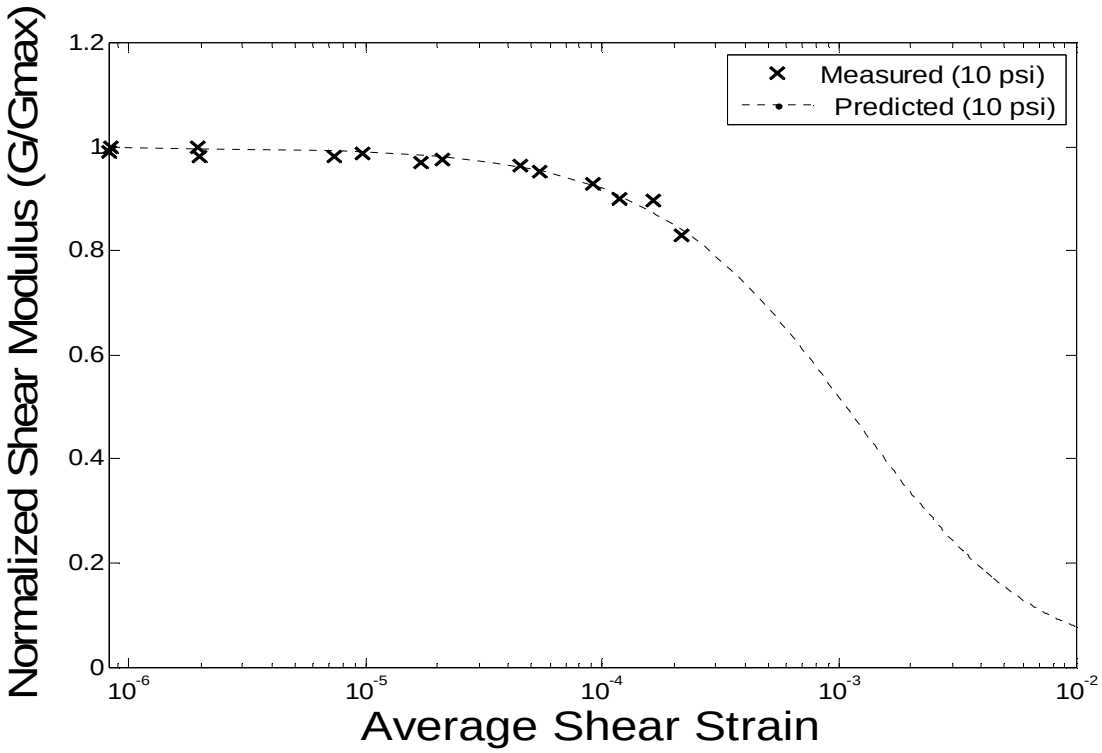
Normalized Shear Modulus (G/Gmax)
Average Shear Strain
Measured (10 psi)
Predicted (10 psi)
1.2
1
0.8
0.6
0.4
0.2
0
10-6
10-5
10-4
10-3
10-2

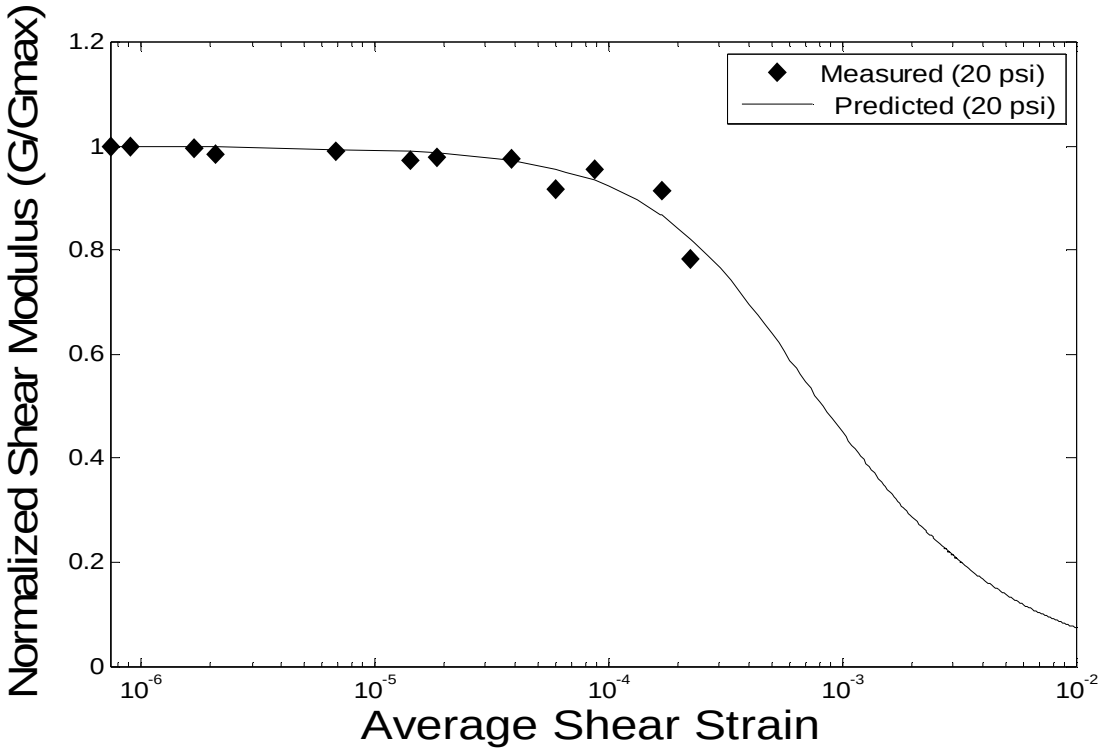
Normalized Shear Modulus (G/Gmax)
1.2
1
0.8
0.6
0.4
0.2
0
Measured (20 psi)
Predicted (20 psi)
10-6
10-5
10-4
10-3
10-2
Average Shear Strain

B.2 UNDISTURBED HEATED

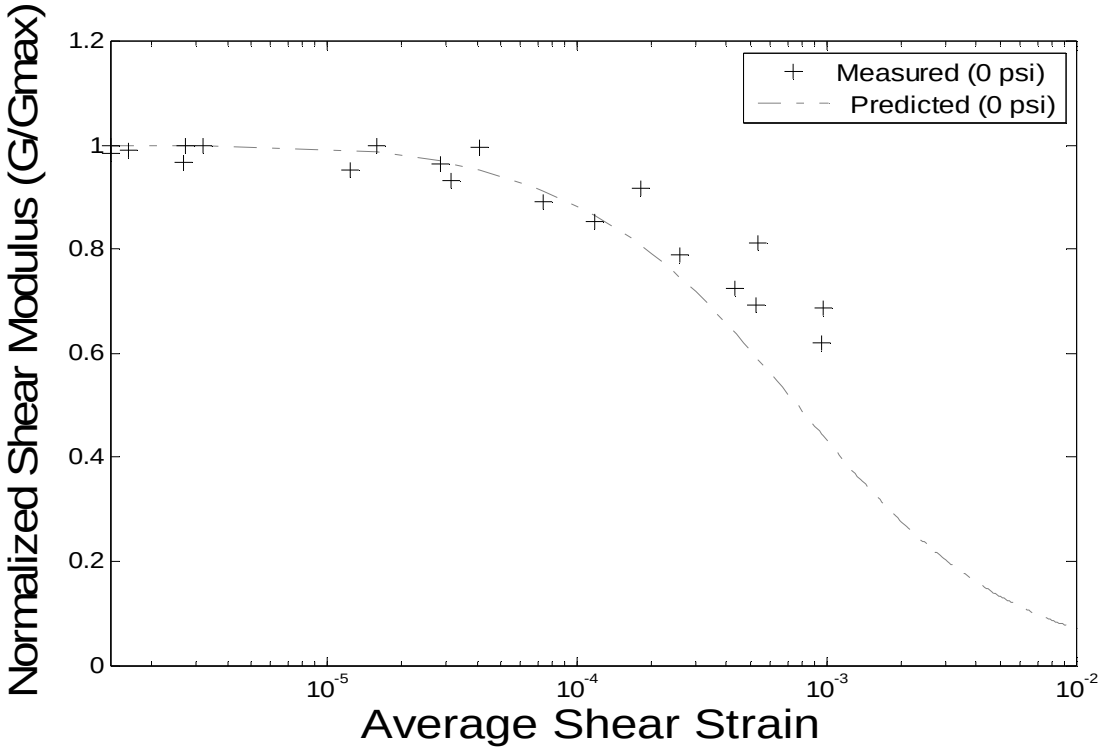

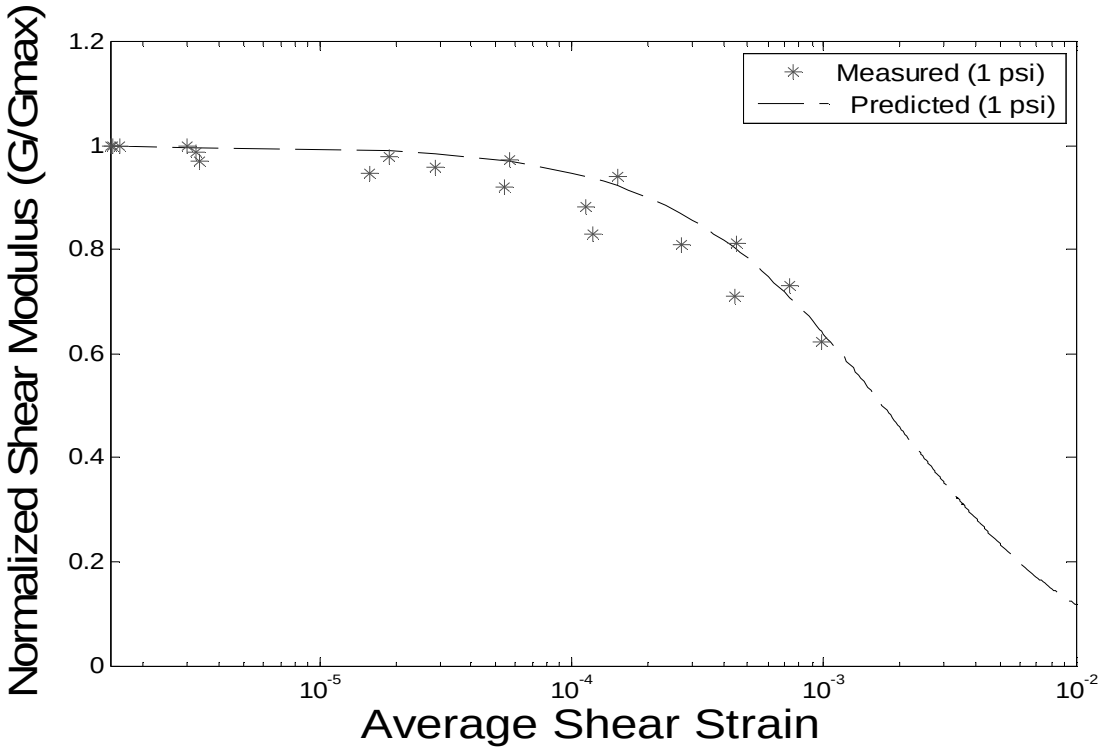

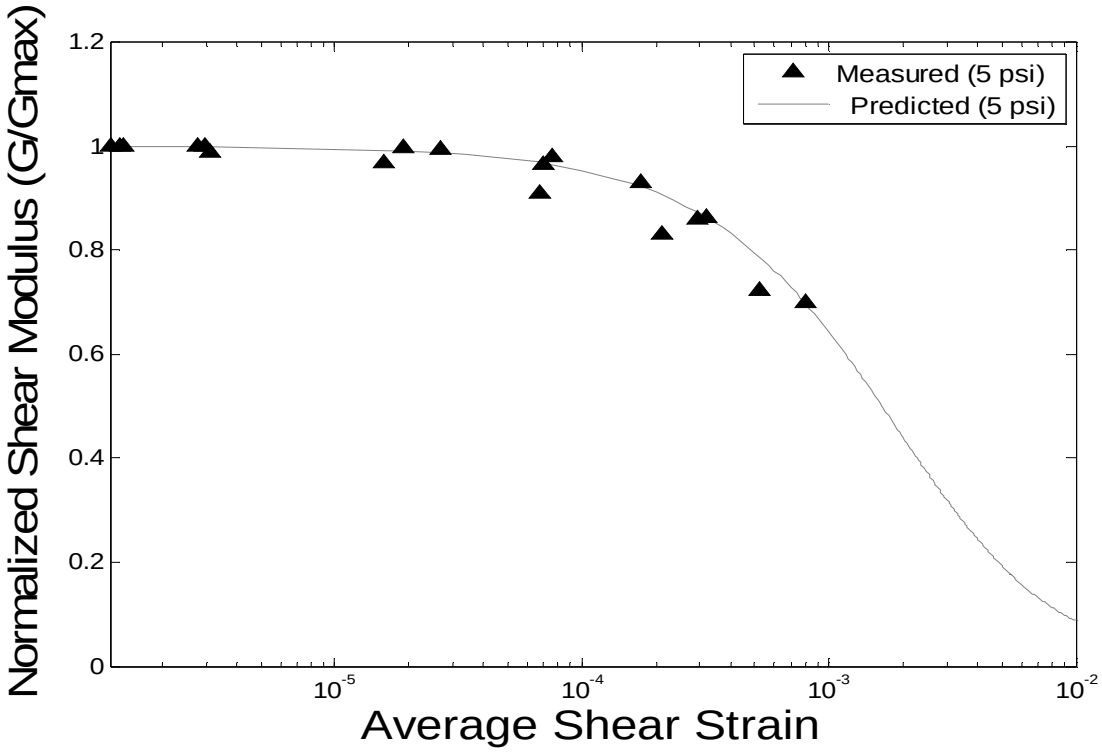
Normalized Shear Modulus (G/Gmax)
Average Shear Strain
Measured (5 psi)
Predicted (5 psi)
1.2
1
0.8
0.6
0.4
0.2
0
10^{-5}
10^{-4}
10^{-3}
10^{-2}

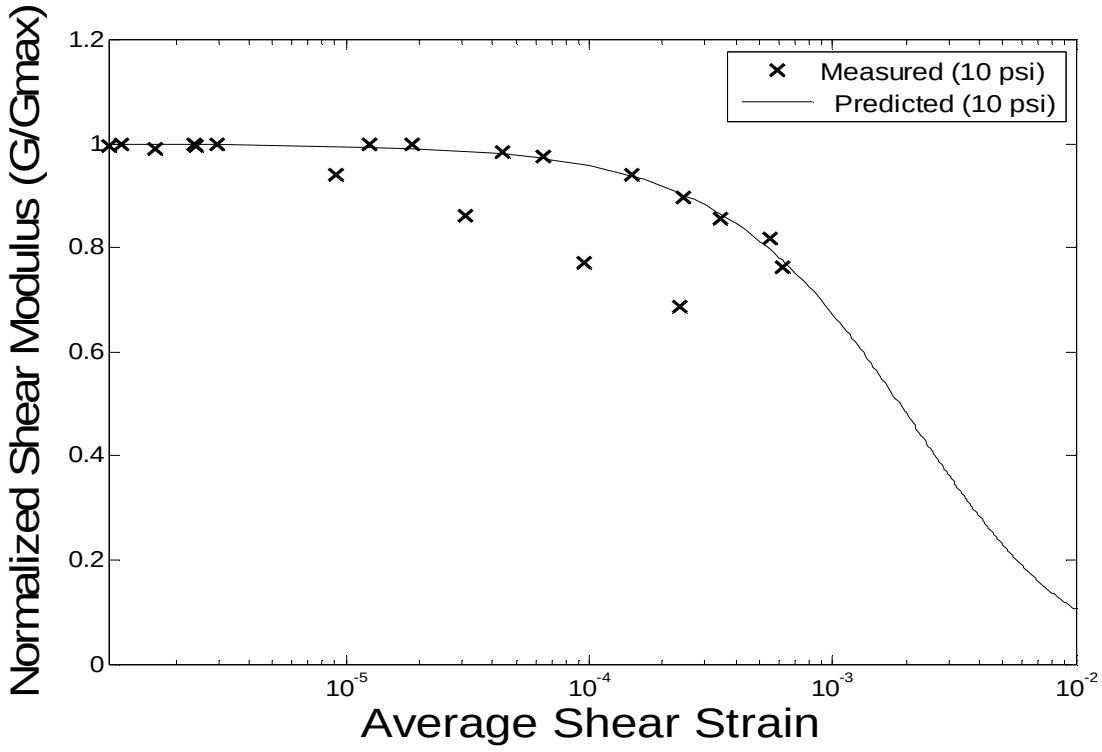
Normalized Shear Modulus (G/Gmax)
Average Shear Strain
Measured (10 psi)
Predicted (10 psi)
1.2
1
0.8
0.6
0.4
0.2
0
10^{-5}
10^{-4}
10^{-3}
10^{-2}

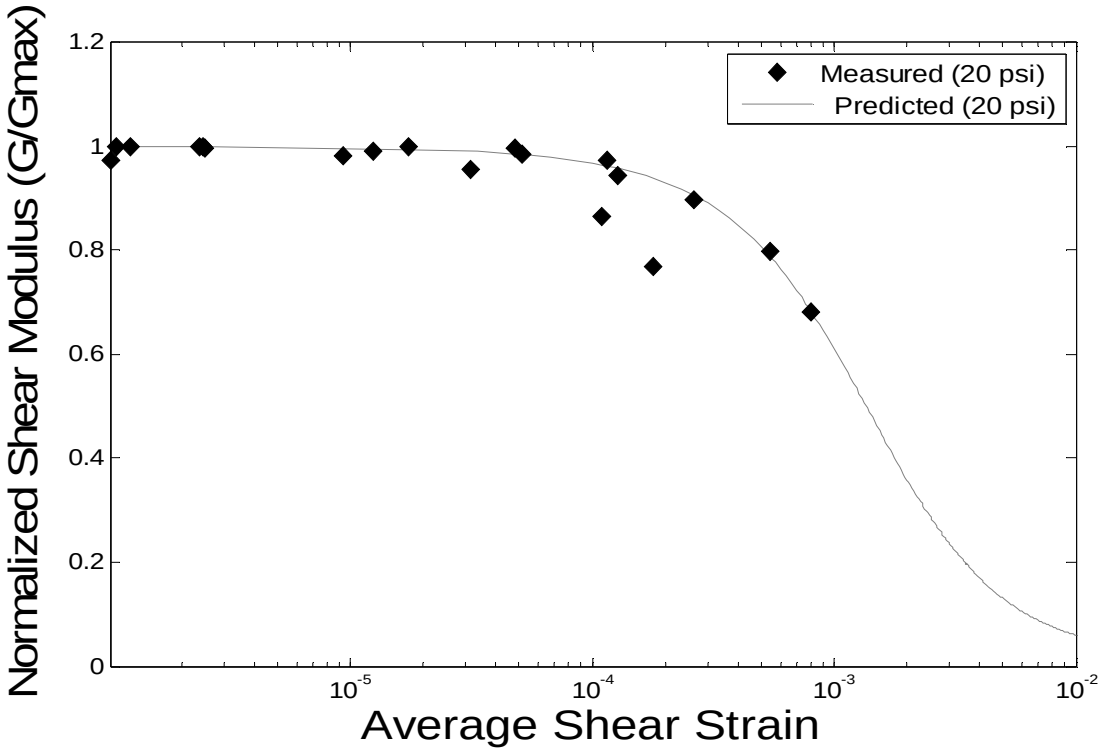
Normalized Shear Modulus (G/Gmax)
1.2
1
0.8
0.6
0.4
0.2
0
Measured (20 psi)
Predicted (20 psi)
10-5
10-4
10-3
10-2
Average Shear Strain

B.3 REMOLDED

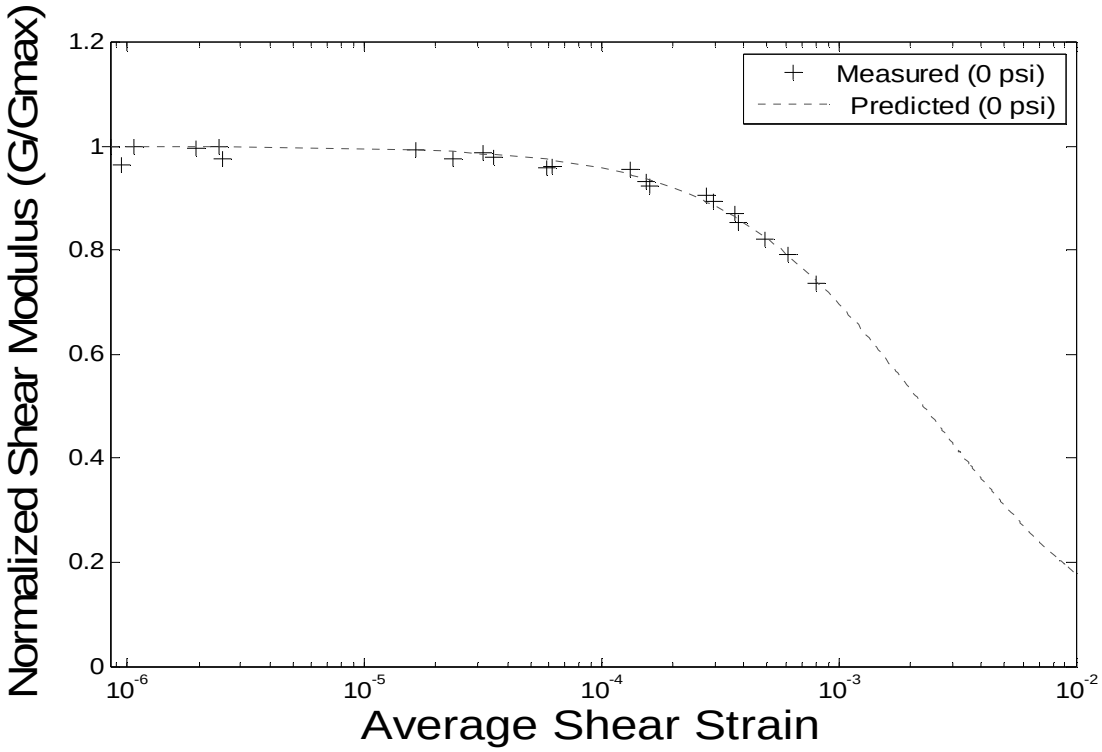
Normalized Shear Modulus (G/Gmax)
Average Shear Strain
Measured (0 psi)
Predicted (0 psi)
1.2
1
0.8
0.6
0.4
0.2
0
10-6
10-5
10-4
10-3
10-2

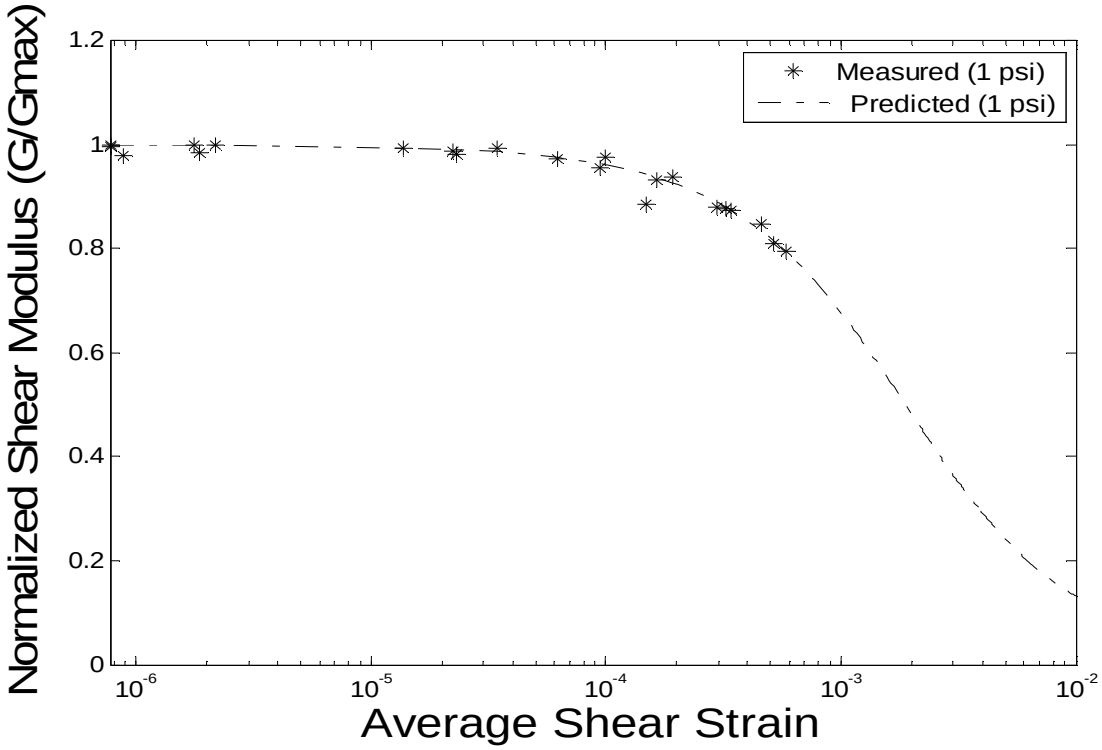
Normalized Shear Modulus (G/Gmax)
Average Shear Strain
Measured (1 psi)
Predicted (1 psi)
1.2
1
0.8
0.6
0.4
0.2
0
10-6
10-5
10-4
10-3
10-2

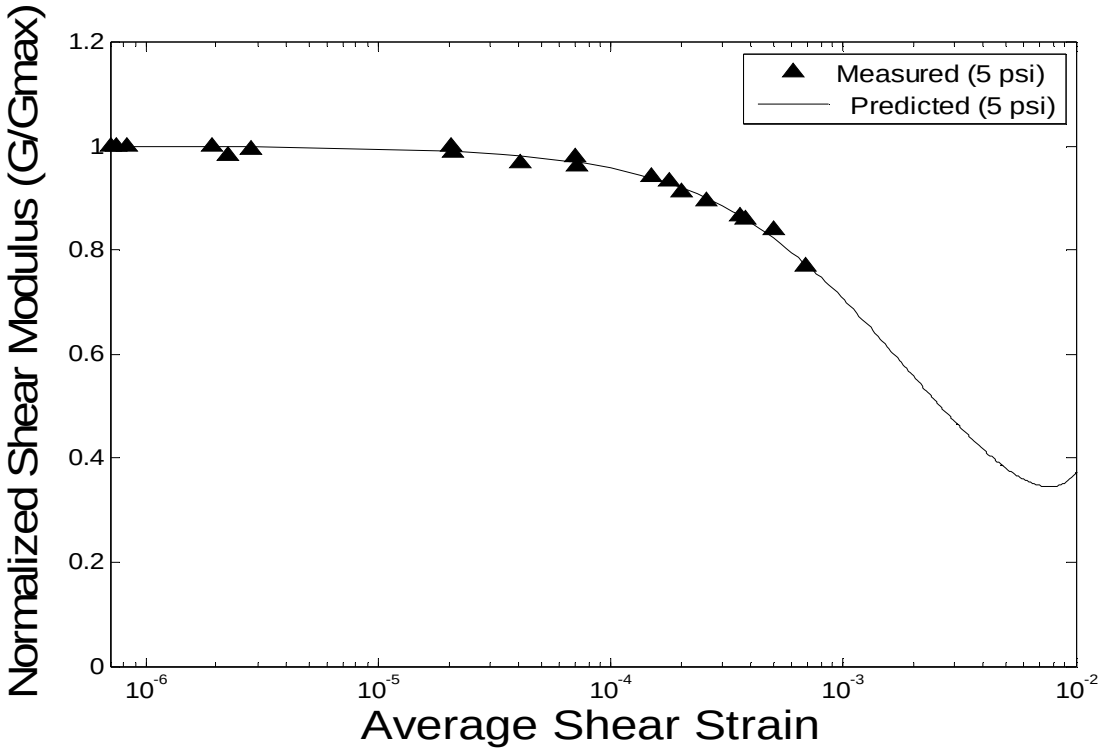
Measured (5 psi)
Predicted (5 psi)
Normalized Shear Modulus (G/Gmax)
Average Shear Strain
1.2
1
0.8
0.6
0.4
0.2
0
10-6
10-5
10-4
10-3
10-2

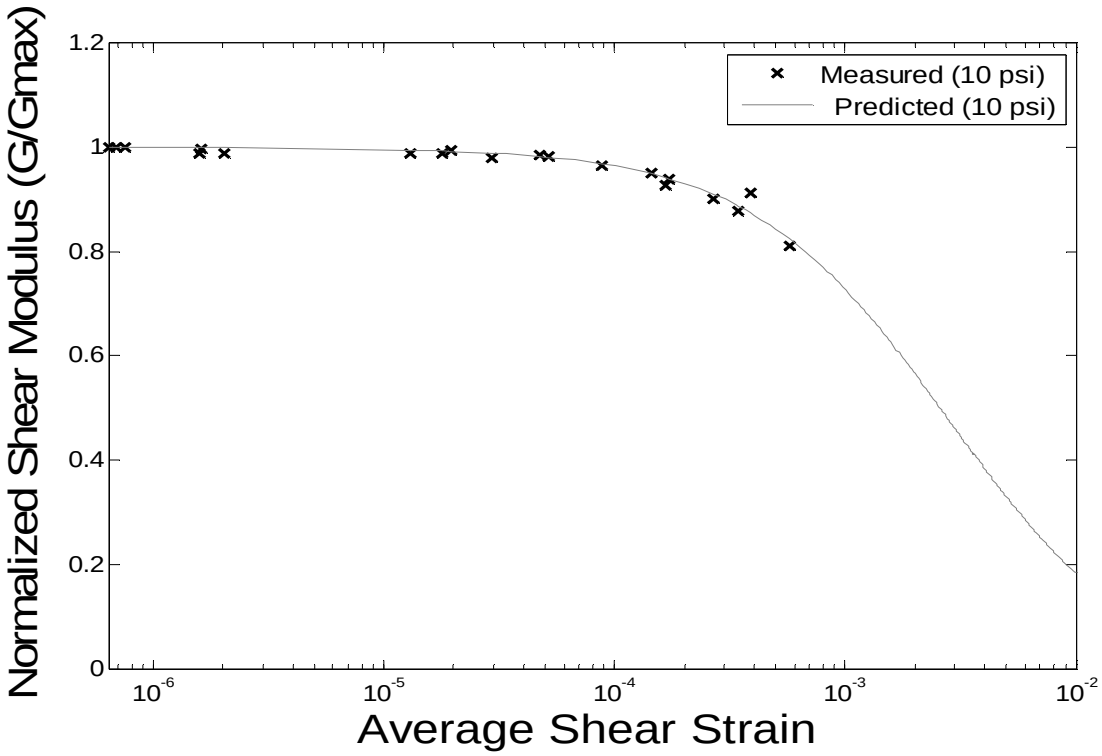
Measured (10 psi)
Predicted (10 psi)
Normalized Shear Modulus (G/Gmax)
Average Shear Strain
1.2
1
0.8
0.6
0.4
0.2
0
10-6
10-5
10-4
10-3
10-2

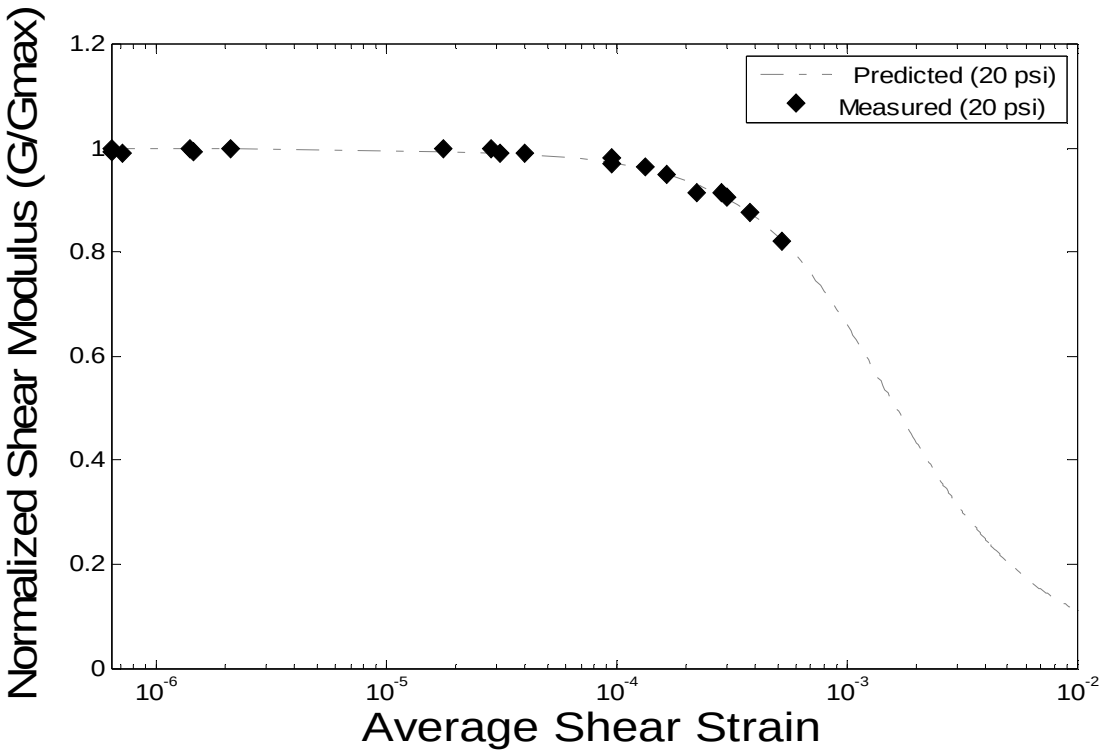
Normalized Shear Modulus (G/Gmax)
1.2
1
0.8
0.6
0.4
0.2
0
10^{-6}
10^{-5}
10^{-4}
10^{-3}
10^{-2}
Average Shear Strain
Predicted (20 psi)
Measured (20 psi)

B.4 REMOLDED HEATED

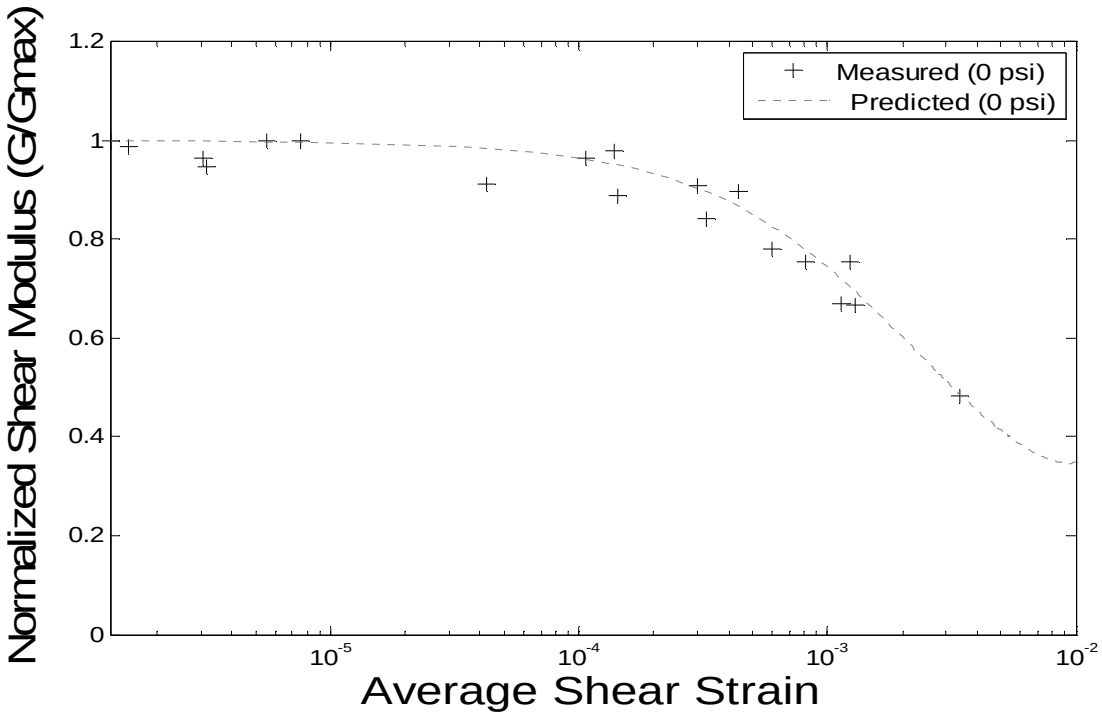

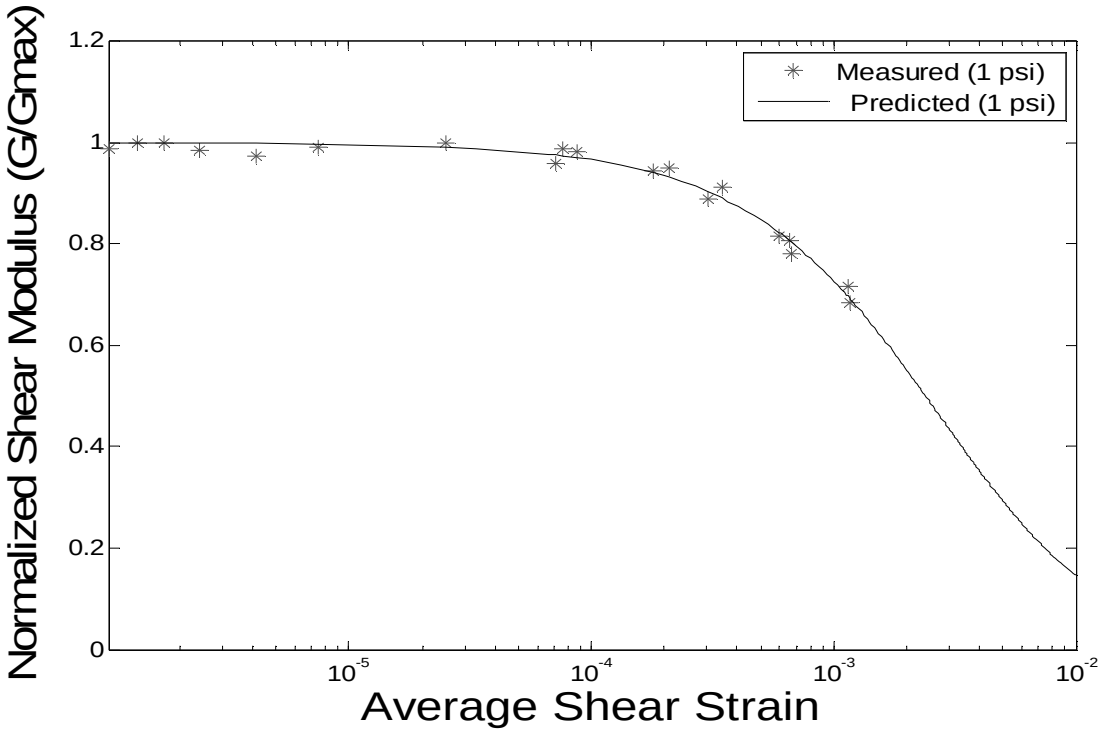

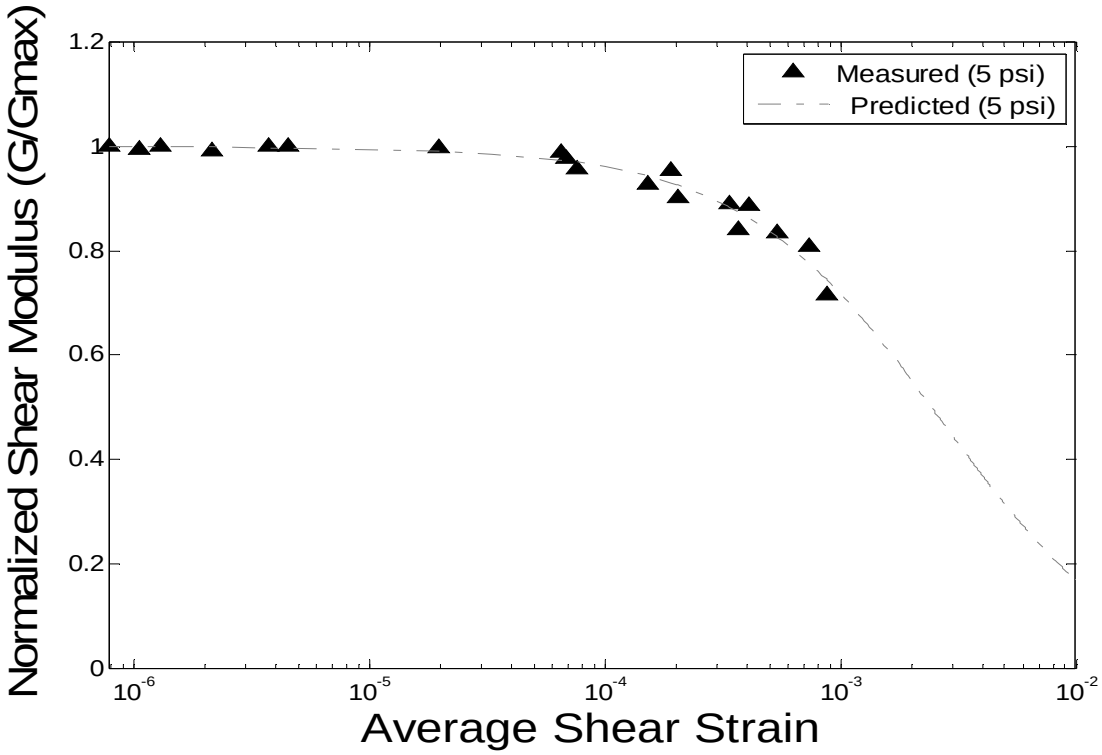
Measured (5 psi)
Predicted (5 psi)
Normalized Shear Modulus (G/Gmax)
Average Shear Strain
0
0.2
0.4
0.6
0.8
1
1.2
10-6
10-5
10-4
10-3
10-2

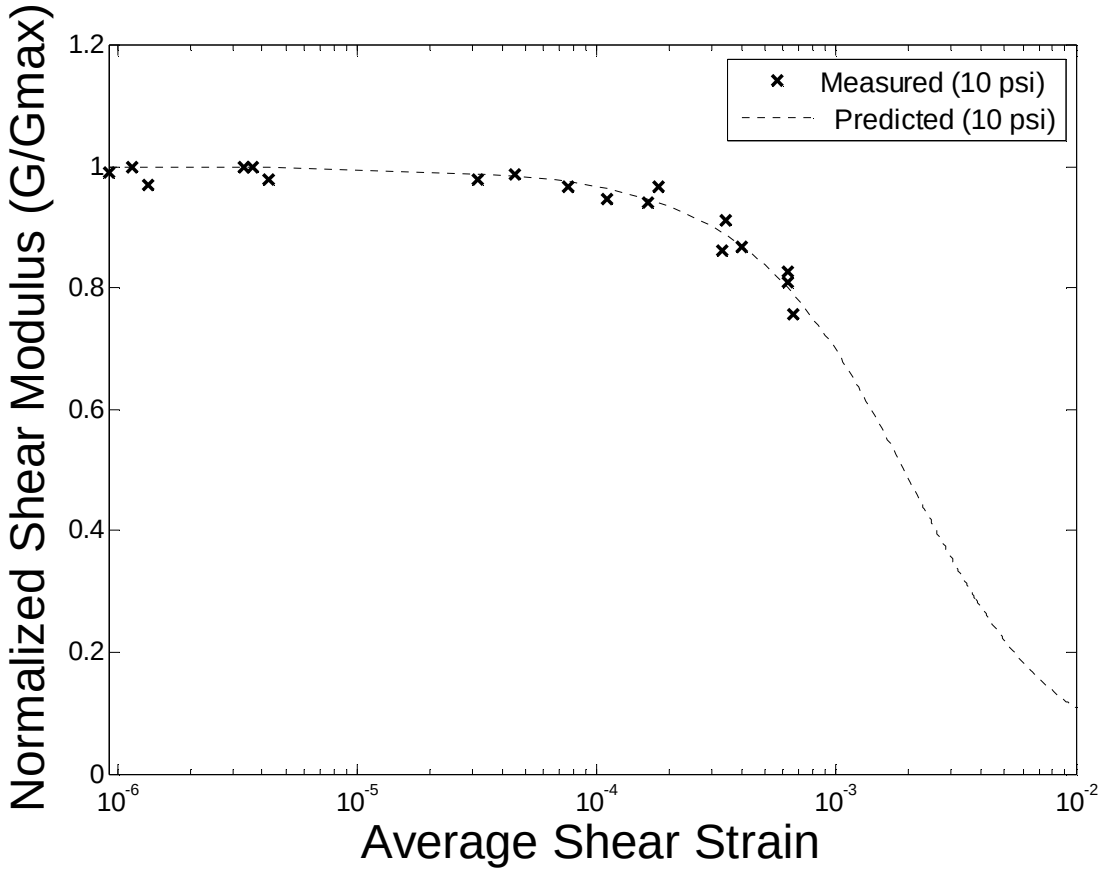
Measured (10 psi)
Predicted (10 psi)
Normalized Shear Modulus (G/Gmax)
Average Shear Strain
0
0.2
0.4
0.6
0.8
1
1.2
10-6
10-5
10-4
10-3
10-2

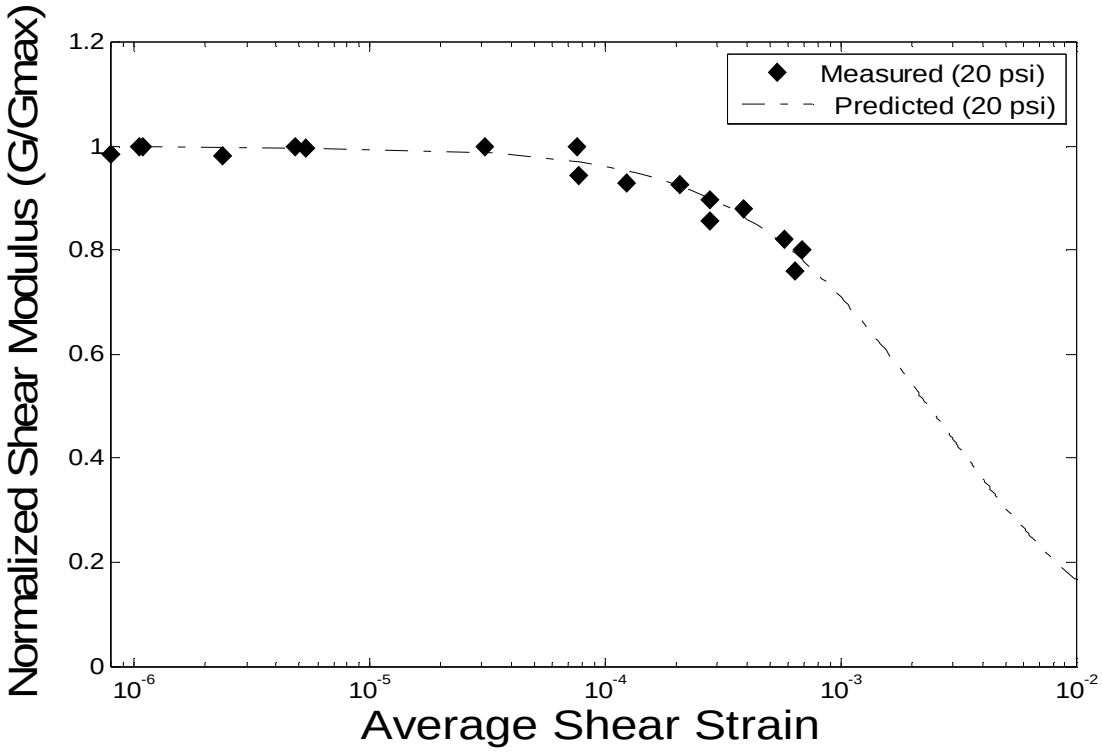
Normalized Shear Modulus (G/Gmax)
1.2
1
0.8
0.6
0.4
0.2
0
Measured (20 psi)
Predicted (20 psi)
10-6
10-5
10-4
10-3
10-2
Average Shear Strain

Appendix C. DATA SHEETS

C.1 UNDISTURBED

M	L	D	ft	RTO	CRT	V	p	Js	Tt	ADFt	RCF	MMFt	Ft	γ	G	A	Dt (%)
0.648	0.134	0.064	65.5	0.005	0.010	4.31E-04	1502	3.32E-04	9.05	2.93E-02	1.04E-03	9.76E-01	0.32	9.96E-07	44.6E+6	19	5.40%
0.648	0.134	0.064	65.6	0.010	0.020	4.31E-04	1502	3.32E-04	9.05	2.93E-02	1.04E-03	9.76E-01	0.32	1.99E-06	44.7E+6	19	5.40%
0.648	0.134	0.064	65.3	0.021	0.041	4.31E-04	1502	3.32E-04	9.05	2.94E-02	1.05E-03	9.99E-01	0.32	8.22E-06	44.3E+6	19	5.27%
0.648	0.134	0.064	64.1	0.054	0.127	4.31E-04	1502	3.32E-04	9.05	3.00E-02	1.09E-03	8.30E-01	0.32	2.64E-05	42.7E+6	19	6.34%
0.648	0.134	0.064	63.2	0.165	0.391	4.31E-04	1502	3.32E-04	9.05	3.04E-02	1.12E-03	8.23E-01	0.32	8.36E-05	41.5E+6	19	6.39%
0.648	0.134	0.064	60.5	0.227	0.687	4.31E-04	1502	3.32E-04	9.05	3.17E-02	1.22E-03	6.45E-01	0.32	1.60E-04	38.1E+6	19	8.16%
0.648	0.134	0.064	56.8	0.339	1.624	4.31E-04	1502	3.32E-04	9.05	3.38E-02	1.39E-03	4.07E-01	0.32	4.30E-04	33.5E+6	19	12.92%

M	L	d	ft	RTO	CRT	V	p	Js	Tt	ADFt	RCF	MMFt	Ft	γ	G	A	Dt (%)
0.648	0.134	0.064	71.9	0.005	0.010	4.31E-04	1502	3.32E-04	9.05	2.67E-02	8.65E-04	9.76E-01	0.32	8.26E-07	53.8E+6	19	5.40%
0.648	0.134	0.064	71.7	0.012	0.026	4.31E-04	1502	3.32E-04	9.05	2.68E-02	8.70E-04	9.01E-01	0.32	1.99E-06	53.5E+6	19	5.84%
0.648	0.134	0.064	70.9	0.026	0.063	4.31E-04	1502	3.32E-04	9.05	2.71E-02	8.90E-04	8.05E-01	0.32	1.07E-05	52.3E+6	19	6.54%
0.648	0.134	0.064	70.0	0.102	0.254	4.31E-04	1502	3.32E-04	9.05	2.74E-02	9.13E-04	7.84E-01	0.32	4.43E-05	51.0E+6	19	6.72%
0.648	0.134	0.064	68.8	0.212	0.523	4.31E-04	1502	3.32E-04	9.05	2.79E-02	9.45E-04	7.91E-01	0.32	9.44E-05	49.2E+6	19	6.65%
0.648	0.134	0.064	68.3	0.291	0.740	4.31E-04	1502	3.32E-04	9.05	2.81E-02	9.59E-04	7.67E-01	0.32	1.36E-04	48.5E+6	19	6.86%
0.648	0.134	0.064	67.5	0.369	0.943	4.31E-04	1502	3.32E-04	9.05	2.84E-02	9.82E-04	7.63E-01	0.32	1.77E-04	47.4E+6	19	6.89%

M	L	d	ft	RTO	CRT	V	p	Js	Tt	ADFt	RCF	MMFt	Ft	γ	G	A	Dt (%)
0.648	0.134	0.064	71.9	0.005	0.010	4.31E-04	1502	3.32E-04	9.05	2.67E-02	8.65E-04	9.76E-01	0.32	8.26E-07	53.8E+6	19	5.40%
0.648	0.134	0.064	71.8	0.010	0.020	4.31E-04	1502	3.32E-04	9.05	2.67E-02	8.68E-04	9.76E-01	0.32	1.66E-06	53.6E+6	19	5.40%
0.648	0.134	0.064	71.8	0.020	0.040	4.31E-04	1502	3.32E-04	9.05	2.67E-02	8.68E-04	9.76E-01	0.32	6.63E-06	53.6E+6	19	5.40%
0.648	0.134	0.064	71.6	0.041	0.091	4.31E-04	1502	3.32E-04	9.05	2.68E-02	8.72E-04	8.79E-01	0.32	1.52E-05	53.3E+6	19	5.99%
0.648	0.134	0.064	71.0	0.096	0.227	4.31E-04	1502	3.32E-04	9.05	2.70E-02	8.87E-04	8.25E-01	0.32	3.85E-05	52.4E+6	19	6.38%
0.648	0.134	0.064	70.2	0.177	0.440	4.31E-04	1502	3.32E-04	9.05	2.74E-02	9.08E-04	7.85E-01	0.32	7.63E-05	51.2E+6	19	6.71%
0.648	0.134	0.064	68.0	0.369	1.054	4.31E-04	1502	3.32E-04	9.05	2.82E-02	9.67E-04	6.83E-01	0.32	1.95E-04	48.1E+6	19	7.71%

M	L	d	ft	RTO	CRT	V	p	Js	Tt	ADFt	RCF	MMFt	Ft	γ	G	A	Dt (%)
0.648	0.134	0.064	73.5	0.005	0.011	4.31E-04	1502	3.32E-04	9.05	2.61E-02	8.28E-04	9.76E-01	0.32	8.38E-07	56.2E+6	19	5.40%
0.648	0.134	0.064	72.9	0.012	0.027	4.31E-04	1502	3.32E-04	9.05	2.63E-02	8.42E-04	8.89E-01	0.32	1.98E-06	55.3E+6	19	5.92%
0.648	0.134	0.064	72.9	0.021	0.046	4.31E-04	1502	3.32E-04	9.05	2.63E-02	8.42E-04	8.99E-01	0.32	7.40E-06	55.3E+6	19	5.85%
0.648	0.134	0.064	72.4	0.048	0.105	4.31E-04	1502	3.32E-04	9.05	2.65E-02	8.53E-04	8.92E-01	0.32	1.71E-05	54.5E+6	19	5.90%
0.648	0.134	0.064	72.2	0.122	0.272	4.31E-04	1502	3.32E-04	9.05	2.66E-02	8.58E-04	8.75E-01	0.32	4.46E-05	54.2E+6	19	6.01%
0.648	0.134	0.064	70.9	0.224	0.536	4.31E-04	1502	3.32E-04	9.05	2.71E-02	8.90E-04	8.15E-01	0.32	9.11E-05	52.3E+6	19	6.45%
0.648	0.134	0.064	69.6	0.345	0.929	4.31E-04	1502	3.32E-04	9.05	2.76E-02	9.23E-04	7.25E-01	0.32	1.64E-04	50.4E+6	19	7.26%

M	L	d	ft	RTO	CRT	V	p	Js	Tt	ADFt	RCF	MMFt	Ft	γ	G	A	Dt (%)
0.648	0.134	0.064	74.0	0.006	0.0108	4.31E-04	1502	3.32E-04	9.05	2.60E-02	8.17E-04	1.05E+00	0.32	9.05E-07	56.9E+6	19	5.02%
0.648	0.134	0.064	73.9	0.011	0.0208	4.31E-04	1502	3.32E-04	9.05	2.60E-02	8.19E-04	1.01E+00	0.32	1.69E-06	56.8E+6	19	5.20%
0.648	0.134	0.064	73.7	0.021	0.0434	4.31E-04	1502	3.32E-04	9.05	2.61E-02	8.23E-04	9.49E-01	0.32	6.83E-06	56.5E+6	19	5.55%
0.648	0.134	0.064	73.2	0.054	0.116	4.31E-04	1502	3.32E-04	9.05	2.62E-02	8.35E-04	9.08E-01	0.32	1.85E-05	55.7E+6	19	5.79%
0.648	0.134	0.064	73.1	0.115	0.243	4.31E-04	1502	3.32E-04	9.05	2.63E-02	8.37E-04	9.23E-01	0.32	3.89E-05	55.6E+6	19	5.70%
0.648	0.134	0.064	72.4	0.242	0.537	4.31E-04	1502	3.32E-04	9.05	2.65E-02	8.53E-04	8.79E-01	0.32	8.75E-05	54.5E+6	19	5.99%
0.648	0.134	0.064	70.8	0.397	0.992	4.31E-04	1502	3.32E-04	9.05	2.71E-02	8.92E-04	7.81E-01	0.32	1.69E-04	52.1E+6	19	6.74%

M	L	d	ft	RTO	CRT	V	p	Js	Tt	ADFt	RCF	MMFt	Ft	γ	G	A	Dt (%)
0.658	0.135	0.064	63.3	0.004	0.010	4.34E-04	1516	3.37E-04	8.90	2.98E-02	1.12E-03	8.33E-01	0.32	8.89E-07	42.7E+6	19	6.32%
0.658	0.135	0.064	63.2	0.008	0.020	4.34E-04	1516	3.37E-04	8.90	2.99E-02	1.12E-03	7.78E-01	0.32	1.66E-06	42.5E+6	19	6.77%
0.658	0.135	0.064	63.1	0.011	0.029	4.34E-04	1516	3.37E-04	8.90	2.99E-02	1.12E-03	7.53E-01	0.32	6.18E-06	42.4E+6	19	6.99%
0.658	0.135	0.064	63.1	0.020	0.054	4.34E-04	1516	3.37E-04	8.90	2.99E-02	1.12E-03	7.35E-01	0.32	1.15E-05	42.4E+6	19	7.16%
0.658	0.135	0.064	62.9	0.044	0.116	4.34E-04	1516	3.37E-04	8.90	3.00E-02	1.13E-03	7.53E-01	0.32	2.49E-05	42.1E+6	19	6.99%
0.658	0.135	0.064	61.9	0.106	0.289	4.34E-04	1516	3.37E-04	8.90	3.05E-02	1.17E-03	7.28E-01	0.32	6.40E-05	40.8E+6	19	7.23%
0.658	0.135	0.064	60.2	0.232	0.663	4.34E-04	1516	3.37E-04	8.90	3.14E-02	1.23E-03	6.94E-01	0.32	1.55E-04	38.6E+6	19	7.58%
0.658	0.135	0.064	58.1	0.325	0.978	4.34E-04	1516	3.37E-04	8.90	3.25E-02	1.32E-03	6.59E-01	0.32	2.46E-04	36.0E+6	19	7.98%

M	L	d	ft	RTO	CRT	V	p	Js	Tt	ADFt	RCF	MMFt	Ft	γ	G	A	Dt (%)
0.658	0.135	0.064	68.0	0.004	0.010	4.34E-04	1516	3.37E-04	8.90	2.78E-02	9.67E-04	8.01E-01	0.32	7.70E-07	49.3E+6	19	6.57%
0.658	0.135	0.064	68.3	0.008	0.021	4.34E-04	1516	3.37E-04	8.90	2.77E-02	9.59E-04	7.90E-01	0.32	1.49E-06	49.7E+6	19	6.66%
0.658	0.135	0.064	68.1	0.015	0.039	4.34E-04	1516	3.37E-04	8.90	2.77E-02	9.64E-04	7.72E-01	0.32	7.19E-06	49.4E+6	19	6.81%
0.658	0.135	0.064	68.1	0.026	0.067	4.34E-04	1516	3.37E-04	8.90	2.77E-02	9.64E-04	7.70E-01	0.32	1.23E-05	49.4E+6	19	6.84%
0.658	0.135	0.064	67.5	0.071	0.186	4.34E-04	1516	3.37E-04	8.90	2.80E-02	9.82E-04	7.57E-01	0.32	3.46E-05	48.5E+6	19	6.95%
0.658	0.135	0.064	66.3	0.147	0.396	4.34E-04	1516	3.37E-04	8.90	2.85E-02	1.02E-03	7.36E-01	0.32	7.64E-05	46.8E+6	19	7.15%
0.658	0.135	0.064	63.8	0.339	0.954	4.34E-04	1516	3.37E-04	8.90	2.96E-02	1.10E-03	7.05E-01	0.32	1.99E-04	43.4E+6	19	7.47%

M	L	d	ft	RTO	CRT	V	p	Js	Tt	ADFt	RCF	MMFt	Ft	γ	G	A	Dt (%)
0.658	0.135	0.064	66.4	0.004	0.011	4.34E-04	1516	3.37E-04	8.90	2.84E-02	1.01E-03	7.72E-01	0.32	8.08E-07	47.0E+6	19	6.82%
0.658	0.135	0.064	66.9	0.010	0.024	4.34E-04	1516	3.37E-04	8.90	2.82E-02	9.99E-04	8.41E-01	0.32	1.89E-06	47.7E+6	19	6.26%
0.658	0.135	0.064	66.5	0.015	0.039	4.34E-04	1516	3.37E-04	8.90	2.84E-02	1.01E-03	7.63E-01	0.32	7.48E-06	47.1E+6	19	6.90%
0.658	0.135	0.064	66.1	0.035	0.090	4.34E-04	1516	3.37E-04	8.90	2.86E-02	1.02E-03	7.72E-01	0.32	1.75E-05	46.5E+6	19	6.82%
0.658	0.135	0.064	64.9	0.102	0.271	4.34E-04	1516	3.37E-04	8.90	2.91E-02	1.06E-03	7.47E-01	0.32	5.46E-05	44.9E+6	19	7.05%
0.658	0.135	0.064	62.5	0.310	0.869	4.34E-04	1516	3.37E-04	8.90	3.02E-02	1.14E-03	7.08E-01	0.32	1.89E-04	41.6E+6	19	7.44%

M	L	d	ft	RTO	CRT	V	p	Js	Tt	ADFt	RCF	MMFt	Ft	γ	G	A	Dt (%)
0.658	0.135	0.064	67.1	0.004	0.011	4.34E-04	1516	3.37E-04	8.90	2.81E-02	9.93E-04	7.72E-01	0.32	7.91E-07	48.0E+6	19	6.82%
0.658	0.135	0.064	67.4	0.010	0.026	4.34E-04	1516	3.37E-04	8.90	2.80E-02	9.84E-04	7.82E-01	0.32	1.94E-06	48.4E+6	19	6.73%
0.658	0.135	0.064	67.0	0.020	0.051	4.34E-04	1516	3.37E-04	8.90	2.82E-02	9.96E-04	7.78E-01	0.32	9.64E-06	47.8E+6	19	6.76%
0.658	0.135	0.064	66.6	0.042	0.110	4.34E-04	1516	3.37E-04	8.90	2.84E-02	1.01E-03	7.58E-01	0.32	2.10E-05	47.2E+6	19	6.95%
0.658	0.135	0.064	65.8	0.103	0.275	4.34E-04	1516	3.37E-04	8.90	2.87E-02	1.03E-03	7.43E-01	0.32	5.39E-05	46.1E+6	19	7.08%
0.658	0.135	0.064	64.0	0.203	0.566	4.34E-04	1516	3.37E-04	8.90	2.95E-02	1.09E-03	7.12E-01	0.32	1.17E-04	43.6E+6	19	7.40%
0.658	0.135	0.064	61.4	0.310	0.954	4.34E-04	1516	3.37E-04	8.90	3.08E-02	1.19E-03	6.45E-01	0.32	2.15E-04	40.2E+6	19	8.16%

M	L	d	ft	RTO	CRT	V	p	Js	Tt	ADFt	RCF	MMFt	Ft	γ	G	A	Dt (%)
0.658	0.135	0.064	68.4	0.004	0.010	4.34E-04	1516	3.37E-04	8.90	2.76E-02	9.56E-04	8.33E-01	0.32	7.61E-07	49.8E+6	19	6.32%
0.658	0.135	0.064	67.9	0.012	0.031	4.34E-04	1516	3.37E-04	8.90	2.78E-02	9.70E-04	7.36E-01	0.32	2.12E-06	49.1E+6	19	7.15%
0.658	0.135	0.064	67.5	0.028	0.077	4.34E-04	1516	3.37E-04	8.90	2.80E-02	9.82E-04	7.21E-01	0.32	1.43E-05	48.5E+6	19	7.30%
0.658	0.135	0.064	65.5	0.101	0.301	4.34E-04	1516	3.37E-04	8.90	2.88E-02	1.04E-03	6.66E-01	0.32	5.95E-05	45.7E+6	19	7.91%
0.658	0.135	0.064	60.6	0.297	0.981	4.34E-04	1516	3.37E-04	8.90	3.12E-02	1.22E-03	6.01E-01	0.32	2.27E-04	39.1E+6	19	8.76%

M	L	d	ft	RTO	CRT	V	p	Js	Tt	ADFt	RCF	MMFt	Ft	γ	G	A	Dt (%)
0.653	0.134	0.064	64.1	0.007	0.011	4.31E-04	1514	3.34E-04	8.98	2.97E-02	1.09E-03	1.25E+00	0.32	1.46E-06	43.1E+6	19	4.21%
0.653	0.134	0.064	64.1	0.013	0.021	4.31E-04	1514	3.34E-04	8.98	2.97E-02	1.09E-03	1.22E+00	0.32	2.70E-06	43.1E+6	19	4.32%
0.653	0.134	0.064	63.9	0.028	0.046	4.31E-04	1514	3.34E-04	8.98	2.98E-02	1.10E-03	1.20E+00	0.32	9.63E-06	42.8E+6	19	4.40%
0.653	0.134	0.064	62.5	0.089	0.181	4.31E-04	1514	3.34E-04	8.98	3.05E-02	1.14E-03	9.67E-01	0.32	3.96E-05	40.9E+6	19	5.44%
0.653	0.134	0.064	61.7	0.142	0.305	4.31E-04	1514	3.34E-04	8.98	3.09E-02	1.17E-03	9.15E-01	0.32	6.85E-05	39.9E+6	19	5.75%
0.653	0.134	0.064	58.0	0.238	0.727	4.31E-04	1514	3.34E-04	8.98	3.29E-02	1.33E-03	6.44E-01	0.32	1.85E-04	35.2E+6	19	8.18%
0.653	0.134	0.064	56.2	0.297	0.943	4.31E-04	1514	3.34E-04	8.98	3.39E-02	1.42E-03	6.19E-01	0.32	2.55E-04	33.1E+6	19	8.50%

M	L	d	ft	RTO	CRT	V	p	Js	Tt	ADFt	RCF	MMFt	Ft	γ	G	A	Dt (%)
0.653	0.134	0.064	64.6	0.006	0.011	4.31E-04	1514	3.34E-04	8.98	2.95E-02	1.07E-03	1.07E+00	0.32	1.23E-06	43.7E+6	19	4.91%
0.653	0.134	0.064	64.4	0.011	0.021	4.31E-04	1514	3.34E-04	8.98	2.96E-02	1.08E-03	1.03E+00	0.32	2.27E-06	43.5E+6	19	5.11%
0.653	0.134	0.064	63.5	0.030	0.059	4.31E-04	1514	3.34E-04	8.98	3.00E-02	1.11E-03	1.00E+00	0.32	1.25E-05	42.3E+6	19	5.26%
0.653	0.134	0.064	62.4	0.052	0.121	4.31E-04	1514	3.34E-04	8.98	3.05E-02	1.15E-03	8.45E-01	0.32	2.66E-05	40.8E+6	19	6.23%

M	L	d	ft	RTO	CRT	V	p	Js	Tt	ADFt	RCF	MMFt	Ft	γ	G	A	Dt (%)
0.653	0.134	0.064	65.6	0.006	0.010	4.31E-04	1514	3.34E-04	8.98	2.90E-02	1.04E-03	1.18E+00	0.32	1.19E-06	45.1E+6	19	4.46%
0.653	0.134	0.064	65.4	0.012	0.023	4.31E-04	1514	3.34E-04	8.98	2.91E-02	1.05E-03	1.03E+00	0.32	2.40E-06	44.8E+6	19	5.13%
0.653	0.134	0.064	64.7	0.023	0.051	4.31E-04	1514	3.34E-04	8.98	2.95E-02	1.07E-03	8.87E-01	0.32	1.04E-05	43.9E+6	19	5.94%

C.2 UNDISTURBED HEATED

M	L	d	ft	RTO	CRT	V	p	Js	Tt	ADFt	RCF	MMFt	Ft	γ	G	A	Dt (%)
0.648	0.134	0.064	56.1	0.005	0.010	4.31E-04	1502	3.32E-04	9.05	3.42E-02	1.42E-03	9.76E-01	0.32	1.36E-06	32.7E+6	19	5.40%
0.648	0.134	0.064	55.2	0.010	0.021	4.31E-04	1502	3.32E-04	9.05	3.48E-02	1.47E-03	8.83E-01	0.32	2.66E-06	31.7E+6	19	5.96%
0.648	0.134	0.064	54.8	0.019	0.044	4.31E-04	1502	3.32E-04	9.05	3.50E-02	1.49E-03	8.43E-01	0.32	1.25E-05	31.2E+6	19	6.25%
0.648	0.134	0.064	54.2	0.047	0.108	4.31E-04	1502	3.32E-04	9.05	3.54E-02	1.52E-03	8.49E-01	0.32	3.14E-05	30.5E+6	19	6.20%
0.648	0.134	0.064	53.0	0.101	0.243	4.31E-04	1502	3.32E-04	9.05	3.62E-02	1.59E-03	8.11E-01	0.32	7.39E-05	29.2E+6	19	6.49%
0.648	0.134	0.064	49.9	0.288	0.762	4.31E-04	1502	3.32E-04	9.05	3.85E-02	1.80E-03	7.37E-01	0.32	2.61E-04	25.9E+6	19	7.14%
0.648	0.134	0.064	46.7	0.455	1.327	4.31E-04	1502	3.32E-04	9.05	4.11E-02	2.05E-03	6.69E-01	0.32	5.20E-04	22.7E+6	19	7.87%

M	L	d	ft	RTO	CRT	V	p	Js	Tt	ADFt	RCF	MMFt	Ft	γ	G	A	Dt (%)
0.648	0.134	0.064	53.8	0.005	0.010	4.31E-04	1502	3.32E-04	9.05	3.57E-02	1.55E-03	9.76E-01	0.32	1.48E-06	30.1E+6	19	5.40%
0.648	0.134	0.064	53.0	0.011	0.023	4.31E-04	1502	3.32E-04	9.05	3.62E-02	1.59E-03	9.33E-01	0.32	3.35E-06	29.2E+6	19	5.64%
0.648	0.134	0.064	52.4	0.022	0.051	4.31E-04	1502	3.32E-04	9.05	3.66E-02	1.63E-03	8.42E-01	0.32	1.59E-05	28.6E+6	19	6.25%
0.648	0.134	0.064	51.6	0.072	0.169	4.31E-04	1502	3.32E-04	9.05	3.72E-02	1.68E-03	8.31E-01	0.32	5.42E-05	27.7E+6	19	6.33%
0.648	0.134	0.064	50.6	0.143	0.344	4.31E-04	1502	3.32E-04	9.05	3.80E-02	1.75E-03	8.11E-01	0.32	1.15E-04	26.6E+6	19	6.49%
0.648	0.134	0.064	48.4	0.285	0.749	4.31E-04	1502	3.32E-04	9.05	3.97E-02	1.91E-03	7.42E-01	0.32	2.73E-04	24.4E+6	19	7.09%

M	L	d	ft	RTO	CRT	V	p	Js	Tt	ADFt	RCF	MMFt	Ft	γ	G	A	Dt (%)
0.648	0.134	0.064	56.4	0.005	0.010	4.31E-04	1502	3.32E-04	9.05	3.40E-02	1.41E-03	9.76E-01	0.32	1.34E-06	33.1E+6	19	5.40%
0.648	0.134	0.064	56.4	0.011	0.024	4.31E-04	1502	3.32E-04	9.05	3.40E-02	1.41E-03	8.94E-01	0.32	2.95E-06	33.1E+6	19	5.89%
0.648	0.134	0.064	56.2	0.044	0.099	4.31E-04	1502	3.32E-04	9.05	3.42E-02	1.42E-03	8.67E-01	0.32	2.68E-05	32.8E+6	19	6.07%
0.648	0.134	0.064	55.8	0.118	0.274	4.31E-04	1502	3.32E-04	9.05	3.44E-02	1.44E-03	8.40E-01	0.32	7.52E-05	32.4E+6	19	6.26%
0.648	0.134	0.064	54.4	0.246	0.602	4.31E-04	1502	3.32E-04	9.05	3.53E-02	1.51E-03	7.97E-01	0.32	1.74E-04	30.8E+6	19	6.60%
0.648	0.134	0.064	52.4	0.391	1.029	4.31E-04	1502	3.32E-04	9.05	3.66E-02	1.63E-03	7.41E-01	0.32	3.20E-04	28.6E+6	19	7.10%

M	L	d	ft	RTO	CRT	V	p	Js	Tt	ADFt	RCF	MMFt	Ft	γ	G	A	Dt (%)
0.648	0.134	0.064	56.4	0.005	0.010	4.31E-04	1502	3.32E-04	9.05	3.40E-02	1.41E-03	9.76E-01	0.32	1.34E-06	33.1E+6	19	5.40%
0.648	0.134	0.064	56.4	0.009	0.021	4.31E-04	1502	3.32E-04	9.05	3.40E-02	1.41E-03	8.36E-01	0.32	2.42E-06	33.1E+6	19	6.29%
0.648	0.134	0.064	56.5	0.019	0.047	4.31E-04	1502	3.32E-04	9.05	3.40E-02	1.40E-03	7.89E-01	0.32	1.26E-05	33.2E+6	19	6.67%
0.648	0.134	0.064	56.1	0.065	0.161	4.31E-04	1502	3.32E-04	9.05	3.42E-02	1.42E-03	7.88E-01	0.32	4.37E-05	32.7E+6	19	6.68%
0.648	0.134	0.064	54.8	0.200	0.523	4.31E-04	1502	3.32E-04	9.05	3.50E-02	1.49E-03	7.46E-01	0.32	1.49E-04	31.2E+6	19	7.05%
0.648	0.134	0.064	52.3	0.388	1.104	4.31E-04	1502	3.32E-04	9.05	3.67E-02	1.64E-03	6.86E-01	0.32	3.45E-04	28.4E+6	19	7.68%
0.648	0.134	0.064	49.4	0.567	1.765	4.31E-04	1502	3.32E-04	9.05	3.89E-02	1.83E-03	6.27E-01	0.32	6.18E-04	25.4E+6	19	8.40%

M	L	d	ft	RTO	CRT	V	p	Js	Tt	ADFt	RCF	MMFt	Ft	γ	G	A	Dt (%)
0.648	0.134	0.064	62.8	0.005	0.011	4.31E-04	1502	3.32E-04	9.05	3.06E-02	1.13E-03	8.87E-01	0.32	1.08E-06	41.0E+6	19	5.93%
0.648	0.134	0.064	62.8	0.011	0.025	4.31E-04	1502	3.32E-04	9.05	3.06E-02	1.13E-03	8.58E-01	0.32	2.38E-06	41.0E+6	19	6.13%
0.648	0.134	0.064	62.8	0.037	0.080	4.31E-04	1502	3.32E-04	9.05	3.06E-02	1.13E-03	9.02E-01	0.32	1.73E-05	41.0E+6	19	5.83%
0.648	0.134	0.064	62.3	0.107	0.234	4.31E-04	1502	3.32E-04	9.05	3.08E-02	1.15E-03	8.92E-01	0.32	5.15E-05	40.4E+6	19	5.90%
0.648	0.134	0.064	61.0	0.240	0.552	4.31E-04	1502	3.32E-04	9.05	3.15E-02	1.20E-03	8.48E-01	0.32	1.27E-04	38.7E+6	19	6.20%
0.648	0.134	0.064	51.8	0.824	2.500	4.31E-04	1502	3.32E-04	9.05	3.71E-02	1.67E-03	6.43E-01	0.32	7.96E-04	27.9E+6	19	8.18%

M	L	d	ft	RTO	CRT	V	p	Js	Tt	ADFt	RCF	MMFt	Ft	γ	G	A	Dt (%)
0.658	0.135	0.064	49.7	0.004	0.010	4.34E-04	1516	3.37E-04	8.90	3.80E-02	1.81E-03	7.94E-01	0.32	1.37E-06	26.3E+6	19	6.63%
0.658	0.135	0.064	50.1	0.008	0.021	4.34E-04	1516	3.37E-04	8.90	3.77E-02	1.78E-03	7.56E-01	0.32	2.70E-06	26.7E+6	19	6.96%
0.658	0.135	0.064	50.1	0.017	0.047	4.34E-04	1516	3.37E-04	8.90	3.77E-02	1.78E-03	7.18E-01	0.32	1.59E-05	26.7E+6	19	7.33%
0.658	0.135	0.064	50.0	0.045	0.121	4.34E-04	1516	3.37E-04	8.90	3.78E-02	1.79E-03	7.38E-01	0.32	4.10E-05	26.6E+6	19	7.13%
0.658	0.135	0.064	48.0	0.171	0.492	4.34E-04	1516	3.37E-04	8.90	3.93E-02	1.94E-03	6.90E-01	0.32	1.81E-04	24.5E+6	19	7.63%
0.658	0.135	0.064	45.2	0.410	1.285	4.34E-04	1516	3.37E-04	8.90	4.18E-02	2.19E-03	6.33E-01	0.32	5.33E-04	21.8E+6	19	8.31%
0.658	0.135	0.064	41.5	0.564	1.973	4.34E-04	1516	3.37E-04	8.90	4.55E-02	2.60E-03	5.67E-01	0.32	9.72E-04	18.3E+6	19	9.28%

M	L	d	ft	RTO	CRT	V	p	Js	Tt	ADFt	RCF	MMFt	Ft	γ	G	A	Dt (%)
0.658	0.135	0.064	47.5	0.004	0.010	4.34E-04	1516	3.37E-04	8.90	3.98E-02	1.98E-03	7.94E-01	0.32	1.50E-06	24.0E+6	19	6.63%
0.658	0.135	0.064	47.5	0.008	0.020	4.34E-04	1516	3.37E-04	8.90	3.98E-02	1.98E-03	7.94E-01	0.32	3.01E-06	24.0E+6	19	6.63%
0.658	0.135	0.064	47.0	0.016	0.049	4.34E-04	1516	3.37E-04	8.90	4.02E-02	2.02E-03	6.48E-01	0.32	1.88E-05	23.5E+6	19	8.12%
0.658	0.135	0.064	46.9	0.045	0.147	4.34E-04	1516	3.37E-04	8.90	4.03E-02	2.03E-03	6.07E-01	0.32	5.67E-05	23.4E+6	19	8.67%
0.658	0.135	0.064	46.1	0.126	0.379	4.34E-04	1516	3.37E-04	8.90	4.10E-02	2.10E-03	6.60E-01	0.32	1.51E-04	22.6E+6	19	7.98%
0.658	0.135	0.064	42.8	0.293	0.975	4.34E-04	1516	3.37E-04	8.90	4.41E-02	2.44E-03	5.96E-01	0.32	4.51E-04	19.5E+6	19	8.83%
0.658	0.135	0.064	40.6	0.403	1.432	4.34E-04	1516	3.37E-04	8.90	4.65E-02	2.71E-03	5.58E-01	0.32	7.37E-04	17.6E+6	19	9.43%

M	L	d	ft	RTO	CRT	V	p	Js	Tt	ADFt	RCF	MMFt	Ft	γ	G	A	Dt (%)
0.658	0.135	0.064	52.6	0.004	0.010	4.34E-04	1516	3.37E-04	8.90	3.59E-02	1.62E-03	7.94E-01	0.32	1.23E-06	29.5E+6	19	6.63%
0.658	0.135	0.064	52.6	0.009	0.025	4.34E-04	1516	3.37E-04	8.90	3.59E-02	1.62E-03	7.14E-01	0.32	2.76E-06	29.5E+6	19	7.37%
0.658	0.135	0.064	52.5	0.022	0.061	4.34E-04	1516	3.37E-04	8.90	3.60E-02	1.62E-03	7.16E-01	0.32	1.88E-05	29.4E+6	19	7.36%
0.658	0.135	0.064	51.7	0.073	0.219	4.34E-04	1516	3.37E-04	8.90	3.65E-02	1.67E-03	6.61E-01	0.32	6.95E-05	28.5E+6	19	7.96%
0.658	0.135	0.064	48.8	0.266	0.821	4.34E-04	1516	3.37E-04	8.90	3.87E-02	1.88E-03	6.43E-01	0.32	2.92E-04	25.4E+6	19	8.19%
0.658	0.135	0.064	44.0	0.513	1.840	4.34E-04	1516	3.37E-04	8.90	4.29E-02	2.31E-03	5.53E-01	0.32	8.06E-04	20.6E+6	19	9.52%

M	L	d	ft	RTO	CRT	V	p	Js	Tt	ADFt	RCF	MMFt	Ft	γ	G	A	Dt (%)
0.658	0.135	0.064	53.4	0.004	0.010	4.34E-04	1516	3.37E-04	8.90	3.54E-02	1.57E-03	7.94E-01	0.32	1.19E-06	30.4E+6	19	6.63%
0.658	0.135	0.064	53.4	0.008	0.022	4.34E-04	1516	3.37E-04	8.90	3.54E-02	1.57E-03	7.21E-01	0.32	2.38E-06	30.4E+6	19	7.30%
0.658	0.135	0.064	53.4	0.023	0.063	4.34E-04	1516	3.37E-04	8.90	3.54E-02	1.57E-03	7.24E-01	0.32	1.87E-05	30.4E+6	19	7.27%
0.658	0.135	0.064	52.8	0.079	0.213	4.34E-04	1516	3.37E-04	8.90	3.58E-02	1.60E-03	7.36E-01	0.32	6.48E-05	29.7E+6	19	7.15%
0.658	0.135	0.064	50.6	0.255	0.740	4.34E-04	1516	3.37E-04	8.90	3.73E-02	1.75E-03	6.84E-01	0.32	2.45E-04	27.3E+6	19	7.70%
0.658	0.135	0.064	48.3	0.481	1.521	4.34E-04	1516	3.37E-04	8.90	3.91E-02	1.92E-03	6.27E-01	0.32	5.53E-04	24.9E+6	19	8.39%

M	L	d	ft	RTO	CRT	V	p	Js	Tt	ADFt	RCF	MMFt	Ft	γ	G	A	Dt (%)
0.658	0.135	0.064	57.8	0.004	0.010	4.34E-04	1516	3.37E-04	8.90	3.27E-02	1.34E-03	7.94E-01	0.32	1.02E-06	35.6E+6	19	6.63%
0.658	0.135	0.064	58.6	0.010	0.026	4.34E-04	1516	3.37E-04	8.90	3.22E-02	1.30E-03	7.63E-01	0.32	2.47E-06	36.6E+6	19	6.90%
0.658	0.135	0.064	58.3	0.018	0.050	4.34E-04	1516	3.37E-04	8.90	3.24E-02	1.32E-03	7.14E-01	0.32	1.25E-05	36.2E+6	19	7.37%
0.658	0.135	0.064	58.5	0.073	0.194	4.34E-04	1516	3.37E-04	8.90	3.23E-02	1.31E-03	7.47E-01	0.32	4.81E-05	36.5E+6	19	7.05%
0.658	0.135	0.064	57.8	0.175	0.454	4.34E-04	1516	3.37E-04	8.90	3.27E-02	1.34E-03	7.65E-01	0.32	1.15E-04	35.6E+6	19	6.88%
0.658	0.135	0.064	55.5	0.352	0.952	4.34E-04	1516	3.37E-04	8.90	3.40E-02	1.45E-03	7.34E-01	0.32	2.62E-04	32.8E+6	19	7.17%
0.658	0.135	0.064	52.4	0.607	1.778	4.34E-04	1516	3.37E-04	8.90	3.60E-02	1.63E-03	6.77E-01	0.32	5.49E-04	29.2E+6	19	7.77%

M	L	d	ft	RTO	CRT	V	p	Js	Tt	ADFt	RCF	MMFt	Ft	γ	G	A	Dt (%)
0.653	0.134	0.064	51.3	0.005	0.010	4.31E-04	1514	3.34E-04	8.98	3.71E-02	1.70E-03	9.83E-01	0.32	1.62E-06	27.6E+6	19	5.35%
0.653	0.134	0.064	51.5	0.010	0.024	4.31E-04	1514	3.34E-04	8.98	3.70E-02	1.69E-03	8.19E-01	0.32	3.22E-06	27.8E+6	19	6.42%
0.653	0.134	0.064	50.6	0.032	0.086	4.31E-04	1514	3.34E-04	8.98	3.77E-02	1.75E-03	7.32E-01	0.32	2.87E-05	26.8E+6	19	7.19%
0.653	0.134	0.064	47.6	0.107	0.313	4.31E-04	1514	3.34E-04	8.98	4.00E-02	1.97E-03	6.72E-01	0.32	1.18E-04	23.7E+6	19	7.83%
0.653	0.134	0.064	43.9	0.307	0.971	4.31E-04	1514	3.34E-04	8.98	4.34E-02	2.32E-03	6.22E-01	0.32	4.30E-04	20.2E+6	19	8.47%
0.653	0.134	0.064	40.6	0.538	1.849	4.31E-04	1514	3.34E-04	8.98	4.69E-02	2.71E-03	5.72E-01	0.32	9.58E-04	17.3E+6	19	9.20%

M	L	d	ft	RTO	CRT	V	p	Js	Tt	ADFt	RCF	MMFt	Ft	γ	G	A	Dt (%)
0.653	0.134	0.064	51.5	0.005	0.010	4.31E-04	1514	3.34E-04	8.98	3.70E-02	1.69E-03	9.83E-01	0.32	1.61E-06	27.8E+6	19	5.35%
0.653	0.134	0.064	51.2	0.010	0.023	4.31E-04	1514	3.34E-04	8.98	3.72E-02	1.71E-03	8.55E-01	0.32	3.26E-06	27.5E+6	19	6.16%
0.653	0.134	0.064	50.4	0.034	0.090	4.31E-04	1514	3.34E-04	8.98	3.78E-02	1.76E-03	7.43E-01	0.32	3.03E-05	26.6E+6	19	7.09%
0.653	0.134	0.064	46.9	0.130	0.384	4.31E-04	1514	3.34E-04	8.98	4.06E-02	2.03E-03	6.66E-01	0.32	1.49E-04	23.0E+6	19	7.91%
0.653	0.134	0.064	43.4	0.312	0.978	4.31E-04	1514	3.34E-04	8.98	4.39E-02	2.37E-03	6.27E-01	0.32	4.44E-04	19.7E+6	19	8.39%
0.653	0.134	0.064	40.7	0.561	1.906	4.31E-04	1514	3.34E-04	8.98	4.68E-02	2.70E-03	5.79E-01	0.32	9.83E-04	17.4E+6	19	9.09%

M	L	d	ft	RTO	CRT	V	p	Js	Tt	ADFt	RCF	MMFt	Ft	γ	G	A	Dt (%)
0.653	0.134	0.064	55.3	0.005	0.010	4.31E-04	1514	3.34E-04	8.98	3.45E-02	1.46E-03	9.83E-01	0.32	1.40E-06	32.0E+6	19	5.35%
0.653	0.134	0.064	55.0	0.011	0.024	4.31E-04	1514	3.34E-04	8.98	3.46E-02	1.48E-03	9.01E-01	0.32	3.11E-06	31.7E+6	19	5.84%
0.653	0.134	0.064	54.4	0.025	0.055	4.31E-04	1514	3.34E-04	8.98	3.50E-02	1.51E-03	8.94E-01	0.32	1.59E-05	31.0E+6	19	5.89%
0.653	0.134	0.064	52.7	0.083	0.218	4.31E-04	1514	3.34E-04	8.98	3.62E-02	1.61E-03	7.49E-01	0.32	6.71E-05	29.1E+6	19	7.03%
0.653	0.134	0.064	50.4	0.225	0.627	4.31E-04	1514	3.34E-04	8.98	3.78E-02	1.76E-03	7.06E-01	0.32	2.11E-04	26.6E+6	19	7.46%
0.653	0.134	0.064	47.0	0.434	1.359	4.31E-04	1514	3.34E-04	8.98	4.05E-02	2.02E-03	6.28E-01	0.32	5.26E-04	23.1E+6	19	8.38%

M	L	d	ft	RTO	CRT	V	p	Js	Tt	ADFt	RCF	MMFt	Ft	γ	G	A	Dt (%)
0.653	0.134	0.064	50.9	0.005	0.010	4.31E-04	1514	3.34E-04	8.98	3.74E-02	1.73E-03	9.83E-01	0.32	1.65E-06	27.1E+6	19	5.35%
0.653	0.134	0.064	51.1	0.009	0.020	4.31E-04	1514	3.34E-04	8.98	3.73E-02	1.71E-03	8.85E-01	0.32	2.94E-06	27.4E+6	19	5.95%
0.653	0.134	0.064	49.6	0.026	0.067	4.31E-04	1514	3.34E-04	8.98	3.84E-02	1.82E-03	7.63E-01	0.32	2.33E-05	25.8E+6	19	6.90%
0.653	0.134	0.064	47.5	0.081	0.235	4.31E-04	1514	3.34E-04	8.98	4.01E-02	1.98E-03	6.78E-01	0.32	8.90E-05	23.6E+6	19	7.77%
0.653	0.134	0.064	44.9	0.225	0.681	4.31E-04	1514	3.34E-04	8.98	4.24E-02	2.22E-03	6.50E-01	0.32	2.89E-04	21.1E+6	19	8.10%
0.653	0.134	0.064	40.4	0.494	1.634	4.31E-04	1514	3.34E-04	8.98	4.72E-02	2.74E-03	5.94E-01	0.32	8.55E-04	17.1E+6	19	8.85%

M	L	d	ft	RTO	CRT	V	p	Js	Tt	ADFt	RCF	MMFt	Ft	γ	G	A	Dt (%)
0.653	0.134	0.064	58.7	0.005	0.010	4.31E-04	1514	3.34E-04	8.98	3.25E-02	1.30E-03	9.83E-01	0.32	1.24E-06	36.1E+6	19	5.35%
0.653	0.134	0.064	58.6	0.010	0.022	4.31E-04	1514	3.34E-04	8.98	3.25E-02	1.30E-03	8.94E-01	0.32	2.49E-06	36.0E+6	19	5.89%
0.653	0.134	0.064	58.2	0.037	0.086	4.31E-04	1514	3.34E-04	8.98	3.27E-02	1.32E-03	8.46E-01	0.32	2.17E-05	35.5E+6	19	6.22%
0.653	0.134	0.064	57.4	0.122	0.281	4.31E-04	1514	3.34E-04	8.98	3.32E-02	1.36E-03	8.54E-01	0.32	7.29E-05	34.5E+6	19	6.17%
0.653	0.134	0.064	54.6	0.383	1.013	4.31E-04	1514	3.34E-04	8.98	3.49E-02	1.50E-03	7.43E-01	0.32	2.90E-04	31.2E+6	19	7.08%
0.653	0.134	0.064	51.5	0.551	1.722	4.31E-04	1514	3.34E-04	8.98	3.70E-02	1.69E-03	6.29E-01	0.32	5.55E-04	27.8E+6	19	8.37%

C.3 REMOLDED

M	L	d	ft	RTO	CRT	V	p	Js	Tt	ADFt	RCF	MMFt	Ft	γ	G	A	Dt (%)
0.859	0.137	0.072	62.5	0.004	0.011	5.57E-04	1543	5.57E-04	5.39	1.83E-02	1.14E-03	1.04E+00	0.41	8.44E-07	26.5E+6	11	8.72%
0.859	0.137	0.072	62.4	0.008	0.025	5.57E-04	1543	5.57E-04	5.39	1.83E-02	1.15E-03	1.05E+00	0.41	1.93E-06	26.4E+6	11	8.67%
0.859	0.137	0.072	62.3	0.021	0.068	5.57E-04	1543	5.57E-04	5.39	1.84E-02	1.15E-03	1.01E+00	0.41	1.65E-05	26.3E+6	11	8.98%
0.859	0.137	0.072	61.9	0.044	0.143	5.57E-04	1543	5.57E-04	5.39	1.85E-02	1.17E-03	1.01E+00	0.41	3.51E-05	26.0E+6	11	9.02%
0.859	0.137	0.072	61.2	0.070	0.233	5.57E-04	1543	5.57E-04	5.39	1.87E-02	1.19E-03	9.84E-01	0.41	5.86E-05	25.4E+6	11	9.24%
0.859	0.137	0.072	60.4	0.180	0.601	5.57E-04	1543	5.57E-04	5.39	1.89E-02	1.23E-03	9.81E-01	0.41	1.55E-04	24.7E+6	11	9.26%
0.859	0.137	0.072	59.5	0.303	1.041	5.57E-04	1543	5.57E-04	5.39	1.92E-02	1.26E-03	9.54E-01	0.41	2.77E-04	24.0E+6	11	9.53%
0.859	0.137	0.072	58.3	0.345	1.311	5.57E-04	1543	5.57E-04	5.39	1.96E-02	1.32E-03	8.62E-01	0.41	3.63E-04	23.0E+6	11	10.54%
0.859	0.137	0.072	56.7	0.418	1.653	5.57E-04	1543	5.57E-04	5.39	2.02E-02	1.39E-03	8.28E-01	0.41	4.84E-04	21.8E+6	11	10.97%

M	L	d	ft	RTO	CRT	V	p	Js	Tt	ADFt	RCF	MMFt	Ft	γ	G	A	Dt (%)
0.859	0.137	0.072	65.4	0.004	0.011	5.57E-04	1543	5.57E-04	5.39	1.75E-02	1.05E-03	1.04E+00	0.41	7.71E-07	29.0E+6	11	0.087205
0.859	0.137	0.072	65.5	0.008	0.027	5.57E-04	1543	5.57E-04	5.39	1.75E-02	1.04E-03	9.71E-01	0.41	1.76E-06	29.1E+6	11	0.093647
0.859	0.137	0.072	65.3	0.019	0.062	5.57E-04	1543	5.57E-04	5.39	1.75E-02	1.05E-03	1.00E+00	0.41	1.37E-05	28.9E+6	11	0.090543
0.859	0.137	0.072	65.3	0.047	0.155	5.57E-04	1543	5.57E-04	5.39	1.75E-02	1.05E-03	9.93E-01	0.41	3.42E-05	28.9E+6	11	0.091507
0.859	0.137	0.072	64.7	0.134	0.442	5.57E-04	1543	5.57E-04	5.39	1.77E-02	1.07E-03	9.93E-01	0.41	9.94E-05	28.4E+6	11	0.091524
0.859	0.137	0.072	61.7	0.254	0.932	5.57E-04	1543	5.57E-04	5.39	1.85E-02	1.17E-03	8.93E-01	0.41	2.31E-04	25.8E+6	11	0.101813
0.859	0.137	0.072	61.3	0.366	1.357	5.57E-04	1543	5.57E-04	5.39	1.87E-02	1.19E-03	8.84E-01	0.41	3.40E-04	25.5E+6	11	0.102877
0.859	0.137	0.072	60.3	0.467	1.765	5.57E-04	1543	5.57E-04	5.39	1.90E-02	1.23E-03	8.67E-01	0.41	4.57E-04	24.6E+6	11	0.104869

M	L	d	ft	RTO	CRT	V	p	Js	Tt	ADFt	RCF	MMFt	Ft	γ	G	A	Dt (%)
0.859	0.137	0.072	68.7	0.004	0.011	5.57E-04	1543	5.57E-04	5.39	1.66E-02	9.48E-04	1.04E+00	0.41	6.98E-07	32.0E+6	11	0.087205
0.859	0.137	0.072	68.5	0.014	0.043	5.57E-04	1543	5.57E-04	5.39	1.67E-02	9.53E-04	1.07E+00	0.41	2.81E-06	31.8E+6	11	0.085224
0.859	0.137	0.072	68.3	0.032	0.103	5.57E-04	1543	5.57E-04	5.39	1.67E-02	9.59E-04	1.02E+00	0.41	2.08E-05	31.6E+6	11	0.089311
0.859	0.137	0.072	67.4	0.110	0.347	5.57E-04	1543	5.57E-04	5.39	1.70E-02	9.84E-04	1.04E+00	0.41	7.19E-05	30.8E+6	11	0.08753
0.859	0.137	0.072	66.4	0.258	0.831	5.57E-04	1543	5.57E-04	5.39	1.72E-02	1.01E-03	1.02E+00	0.41	1.77E-04	29.9E+6	11	0.089372
0.859	0.137	0.072	63.7	0.424	1.616	5.57E-04	1543	5.57E-04	5.39	1.80E-02	1.10E-03	8.60E-01	0.41	3.75E-04	27.5E+6	11	0.105753

M	L	d	ft	RTO	CRT	V	p	Js	Tt	ADFt	RCF	MMFt	Ft	γ	G	A	Dt (%)
0.859	0.137	0.072	71.5	0.004	0.011	5.57E-04	1543	5.57E-04	5.39	1.60E-02	8.75E-04	1.04E+00	0.41	6.45E-07	34.7E+6	11	8.72%
0.859	0.137	0.072	71.1	0.009	0.033	5.57E-04	1543	5.57E-04	5.39	1.61E-02	8.85E-04	8.44E-01	0.41	1.58E-06	34.3E+6	11	10.77%
0.859	0.137	0.072	71.1	0.018	0.069	5.57E-04	1543	5.57E-04	5.39	1.61E-02	8.85E-04	8.55E-01	0.41	1.29E-05	34.3E+6	11	10.64%
0.859	0.137	0.072	70.8	0.039	0.155	5.57E-04	1543	5.57E-04	5.39	1.62E-02	8.92E-04	8.24E-01	0.41	2.91E-05	34.0E+6	11	11.03%
0.859	0.137	0.072	70.3	0.115	0.461	5.57E-04	1543	5.57E-04	5.39	1.63E-02	9.05E-04	8.17E-01	0.41	8.78E-05	33.5E+6	11	11.12%
0.859	0.137	0.072	68.9	0.205	0.84	5.57E-04	1543	5.57E-04	5.39	1.66E-02	9.42E-04	8.00E-01	0.41	1.67E-04	32.2E+6	11	11.37%
0.859	0.137	0.072	67	0.379	1.628	5.57E-04	1543	5.57E-04	5.39	1.71E-02	9.96E-04	7.63E-01	0.41	3.41E-04	30.4E+6	11	11.92%

M	L	d	ft	RTO	CRT	V	p	Js	Tt	ADFt	RCF	MMFt	Ft	γ	G	A	Dt (%)
0.859	0.137	0.072	71.9	0.004	0.011	5.57E-04	1543	5.57E-04	5.39	1.59E-02	8.65E-04	1.04E+00	0.41	6.37E-07	35.0E+6	11	8.72%
0.859	0.137	0.072	71.9	0.008	0.035	5.57E-04	1543	5.57E-04	5.39	1.59E-02	8.65E-04	7.49E-01	0.41	1.46E-06	35.0E+6	11	12.14%
0.859	0.137	0.072	72.1	0.037	0.157	5.57E-04	1543	5.57E-04	5.39	1.59E-02	8.60E-04	7.72E-01	0.41	2.84E-05	35.2E+6	11	11.77%
0.859	0.137	0.072	71.5	0.115	0.515	5.57E-04	1543	5.57E-04	5.39	1.60E-02	8.75E-04	7.32E-01	0.41	9.49E-05	34.7E+6	11	12.43%
0.859	0.137	0.072	70.3	0.192	0.873	5.57E-04	1543	5.57E-04	5.39	1.63E-02	9.05E-04	7.21E-01	0.41	1.66E-04	33.5E+6	11	12.62%
0.859	0.137	0.072	68.6	0.323	1.504	5.57E-04	1543	5.57E-04	5.39	1.67E-02	9.50E-04	7.04E-01	0.41	3.01E-04	31.9E+6	11	12.92%

M	L	d	ft	RTO	CRT	V	p	Js	Tt	ADFt	RCF	MMFt	Ft	γ	G	A	Dt (%)
0.877	0.138	0.072	54.6	0.003	0.011	5.61E-04	1564	5.69E-04	5.28	2.05E-02	1.50E-03	9.13E-01	0.41	9.41E-07	20.8E+6	11	9.96%
0.877	0.138	0.072	55.6	0.008	0.032	5.61E-04	1564	5.69E-04	5.28	2.01E-02	1.45E-03	8.37E-01	0.41	2.42E-06	21.6E+6	11	10.87%
0.877	0.138	0.072	55.3	0.025	0.104	5.61E-04	1564	5.69E-04	5.28	2.02E-02	1.46E-03	8.04E-01	0.41	3.18E-05	21.3E+6	11	11.30%
0.877	0.138	0.072	54.4	0.098	0.414	5.61E-04	1564	5.69E-04	5.28	2.06E-02	1.51E-03	7.92E-01	0.41	1.31E-04	20.6E+6	11	11.48%
0.877	0.138	0.072	52.6	0.197	0.871	5.61E-04	1564	5.69E-04	5.28	2.13E-02	1.62E-03	7.57E-01	0.41	2.94E-04	19.3E+6	11	12.01%
0.877	0.138	0.072	49.5	0.340	1.612	5.61E-04	1564	5.69E-04	5.28	2.26E-02	1.83E-03	7.06E-01	0.41	6.15E-04	17.1E+6	11	12.88%

M	L	d	ft	RTO	CRT	V	p	Js	Tt	ADFt	RCF	MMFt	Ft	γ	G	A	Dt (%)
0.877	0.138	0.072	59.8	0.003	0.011	5.61E-04	1564	5.69E-04	5.28	1.87E-02	1.25E-03	9.13E-01	0.41	7.84E-07	24.9E+6	11	9.96%
0.877	0.138	0.072	59.4	0.007	0.026	5.61E-04	1564	5.69E-04	5.28	1.89E-02	1.27E-03	9.01E-01	0.41	1.85E-06	24.6E+6	11	10.09%
0.877	0.138	0.072	59.3	0.023	0.087	5.61E-04	1564	5.69E-04	5.28	1.89E-02	1.27E-03	8.85E-01	0.41	2.31E-05	24.5E+6	11	10.28%
0.877	0.138	0.072	58.5	0.083	0.345	5.61E-04	1564	5.69E-04	5.28	1.91E-02	1.31E-03	8.05E-01	0.41	9.43E-05	23.9E+6	11	11.29%
0.877	0.138	0.072	57.9	0.160	0.689	5.61E-04	1564	5.69E-04	5.28	1.93E-02	1.33E-03	7.77E-01	0.41	1.92E-04	23.4E+6	11	11.70%
0.877	0.138	0.072	56.1	0.227	1.003	5.61E-04	1564	5.69E-04	5.28	2.00E-02	1.42E-03	7.57E-01	0.41	2.98E-04	21.9E+6	11	12.00%
0.877	0.138	0.072	53.8	0.345	1.591	5.61E-04	1564	5.69E-04	5.28	2.08E-02	1.55E-03	7.26E-01	0.41	5.14E-04	20.2E+6	11	12.53%

M	L	d	ft	RTO	CRT	V	p	Js	Tt	ADFt	RCF	MMFt	Ft	γ	G	A	Dt (%)
0.877	0.138	0.072	61.6	0.003	0.011	5.61E-04	1564	5.69E-04	5.28	1.82E-02	1.18E-03	9.13E-01	0.41	7.39E-07	26.5E+6	11	9.96%
0.877	0.138	0.072	61.1	0.009	0.035	5.61E-04	1564	5.69E-04	5.28	1.83E-02	1.20E-03	8.60E-01	0.41	2.25E-06	26.0E+6	11	10.57%
0.877	0.138	0.072	60.6	0.039	0.160	5.61E-04	1564	5.69E-04	5.28	1.85E-02	1.22E-03	8.16E-01	0.41	4.07E-05	25.6E+6	11	11.15%
0.877	0.138	0.072	59.8	0.140	0.566	5.61E-04	1564	5.69E-04	5.28	1.87E-02	1.25E-03	8.28E-01	0.41	1.48E-04	24.9E+6	11	10.98%
0.877	0.138	0.072	58.3	0.227	0.943	5.61E-04	1564	5.69E-04	5.28	1.92E-02	1.32E-03	8.05E-01	0.41	2.59E-04	23.7E+6	11	11.29%
0.877	0.138	0.072	56.4	0.394	1.693	5.61E-04	1564	5.69E-04	5.28	1.99E-02	1.41E-03	7.79E-01	0.41	4.98E-04	22.2E+6	11	11.67%

M	L	d	ft	RTO	CRT	V	p	Js	Tt	ADFt	RCF	MMFt	Ft	γ	G	A	Dt (%)
0.877	0.138	0.072	63.8	0.003	0.011	5.61E-04	1564	5.69E-04	5.28	1.76E-02	1.10E-03	9.13E-01	0.41	6.89E-07	28.4E+6	11	9.96%
0.877	0.138	0.072	63.7	0.007	0.024	5.61E-04	1564	5.69E-04	5.28	1.76E-02	1.10E-03	9.76E-01	0.41	1.61E-06	28.3E+6	11	9.31%
0.877	0.138	0.072	63.6	0.021	0.085	5.61E-04	1564	5.69E-04	5.28	1.76E-02	1.11E-03	8.27E-01	0.41	1.96E-05	28.2E+6	11	11.00%
0.877	0.138	0.072	63.3	0.056	0.221	5.61E-04	1564	5.69E-04	5.28	1.77E-02	1.12E-03	8.48E-01	0.41	5.16E-05	27.9E+6	11	10.72%
0.877	0.138	0.072	61.8	0.181	0.707	5.61E-04	1564	5.69E-04	5.28	1.81E-02	1.17E-03	8.57E-01	0.41	1.73E-04	26.6E+6	11	10.61%
0.877	0.138	0.072	61.0	0.378	1.547	5.61E-04	1564	5.69E-04	5.28	1.84E-02	1.20E-03	8.18E-01	0.41	3.89E-04	25.9E+6	11	11.12%

M	L	d	ft	RTO	CRT	V	p	Js	Tt	ADFt	RCF	MMFt	Ft	γ	G	A	Dt (%)
0.877	0.138	0.072	66.2	0.003	0.011	5.61E-04	1564	5.69E-04	5.28	1.69E-02	1.02E-03	9.13E-01	0.41	6.40E-07	30.6E+6	11	9.96%
0.877	0.138	0.072	66.2	0.007	0.025	5.61E-04	1564	5.69E-04	5.28	1.69E-02	1.02E-03	8.70E-01	0.41	1.39E-06	30.6E+6	11	10.45%
0.877	0.138	0.072	65.9	0.038	0.146	5.61E-04	1564	5.69E-04	5.28	1.70E-02	1.03E-03	8.71E-01	0.41	3.14E-05	30.3E+6	11	10.44%
0.877	0.138	0.072	65.2	0.113	0.431	5.61E-04	1564	5.69E-04	5.28	1.72E-02	1.05E-03	8.77E-01	0.41	9.48E-05	29.6E+6	11	10.36%
0.877	0.138	0.072	63.3	0.235	0.955	5.61E-04	1564	5.69E-04	5.28	1.77E-02	1.12E-03	8.23E-01	0.41	2.23E-04	27.9E+6	11	11.04%
0.877	0.138	0.072	62.0	0.377	1.555	5.61E-04	1564	5.69E-04	5.28	1.81E-02	1.16E-03	8.11E-01	0.41	3.78E-04	26.8E+6	11	11.21%

M	L	d	ft	RTO	CRT	V	p	Js	Tt	ADFt	RCF	MMFt	Ft	γ	G	A	Dt (%)
0.851	0.136	0.072	51.9	0.003	0.011	5.53E-04	1540	5.52E-04	5.44	2.22E-02	1.66E-03	8.85E-01	0.409	1.06E-06	18.0E+6	11.1	10.18%
0.851	0.136	0.072	51.3	0.007	0.027	5.53E-04	1540	5.52E-04	5.44	2.25E-02	1.70E-03	8.42E-01	0.409	2.52E-06	17.6E+6	11.1	10.70%
0.851	0.136	0.072	51.3	0.016	0.065	5.53E-04	1540	5.52E-04	5.44	2.25E-02	1.70E-03	7.99E-01	0.409	2.34E-05	17.6E+6	11.1	11.27%
0.851	0.136	0.072	50.9	0.042	0.169	5.53E-04	1540	5.52E-04	5.44	2.27E-02	1.73E-03	8.07E-01	0.409	6.19E-05	17.4E+6	11.1	11.17%
0.851	0.136	0.072	49.9	0.103	0.418	5.53E-04	1540	5.52E-04	5.44	2.31E-02	1.80E-03	8.00E-01	0.409	1.59E-04	16.7E+6	11.1	11.26%
0.851	0.136	0.072	48.0	0.214	0.910	5.53E-04	1540	5.52E-04	5.44	2.40E-02	1.94E-03	7.63E-01	0.409	3.75E-04	15.4E+6	11.1	11.80%
0.851	0.136	0.072	44.6	0.366	1.695	5.53E-04	1540	5.52E-04	5.44	2.59E-02	2.25E-03	7.01E-01	0.409	8.09E-04	13.3E+6	11.1	12.85%

M	L	d	ft	RTO	CRT	V	p	Js	Tt	ADFt	RCF	MMFt	Ft	γ	G	A	Dt (%)
0.851	0.136	0.072	56.9	0.003	0.011	5.53E-04	1540	5.52E-04	5.44	2.03E-02	1.38E-03	8.85E-01	0.409	8.79E-07	21.7E+6	11.1	10.18%
0.851	0.136	0.072	57.5	0.008	0.029	5.53E-04	1540	5.52E-04	5.44	2.01E-02	1.35E-03	8.40E-01	0.409	2.15E-06	22.1E+6	11.1	10.73%
0.851	0.136	0.072	57.2	0.020	0.077	5.53E-04	1540	5.52E-04	5.44	2.02E-02	1.37E-03	8.43E-01	0.409	2.23E-05	21.9E+6	11.1	10.68%
0.851	0.136	0.072	56.7	0.054	0.211	5.53E-04	1540	5.52E-04	5.44	2.04E-02	1.39E-03	8.31E-01	0.409	6.23E-05	21.5E+6	11.1	10.84%
0.851	0.136	0.072	55.5	0.133	0.536	5.53E-04	1540	5.52E-04	5.44	2.08E-02	1.45E-03	8.05E-01	0.409	1.65E-04	20.6E+6	11.1	11.18%
0.851	0.136	0.072	53.9	0.240	0.993	5.53E-04	1540	5.52E-04	5.44	2.14E-02	1.54E-03	7.85E-01	0.409	3.24E-04	19.5E+6	11.1	11.48%
0.851	0.136	0.072	51.3	0.371	1.626	5.53E-04	1540	5.52E-04	5.44	2.25E-02	1.70E-03	7.41E-01	0.409	5.86E-04	17.6E+6	11.1	12.16%

M	L	d	ft	RTO	CRT	V	p	Js	Tt	ADFt	RCF	MMFt	Ft	γ	G	A	Dt (%)
0.851	0.136	0.072	58.7	0.003	0.011	5.53E-04	1540	5.52E-04	5.44	1.97E-02	1.30E-03	8.85E-01	0.409	8.26E-07	23.1E+6	11.1	10.18%
0.851	0.136	0.072	58.7	0.007	0.027	5.53E-04	1540	5.52E-04	5.44	1.97E-02	1.30E-03	8.42E-01	0.409	1.93E-06	23.1E+6	11.1	10.70%
0.851	0.136	0.072	58.7	0.019	0.074	5.53E-04	1540	5.52E-04	5.44	1.97E-02	1.30E-03	8.33E-01	0.409	2.04E-05	23.1E+6	11.1	10.81%
0.851	0.136	0.072	58.1	0.065	0.251	5.53E-04	1540	5.52E-04	5.44	1.99E-02	1.32E-03	8.41E-01	0.409	7.06E-05	22.6E+6	11.1	10.72%
0.851	0.136	0.072	56.1	0.166	0.668	5.53E-04	1540	5.52E-04	5.44	2.06E-02	1.42E-03	8.07E-01	0.409	2.01E-04	21.1E+6	11.1	11.17%
0.851	0.136	0.072	54.6	0.272	1.122	5.53E-04	1540	5.52E-04	5.44	2.11E-02	1.50E-03	7.87E-01	0.409	3.57E-04	20.0E+6	11.1	11.45%
0.851	0.136	0.072	51.5	0.434	1.915	5.53E-04	1540	5.52E-04	5.44	2.24E-02	1.69E-03	7.36E-01	0.409	6.85E-04	17.8E+6	11.1	12.25%

M	L	d	ft	RTO	CRT	V	p	Js	Tt	ADFt	RCF	MMFt	Ft	γ	G	A	Dt (%)
0.851	0.136	0.072	61.6	0.003	0.011	5.53E-04	1540	5.52E-04	5.44	1.87E-02	1.18E-03	8.85E-01	0.409	7.50E-07	25.4E+6	11.1	10.18%
0.851	0.136	0.072	61.3	0.008	0.030	5.53E-04	1540	5.52E-04	5.44	1.88E-02	1.19E-03	8.66E-01	0.409	2.02E-06	25.2E+6	11.1	10.41%
0.851	0.136	0.072	61.3	0.018	0.071	5.53E-04	1540	5.52E-04	5.44	1.88E-02	1.19E-03	8.23E-01	0.409	1.79E-05	25.2E+6	11.1	10.95%
0.851	0.136	0.072	61.2	0.048	0.185	5.53E-04	1540	5.52E-04	5.44	1.89E-02	1.19E-03	8.42E-01	0.409	4.69E-05	25.1E+6	11.1	10.70%
0.851	0.136	0.072	60.1	0.141	0.550	5.53E-04	1540	5.52E-04	5.44	1.92E-02	1.24E-03	8.32E-01	0.409	1.44E-04	24.2E+6	11.1	10.83%
0.851	0.136	0.072	58.5	0.237	0.960	5.53E-04	1540	5.52E-04	5.44	1.97E-02	1.31E-03	8.01E-01	0.409	2.66E-04	22.9E+6	11.1	11.24%
0.851	0.136	0.072	55.5	0.430	1.863	5.53E-04	1540	5.52E-04	5.44	2.08E-02	1.45E-03	7.49E-01	0.409	5.74E-04	20.6E+6	11.1	12.02%

M	L	d	ft	RTO	CRT	V	p	Js	Tt	ADFt	RCF	MMFt	Ft	γ	G	A	Dt (%)
0.851	0.136	0.072	63.3	0.003	0.011	5.53E-04	1540	5.52E-04	5.44	1.82E-02	1.12E-03	8.85E-01	0.409	7.10E-07	26.8E+6	11.1	10.18%
0.851	0.136	0.072	63.6	0.009	0.034	5.53E-04	1540	5.52E-04	5.44	1.81E-02	1.11E-03	8.59E-01	0.409	2.11E-06	27.1E+6	11.1	10.48%
0.851	0.136	0.072	63.6	0.020	0.076	5.53E-04	1540	5.52E-04	5.44	1.81E-02	1.11E-03	8.54E-01	0.409	1.78E-05	27.1E+6	11.1	10.55%
0.851	0.136	0.072	63.3	0.045	0.169	5.53E-04	1540	5.52E-04	5.44	1.82E-02	1.12E-03	8.64E-01	0.409	4.00E-05	26.8E+6	11.1	10.42%
0.851	0.136	0.072	62.5	0.144	0.547	5.53E-04	1540	5.52E-04	5.44	1.85E-02	1.14E-03	8.55E-01	0.409	1.33E-04	26.2E+6	11.1	10.54%
0.851	0.136	0.072	60.8	0.282	1.114	5.53E-04	1540	5.52E-04	5.44	1.90E-02	1.21E-03	8.22E-01	0.409	2.86E-04	24.8E+6	11.1	10.96%
0.851	0.136	0.072	57.7	0.424	1.846	5.53E-04	1540	5.52E-04	5.44	2.00E-02	1.34E-03	7.46E-01	0.409	5.26E-04	22.3E+6	11.1	12.08%

C.4 REMOLDED HEATED

M	L	d	ft	RTO	CRT	V	p	Js	Tt	ADFt	RCF	MMFt	Ft	γ	G	A	Dt (%)
0.919	0.146	0.072	45.3	0.003	0.011	5.96E-04	1541	5.95E-04	5.04	2.36E-02	2.18E-03	9.56E-01	0.415	1.29E-06	15.5E+6	10.5	9.97%
0.919	0.146	0.072	44.1	0.007	0.027	5.96E-04	1541	5.95E-04	5.04	2.42E-02	2.30E-03	9.08E-01	0.415	3.17E-06	14.7E+6	10.5	10.48%
0.919	0.146	0.072	43.3	0.022	0.091	5.96E-04	1541	5.95E-04	5.04	2.47E-02	2.39E-03	8.47E-01	0.415	4.27E-05	14.2E+6	10.5	11.24%
0.919	0.146	0.072	42.7	0.070	0.294	5.96E-04	1541	5.95E-04	5.04	2.50E-02	2.45E-03	8.34E-01	0.415	1.42E-04	13.8E+6	10.5	11.42%
0.919	0.146	0.072	41.6	0.148	0.635	5.96E-04	1541	5.95E-04	5.04	2.57E-02	2.58E-03	8.17E-01	0.415	3.23E-04	13.1E+6	10.5	11.66%
0.919	0.146	0.072	40	0.238	1.086	5.96E-04	1541	5.95E-04	5.04	2.67E-02	2.80E-03	7.68E-01	0.415	5.97E-04	12.1E+6	10.5	12.40%
0.919	0.146	0.072	37.1	0.354	1.763	5.96E-04	1541	5.95E-04	5.04	2.88E-02	3.25E-03	7.04E-01	0.415	1.13E-03	10.4E+6	10.5	13.54%

M	L	d	ft	RTO	CRT	V	p	Js	Tt	ADFt	RCF	MMFt	Ft	γ	G	A	Dt (%)
0.919	0.146	0.072	50.6	0.003	0.011	5.96E-04	1541	5.95E-04	5.04	2.11E-02	1.75E-03	9.56E-01	0.415	1.03E-06	19.4E+6	10.5	9.97%
0.919	0.146	0.072	50.5	0.007	0.030	5.96E-04	1541	5.95E-04	5.04	2.12E-02	1.75E-03	8.18E-01	0.415	2.41E-06	19.3E+6	10.5	11.65%
0.919	0.146	0.072	50.9	0.019	0.074	5.96E-04	1541	5.95E-04	5.04	2.10E-02	1.73E-03	9.00E-01	0.415	2.51E-05	19.6E+6	10.5	10.59%
0.919	0.146	0.072	50.6	0.055	0.220	5.96E-04	1541	5.95E-04	5.04	2.11E-02	1.75E-03	8.76E-01	0.415	7.56E-05	19.4E+6	10.5	10.87%
0.919	0.146	0.072	49.6	0.144	0.588	5.96E-04	1541	5.95E-04	5.04	2.16E-02	1.82E-03	8.58E-01	0.415	2.10E-04	18.6E+6	10.5	11.10%
0.919	0.146	0.072	48.6	0.220	0.926	5.96E-04	1541	5.95E-04	5.04	2.20E-02	1.89E-03	8.32E-01	0.415	3.45E-04	17.9E+6	10.5	11.44%
0.919	0.146	0.072	45.7	0.344	1.567	5.96E-04	1541	5.95E-04	5.04	2.34E-02	2.14E-03	7.69E-01	0.415	6.60E-04	15.8E+6	10.5	12.38%

M	L	d	ft	RTO	CRT	V	p	Js	Tt	ADFt	RCF	MMFt	Ft	γ	G	A	Dt (%)
0.919	0.146	0.072	57.7	0.003	0.011	5.96E-04	1541	5.95E-04	5.04	1.85E-02	1.34E-03	9.56E-01	0.415	7.93E-07	25.2E+6	10.5	9.97%
0.919	0.146	0.072	57.5	0.008	0.030	5.96E-04	1541	5.95E-04	5.04	1.86E-02	1.35E-03	9.34E-01	0.415	2.13E-06	25.0E+6	10.5	10.19%
0.919	0.146	0.072	57.6	0.019	0.074	5.96E-04	1541	5.95E-04	5.04	1.86E-02	1.35E-03	9.00E-01	0.415	1.96E-05	25.1E+6	10.5	10.59%
0.919	0.146	0.072	56.4	0.069	0.276	5.96E-04	1541	5.95E-04	5.04	1.90E-02	1.41E-03	8.76E-01	0.415	7.63E-05	24.1E+6	10.5	10.87%
0.919	0.146	0.072	55.6	0.125	0.535	5.96E-04	1541	5.95E-04	5.04	1.92E-02	1.45E-03	8.19E-01	0.415	1.52E-04	23.4E+6	10.5	11.63%
0.919	0.146	0.072	54.4	0.260	1.144	5.96E-04	1541	5.95E-04	5.04	1.97E-02	1.51E-03	7.96E-01	0.415	3.40E-04	22.4E+6	10.5	11.96%
0.919	0.146	0.072	52.7	0.372	1.702	5.96E-04	1541	5.95E-04	5.04	2.03E-02	1.61E-03	7.66E-01	0.415	5.39E-04	21.0E+6	10.5	12.44%

M	L	d	ft	RTO	CRT	V	p	Js	Tt	ADFt	RCF	MMFt	Ft	γ	G	A	Dt (%)
0.919	0.146	0.072	53.4	0.003	0.011	5.96E-04	1541	5.95E-04	5.04	2.00E-02	1.57E-03	9.56E-01	0.415	9.25E-07	21.6E+6	10.5	9.97%
0.919	0.146	0.072	53.6	0.012	0.048	5.96E-04	1541	5.95E-04	5.04	2.00E-02	1.56E-03	8.76E-01	0.415	3.67E-06	21.8E+6	10.5	10.87%
0.919	0.146	0.072	53.3	0.036	0.146	5.96E-04	1541	5.95E-04	5.04	2.01E-02	1.57E-03	8.64E-01	0.415	4.52E-05	21.5E+6	10.5	11.02%
0.919	0.146	0.072	52.7	0.139	0.569	5.96E-04	1541	5.95E-04	5.04	2.03E-02	1.61E-03	8.56E-01	0.415	1.80E-04	21.0E+6	10.5	11.13%
0.919	0.146	0.072	51.2	0.244	1.023	5.96E-04	1541	5.95E-04	5.04	2.09E-02	1.71E-03	8.36E-01	0.415	3.43E-04	19.9E+6	10.5	11.40%
0.919	0.146	0.072	48.8	0.375	1.691	5.96E-04	1541	5.95E-04	5.04	2.19E-02	1.88E-03	7.77E-01	0.415	6.25E-04	18.0E+6	10.5	12.26%

M	L	d	ft	RTO	CRT	V	p	Js	Tt	ADFt	RCF	MMFt	Ft	γ	G	A	Dt (%)
0.919	0.146	0.072	57.9	0.003	0.011	5.96E-04	1541	5.95E-04	5.04	1.85E-02	1.33E-03	9.56E-01	0.415	7.87E-07	25.4E+6	10.5	9.97%
0.919	0.146	0.072	57.8	0.009	0.033	5.96E-04	1541	5.95E-04	5.04	1.85E-02	1.34E-03	9.56E-01	0.415	2.37E-06	25.3E+6	10.5	9.97%
0.919	0.146	0.072	58.3	0.035	0.119	5.96E-04	1541	5.95E-04	5.04	1.83E-02	1.32E-03	1.03E+00	0.415	3.08E-05	25.7E+6	10.5	9.24%
0.919	0.146	0.072	56.2	0.104	0.441	5.96E-04	1541	5.95E-04	5.04	1.90E-02	1.42E-03	8.26E-01	0.415	1.23E-04	23.9E+6	10.5	11.53%
0.919	0.146	0.072	55.2	0.212	0.973	5.96E-04	1541	5.95E-04	5.04	1.94E-02	1.47E-03	7.63E-01	0.415	2.81E-04	23.1E+6	10.5	12.48%
0.919	0.146	0.072	52.9	0.391	1.827	5.96E-04	1541	5.95E-04	5.04	2.02E-02	1.60E-03	7.50E-01	0.415	5.74E-04	21.2E+6	10.5	12.70%

M	L	d	ft	RTO	CRT	V	p	Js	Tt	ADFt	RCF	MMFt	Ft	γ	G	A	Dt (%)
0.923	0.147	0.072	37.8	0.003	0.011	5.96E-04	1548	5.98E-04	5.01	2.81E-02	3.13E-03	8.00E-01	0.418	1.54E-06	10.7E+6	10.5	11.90%
0.923	0.147	0.072	38.0	0.009	0.048	5.96E-04	1548	5.98E-04	5.01	2.80E-02	3.10E-03	6.60E-01	0.418	5.48E-06	10.8E+6	10.5	14.43%
0.923	0.147	0.072	37.6	0.042	0.223	5.96E-04	1548	5.98E-04	5.01	2.83E-02	3.16E-03	6.63E-01	0.418	1.39E-04	10.6E+6	10.5	14.36%
0.923	0.147	0.072	36.0	0.103	0.641	5.96E-04	1548	5.98E-04	5.01	2.96E-02	3.45E-03	5.66E-01	0.418	4.35E-04	9.7E+6	10.5	16.83%
0.923	0.147	0.072	33.0	0.226	1.525	5.96E-04	1548	5.98E-04	5.01	3.22E-02	4.11E-03	5.22E-01	0.418	1.23E-03	8.2E+6	10.5	18.25%

M	L	d	ft	RTO	CRT	V	p	Js	Tt	ADFt	RCF	MMFt	Ft	γ	G	A	Dt (%)
0.923	0.147	0.072	44.3	0.003	0.011	5.96E-04	1548	5.98E-04	5.01	2.40E-02	2.28E-03	9.60E-01	0.418	1.34E-06	14.7E+6	10.5	9.92%
0.923	0.147	0.072	43.7	0.009	0.035	5.96E-04	1548	5.98E-04	5.01	2.43E-02	2.34E-03	9.05E-01	0.418	4.14E-06	14.3E+6	10.5	10.52%
0.923	0.147	0.072	43.4	0.038	0.153	5.96E-04	1548	5.98E-04	5.01	2.45E-02	2.37E-03	8.75E-01	0.418	7.14E-05	14.1E+6	10.5	10.89%
0.923	0.147	0.072	41.8	0.141	0.598	5.96E-04	1548	5.98E-04	5.01	2.55E-02	2.56E-03	8.30E-01	0.418	3.01E-04	13.1E+6	10.5	11.47%
0.923	0.147	0.072	40.0	0.242	1.081	5.96E-04	1548	5.98E-04	5.01	2.66E-02	2.80E-03	7.88E-01	0.418	5.94E-04	12.0E+6	10.5	12.08%
0.923	0.147	0.072	37.5	0.383	1.829	5.96E-04	1548	5.98E-04	5.01	2.84E-02	3.18E-03	7.37E-01	0.418	1.14E-03	10.6E+6	10.5	12.92%

M	L	d	ft	RTO	CRT	V	p	Js	Tt	ADFt	RCF	MMFt	Ft	γ	G	A	Dt (%)
0.923	0.147	0.072	50.2	0.003	0.011	5.96E-04	1548	5.98E-04	5.01	2.12E-02	1.77E-03	9.60E-01	0.418	1.05E-06	18.9E+6	10.5	9.92%
0.923	0.147	0.072	50.3	0.013	0.049	5.96E-04	1548	5.98E-04	5.01	2.12E-02	1.77E-03	9.34E-01	0.418	4.52E-06	19.0E+6	10.5	10.19%
0.923	0.147	0.072	50.0	0.049	0.186	5.96E-04	1548	5.98E-04	5.01	2.13E-02	1.79E-03	9.28E-01	0.418	6.54E-05	18.8E+6	10.5	10.27%
0.923	0.147	0.072	49.1	0.131	0.523	5.96E-04	1548	5.98E-04	5.01	2.17E-02	1.86E-03	8.82E-01	0.418	1.91E-04	18.1E+6	10.5	10.80%
0.923	0.147	0.072	47.4	0.252	1.053	5.96E-04	1548	5.98E-04	5.01	2.24E-02	1.99E-03	8.43E-01	0.418	4.12E-04	16.9E+6	10.5	11.30%
0.923	0.147	0.072	45.2	0.386	1.724	5.96E-04	1548	5.98E-04	5.01	2.35E-02	2.19E-03	7.88E-01	0.418	7.42E-04	15.3E+6	10.5	12.08%

M	L	d	ft	RTO	CRT	V	p	Js	Tt	ADFt	RCF	MMFt	Ft	γ	G	A	Dt (%)
0.923	0.147	0.072	48.1	0.003	0.011	5.96E-04	1548	5.98E-04	5.01	2.21E-02	1.93E-03	9.60E-01	0.418	1.14E-06	17.4E+6	10.5	9.92%
0.923	0.147	0.072	47.6	0.011	0.043	5.96E-04	1548	5.98E-04	5.01	2.24E-02	1.97E-03	9.01E-01	0.418	4.27E-06	17.0E+6	10.5	10.57%
0.923	0.147	0.072	47.3	0.051	0.193	5.96E-04	1548	5.98E-04	5.01	2.25E-02	2.00E-03	9.30E-01	0.418	7.58E-05	16.8E+6	10.5	10.24%
0.923	0.147	0.072	46.7	0.104	0.404	5.96E-04	1548	5.98E-04	5.01	2.28E-02	2.05E-03	9.06E-01	0.418	1.63E-04	16.4E+6	10.5	10.51%
0.923	0.147	0.072	44.8	0.227	0.923	5.96E-04	1548	5.98E-04	5.01	2.38E-02	2.23E-03	8.66E-01	0.418	4.04E-04	15.1E+6	10.5	11.00%
0.923	0.147	0.072	43.3	0.318	1.334	5.96E-04	1548	5.98E-04	5.01	2.46E-02	2.39E-03	8.39E-01	0.418	6.26E-04	14.1E+6	10.5	11.35%

M	L	d	ft	RTO	CRT	V	p	Js	Tt	ADFt	RCF	MMFt	Ft	γ	G	A	Dt (%)
0.923	0.147	0.072	50.4	0.003	0.011	5.96E-04	1548	5.98E-04	5.01	2.11E-02	1.76E-03	9.60E-01	0.418	1.04E-06	19.1E+6	10.5	9.92%
0.923	0.147	0.072	50.4	0.014	0.052	5.96E-04	1548	5.98E-04	5.01	2.11E-02	1.76E-03	9.48E-01	0.418	4.85E-06	19.1E+6	10.5	10.05%
0.923	0.147	0.072	50.4	0.060	0.219	5.96E-04	1548	5.98E-04	5.01	2.11E-02	1.76E-03	9.65E-01	0.418	7.58E-05	19.1E+6	10.5	9.87%
0.923	0.147	0.072	48.5	0.132	0.555	5.96E-04	1548	5.98E-04	5.01	2.19E-02	1.90E-03	8.37E-01	0.418	2.07E-04	17.7E+6	10.5	11.37%
0.923	0.147	0.072	47.3	0.226	0.980	5.96E-04	1548	5.98E-04	5.01	2.25E-02	2.00E-03	8.12E-01	0.418	3.85E-04	16.8E+6	10.5	11.73%
0.923	0.147	0.072	45.1	0.342	1.582	5.96E-04	1548	5.98E-04	5.01	2.36E-02	2.20E-03	7.61E-01	0.418	6.84E-04	15.3E+6	10.5	12.51%

M	L	d	ft	RTO	CRT	V	p	Js	Tt	ADFt	RCF	MMFt	Ft	γ	G	A	Dt (%)
0.889	0.142	0.072	32.3	0.004	0.011	5.77E-04	1540	5.76E-04	5.21	3.42E-02	4.29E-03	1.08E+00	0.41	3.05E-06	7.8E+6	10.5	8.82%
0.889	0.142	0.072	32.9	0.009	0.030	5.77E-04	1540	5.76E-04	5.21	3.36E-02	4.13E-03	1.02E+00	0.41	7.55E-06	8.1E+6	10.5	9.36%
0.889	0.142	0.072	32.3	0.034	0.122	5.77E-04	1540	5.76E-04	5.21	3.42E-02	4.29E-03	9.45E-01	0.41	1.06E-04	7.8E+6	10.5	10.08%
0.889	0.142	0.072	31.4	0.083	0.325	5.77E-04	1540	5.76E-04	5.21	3.52E-02	4.54E-03	8.66E-01	0.41	2.99E-04	7.4E+6	10.5	10.99%
0.889	0.142	0.072	28.6	0.174	0.735	5.77E-04	1540	5.76E-04	5.21	3.86E-02	5.47E-03	8.03E-01	0.41	8.16E-04	6.1E+6	10.5	11.86%
0.889	0.142	0.072	26.9	0.234	1.037	5.77E-04	1540	5.76E-04	5.21	4.11E-02	6.18E-03	7.65E-01	0.41	1.30E-03	5.4E+6	10.5	12.44%
0.889	0.142	0.072	22.9	0.389	1.978	5.77E-04	1540	5.76E-04	5.21	4.82E-02	8.53E-03	6.67E-01	0.41	3.43E-03	3.9E+6	10.5	14.28%

M	L	d	ft	RTO	CRT	V	p	Js	Tt	ADFt	RCF	MMFt	Ft	γ	G	A	Dt (%)
0.889	0.142	0.072	43.1	0.004	0.011	5.77E-04	1540	5.76E-04	5.21	2.56E-02	2.41E-03	1.08E+00	0.41	1.71E-06	13.9E+6	10.5	8.82%
0.889	0.142	0.072	42.9	0.015	0.052	5.77E-04	1540	5.76E-04	5.21	2.57E-02	2.43E-03	9.78E-01	0.41	7.40E-06	13.7E+6	10.5	9.73%
0.889	0.142	0.072	42.7	0.050	0.174	5.77E-04	1540	5.76E-04	5.21	2.59E-02	2.45E-03	9.75E-01	0.41	8.67E-05	13.6E+6	10.5	9.77%
0.889	0.142	0.072	41.9	0.098	0.349	5.77E-04	1540	5.76E-04	5.21	2.64E-02	2.55E-03	9.52E-01	0.41	1.81E-04	13.1E+6	10.5	10.00%
0.889	0.142	0.072	38.1	0.263	1.061	5.77E-04	1540	5.76E-04	5.21	2.90E-02	3.08E-03	8.41E-01	0.41	6.64E-04	10.8E+6	10.5	11.33%
0.889	0.142	0.072	35.7	0.374	1.632	5.77E-04	1540	5.76E-04	5.21	3.09E-02	3.51E-03	7.77E-01	0.41	1.16E-03	9.5E+6	10.5	12.25%

M	L	d	ft	RTO	CRT	V	p	Js	Tt	ADFt	RCF	MMFt	Ft	γ	G	A	Dt (%)
0.889	0.142	0.072	49.5	0.004	0.011	5.77E-04	1540	5.76E-04	5.21	2.23E-02	1.83E-03	1.08E+00	0.41	1.30E-06	18.3E+6	10.5	8.82%
0.889	0.142	0.072	49.5	0.010	0.032	5.77E-04	1540	5.76E-04	5.21	2.23E-02	1.83E-03	1.06E+00	0.41	3.71E-06	18.3E+6	10.5	8.99%
0.889	0.142	0.072	48.9	0.052	0.180	5.77E-04	1540	5.76E-04	5.21	2.26E-02	1.87E-03	9.80E-01	0.41	6.84E-05	17.8E+6	10.5	9.72%
0.889	0.142	0.072	47.0	0.135	0.495	5.77E-04	1540	5.76E-04	5.21	2.35E-02	2.02E-03	9.25E-01	0.41	2.04E-04	16.5E+6	10.5	10.30%
0.889	0.142	0.072	45.4	0.223	0.841	5.77E-04	1540	5.76E-04	5.21	2.43E-02	2.17E-03	8.99E-01	0.41	3.71E-04	15.4E+6	10.5	10.59%
0.889	0.142	0.072	41.9	0.420	1.696	5.77E-04	1540	5.76E-04	5.21	2.64E-02	2.55E-03	8.40E-01	0.41	8.77E-04	13.1E+6	10.5	11.34%

M	L	d	ft	RTO	CRT	V	p	Js	Tt	ADFt	RCF	MMFt	Ft	γ	G	A	Dt (%)
0.889	0.142	0.072	48.7	0.004	0.011	5.77E-04	1540	5.76E-04	5.21	2.27E-02	1.89E-03	1.08E+00	0.41	1.34E-06	17.7E+6	10.5	8.82%
0.889	0.142	0.072	49.4	0.009	0.031	5.77E-04	1540	5.76E-04	5.21	2.24E-02	1.83E-03	9.85E-01	0.41	3.35E-06	18.2E+6	10.5	9.67%
0.889	0.142	0.072	48.9	0.024	0.084	5.77E-04	1540	5.76E-04	5.21	2.26E-02	1.87E-03	9.69E-01	0.41	3.19E-05	17.8E+6	10.5	9.83%
0.889	0.142	0.072	48.1	0.081	0.283	5.77E-04	1540	5.76E-04	5.21	2.30E-02	1.93E-03	9.71E-01	0.41	1.11E-04	17.2E+6	10.5	9.81%
0.889	0.142	0.072	45.9	0.204	0.775	5.77E-04	1540	5.76E-04	5.21	2.41E-02	2.12E-03	8.93E-01	0.41	3.34E-04	15.7E+6	10.5	10.67%
0.889	0.142	0.072	43.0	0.332	1.340	5.77E-04	1540	5.76E-04	5.21	2.57E-02	2.42E-03	8.40E-01	0.41	6.58E-04	13.8E+6	10.5	11.33%

M	L	d	ft	RTO	CRT	V	p	Js	Tt	ADFt	RCF	MMFt	Ft	γ	G	A	Dt (%)
0.889	0.142	0.072	54.0	0.004	0.011	5.77E-04	1540	5.76E-04	5.21	2.05E-02	1.53E-03	1.08E+00	0.41	1.09E-06	21.7E+6	10.5	8.82%
0.889	0.142	0.072	53.9	0.017	0.058	5.77E-04	1540	5.76E-04	5.21	2.05E-02	1.54E-03	9.94E-01	0.41	5.31E-06	21.7E+6	10.5	9.58%
0.889	0.142	0.072	52.5	0.067	0.233	5.77E-04	1540	5.76E-04	5.21	2.10E-02	1.62E-03	9.75E-01	0.41	7.68E-05	20.6E+6	10.5	9.76%
0.889	0.142	0.072	50.0	0.195	0.763	5.77E-04	1540	5.76E-04	5.21	2.21E-02	1.79E-03	8.67E-01	0.41	2.77E-04	18.6E+6	10.5	10.99%
0.889	0.142	0.072	47.1	0.379	1.562	5.77E-04	1540	5.76E-04	5.21	2.35E-02	2.02E-03	8.23E-01	0.41	6.40E-04	16.5E+6	10.5	11.57%

Bibliography

Carrol, A., & Soderstrom, C. (1978). A New Nonpenetrating Ballistic Injury. *Ann Surg* , 753-757.

Chen, W. F., & Han, D. J. (1988). *Plasticity for Structural engineers.* New York: Springer-Verlag.

Chopra, A. K. (2007). *Dynamics of Structures: Theory and Applications to Earthquake Engineering.* Upper Saddle River, NJ: Pearson Prentice Hall.

Drnevich, V., Hardin, B., & Shippy, D. (1978). Modulus and Damping of Soils by the Resonant-Column Method. *Dynamic Geotechnical Testing* , 91-125.

Fratta, D., & Santamarina, J. C. (1996). Wave Propagation in Soils: Multi-Mode, Wide-Band Testing in a Waveguide Device. *Geotechnical Testing Journal* , 130-140.

Hardin, B. O., & Blandford, G. E. (1989). Elasticity of Particulate Materials. *Journal of Geotechnical Engineering* , 788-805.

Hardin, B. O., & Drnevich, V. P. (1972). Shear Modulus and Damping in Soils: Design Equations and Curves. *Journal of the Soil Mechanics and Foundations Division* , 1459-1484.

Ishibashi, I., & Zhang, X. (1993). Unified Dynamic Shear Modulus and Damping Ratios of Sand and Clay. *Soils and Foundations* , 182-191.

Jeremic', B., Putnam, J., Sett, K., Humphrey, D., & Patenaude, S. (2004). Calibration of Elastic-Plastic Material Model for Tire Shreds. *Geotechnical Engineering for Transportation Projects* , 760-767.

Lewis, M. J., & Blaney, G. W. (1990). Design and Testing of a Synthetic Clay Soil. *Geotechnical Testing Journal* , 269-270.

Moseley, R., & Doty, D. (1969). Physiologic Changes Following Chest Injury in Combat Casualties. *Surg Gyneg Obstet* , 233-242.

Munusamy, R., & Barton, D. J. *Behaviour of Roma Plastilina Upon Blunt Projectile Impact.* UK: School of Mechanical Engineering, University of Leeds.

Pamukcu, S., Poplin, J. K., Suhayda, J. N., & Tumay, M. T. (1983). Dynamic Sediment Properties, Mississippi Delta. *Geotechnical Practice in Offshore Engineering*, (pp. 111-132). Austin, Texas.

Park, D., & Hashash, Y. M. (2003). Soil Damping Formulationin Nonlinear Time Domain Site Response Analysis. *Journal of Earthquake Engineering* , 249-274.

Parrales, R. M. (2004). Different Definitions of Energy Dissipation in Geological Materials. *Engineering Geology* .

Resende, L., & Martin, J. B. (1985). Formulation of Drucker-Prager Cap Model. *Journal of Engineering Mechanics* , 855-881.

Roberts, J. C., Ward, E. E., Merkle, A. C., & O'Connor, J. V. (2007). Assessing Behind Armor Blunt Trauma in Accordance With the National Institute of Justice Standard for Personal Body Armor Protection Using Finite Element Modeling. *The Journal of TRAUMA* , 1127-1133.

Sasanakul, I., & Bay, J. A. (2008). Stress Integration Approach in Resonant Column and Torsional Shear Testing for Soils. *Journal of Geotechnical and Geoenviromental Engineering* , 1757-1762.

Shahnazari, H., Dehnavi, Y., & Alavi, A. H. (2010). Numerical Modeling of Stress-Strain Behavior of Sand Under Cyclic Loading. *Engineering Geology* , 53-72.

Steven L.Kramer. (1996). *Geotechnical Earthquake Engineering.* Upper Saddle River, NJ: Prentice Hall.

Stokoe, K., Darendeli, M., Gilbert, R., Meng, F., & Choi, W. (2004). Development of new family of normalized modulus reduction and material damping curves. *Proc., NSF/PEER Int. Workshop.* Berkeley, CA.

Tatsuoka, F., & Silver, M. (1980). New Method for the Calibration of the Inertia of Resonant Column Devices. *Geotechnical Testing Journal* , 30-34.

Valdes, J. R. (1999, March). Simultaneous Determination of Frequency Dependent Modulus and Damping From Resonant Column Test. 186. Georgia Institute of Technology.

Wang, Z., & Lu, Y. (2003). Numerical Analysis on Dynamic Deformation Mechanism of Soils under Blast Loading. *Soil Dynamics and Earthquake Engineering* , 705-714.

Zhang, J., Andrus, R. D., & Juang, C. H. (2005). Normalized Shear Modulus and Material Damping Ratio Relationship. *Journal of Geotechnical and Geoenvironmental Engineering* , 453-464.

VITA

Carlos I. Medina was born on September 21, 1985 in San Juan, Puerto Rico to Lorna Rodriguez-Medina and Ismael Medina. He moved to the state of Washington in 1990 with his parents and younger sister. In 1991 he relocated with his family to Bethlehem, PA. Carlos graduated from Liberty High School in Bethlehem, PA in 2004 and attended Lehigh University in Bethlehem to pursue a degree in civil engineering. He received his Bachelor of Science in Civil Engineering from Lehigh University in May, 2008. After working for the Pennsylvania Department of Transportation for a year, Carlos continued his education at Lehigh receiving his Master of Science in Geotechnical Engineering in August, 2011.